DESIGN AND OPTIMIZATION OF BROADBAND HIGH IMPEDANCE GROUND PLANES (HIGP) FOR SURFACE MOUNT ANTENNAS

THESIS

Murat Dogrul, First Lieutenant, TUAF

AFIT/GE/ENG/08-08

DEPARTMENT OF THE AIR FORCE
AIR UNIVERSITY

AIR FORCE INSTITUTE OF TECHNOLOGY

Wright-Patterson Air Force Base, Ohio

The views expressed in this thesis are those of the author and do not reflect the official policy or position of the United States Air Force, Department of Defense, or the United States Government.

AFIT/GE/ENG/08-08

DESIGN AND OPTIMIZATION OF BROADBAND HIGH IMPEDANCE GROUND PLANES (HIGP) FOR SURFACE MOUNT ANTENNAS

THESIS

Presented to the Faculty

Department of Electrical and Computer Engineering

Graduate School of Engineering and Management

Air Force Institute of Technology

Air University

Air Education and Training Command

In Partial Fulfillment of the Requirements for the

Degree of Master of Science in Electrical Engineering

Murat Dogrul, BS

First Lieutenant, TuAF

March 2008

AFIT/GE/ENG/08-08

DESIGN AND OPTIMIZATION OF BROADBAND HIGH IMPEDANCE GROUND PLANES (HIGP) FOR SURFACE MOUNT ANTENNAS

Murat Dogrul, BS
First Lieutenant, TuAF

Approved:

/signed	27 Feb 2008
Dr. Peter J. Collins (Chairman)	date
/signed	27 Feb 2008
Dr. Andrew J. Terzuoli (Member)	date
/signed	27 Feb 2008
Maj. Michael A. Saville, Ph.D. (Member)	date

Acknowledgments

First of all, I would like to thank Turkish Air Force for providing the great opportunity to complete my Master's degree in AFIT.

I would like to express my sincere appreciation to my faculty advisor, Dr. Peter J. Collins, for his guidance and support throughout the course of this thesis effort. I would, also, like to thank Dr. Kubilay Sertel from The Ohio State University, my committee and faculty members Dr. A. Terzuoli, Maj. M. Saville and Dr. M. Havrilla for their insight and experience.

I would also like to thank my fellow classmate Lt. Bora Cakiroglu and his wife, for their support and very kind friendship.

Finally, I wish to thank my mother. It was her inspiration, guidance and teaching throughout my life that helped me to be successful in my education.

Murat DOGRUL

Table of Contents

Page

Page

Page

List of Figures

Page

Page

Page

Page

Page

Page

List of Tables

Page

Abstract

Gain and bandwidth metrics of broad-band low-profile antennas severely deteriorate when they are placed conformally onto the conductive skins of air, sea, and ground platforms. This detrimental effect is primarily due to out-of-phase reflections from the conductive body interfering with the antenna's self radiation. Furthermore, lateral waves launched by the antenna couple into the thin substrate placed between the antenna and the platform, giving rise to surface waves resulting in significant diffraction from the edges of the substrate.

To remedy these two major mechanisms degrading antenna performance, high impedance ground planes (HIGP) were designed. HIGPs made of a 2-dimensional periodic arrangement of a mushroom structure not only provide perfect-magnetic-conductor (PMC)-like reflection but also suppress the surface waves within the stop-band of the substrate modes.

This thesis presents new geometrical shape HIGP-antenna designs and optimizations. Dipole antenna, log periodic antenna and finally bow-tie antennas are used in the research. Operating frequency bands of these antennas over different types of optimized HIGP's are investigated. Multi-scale HIGP and antenna designs are introduced in the final part of the thesis. Broadband nature of the HIGP-antenna designs is increased by using multi-scale HIGP.

DESIGN AND OPTIMIZATION OF BROADBAND HIGH IMPEDANCE GROUND PLANES (HIGP) FOR SURFACE MOUNT ANTENNAS

I. Introduction

In recent years there has been an increase in the amount of studies and articles on new type of man-made materials, generally called “metamaterials”. Modern computational electromagnetics techniques and developments in the area of the electromagnetics and antenna simulation software along with improvements in modern manufacturing and testing have enabled the analysis design and construction of inhomogeneous structured materials. These inhomogeneities are generally on a sub-wavelength scale. The interaction of electromagnetic fields is then dictated by different material properties not available in the materials that are found in the nature on its own.

This ability to shape and change a natural material’s electromagnetic properties has opened many interesting and useful opportunities for the people who are working on antenna and electromagnetics. Recently, these kinds of materials have been used in many commercial and Air Force applications. As a commercial application, metamaterials are being used in the mobile technology to not only reduce the cell phone antenna size, but also to improve its radiation efficiency (Broas and others, 2001:1262-1265). In this area, broadband antennas that work on conducting surfaces are required for these kinds of

commercial and Air Force applications. Up to now, standard antenna designs have not had such features.

Designing an antenna has come to a point that most of the desired antennas can be created by using any antenna handbook. However many antenna designs suffer from fundamental material limitations. If a new, low profile thin antenna and ground plane system is desired, many problems can occur. Metals are generally used as the radiator element of the antenna systems. The conventional ground planes and reflectors are also made up of metal. These metal materials are approximated as having perfect conductivity and called as Perfect Electric Conductor (PEC). And dielectric materials are used to provide isolation between the antenna's radiating element and ground plane or reflector. But an ideal material for the reflector applications has not been developed yet. PEC ground planes and reflectors are designed practically for most applications, but they cause many major problems when combined with PEC antennas. The latest developments in electronic band gap materials (EBG) or photonic band gap materials (PBG) offer an opportunity to design alternative forms of structures that exhibit high impedance for microwave fields (Sievenpiper and others, 1999: 2059-2074), (Broas and others, 2001:1262-1265), (Yang and Rahmat-Samii, 2003: 2691-2703), (Broas and others, 2005:1377-1381), (Linton and others, 2006). These kinds of structures could replace conventional PEC ground planes and could result in a new design area by the way of suppressing the surface waves and reflecting the electromagnetic waves in phase.

This chapter introduces the background of the research, the problem to be investigated, the research question and the investigative questions, scope/methodology and the organization of the thesis.

Background

Engineered electromagnetic surface textures can be used to change the properties of the metal surfaces to perform a variety of desired functions. For example, specific textures can be designed to change the surface impedance for one or both polarizations, to manipulate the propagation of surface waves, or to control the reflection phase.
New boundary conditions for building electromagnetic structures, such as for varying the radiation patterns of small antennas are provided by these surfaces (Sievenpiper and others, 1999: 2059-2074).

These novel artificial materials, such as photonic crystals, electromagnetic band gap (EBG) structures, and double-negative (DNG) materials, have opened up many research areas in electromagnetics. These structures are called metamaterials and are typically generated by periodic dielectric substrates and metallization patterns. Metamaterials lead a wide range of applications in the electromagnetics area with their novel features (Yang and Rahmat-Samii, 2003: 2691-2703).

Periodic metamaterials can be classified into two groups: (1) three dimensional volumetric structures and (2) two-dimensional surface designs. This thesis research

focuses on the second area that gives the opportunity of low profile, light weight, and low fabrication cost designs.

In recent years, compact structures have been developed that can also alter the electromagnetic boundary condition of a metal surface but which are much less than one-quarter-wavelength thick. These textured structures are typically designed and manufactured as sub-wavelength mushroom type metal protrusions (Fig.1). They are generally analyzed as resonant LC circuits. The thickness of these structures is reduced by capacitive loading. These materials provide a high-impedance boundary condition for both polarizations and for all propagation directions (Sievenpiper and others, 1999: 2059-2074).

So far, electrical conductor materials have been widely used as unique material available for reflecting structures. Unfortunately, using electrical conductors for both the radiating element of the antenna and the reflector or ground plane causes some problems such as shorting out radiating element, and diffracting waves from edges and corners of the structure. In order to avoid these problems, an isolation between them is required to keep the PEC reflector from shorting out the radiating element. Electromagnetic waves incident on a PEC surface are reflected with a 180-degree phase shift. An antenna which is directly placed over a PEC surface does not radiate because the radiation of the antenna is cancelled by the out of phase waves reflected from the PEC ground plane. If it is desired that the antenna radiate efficiently, then the separation between the ground plane

and the radiating element must be increased. Increasing the separation provides a solution by changing the phase of the reflected wave closer to in-phase. But this approach brings about dimension problems for designs. Not only overall dimensions are increased, but also this approach limits the frequency bandwidth of the antenna system (Sievenpiper and others, 1999: 2059-2074).

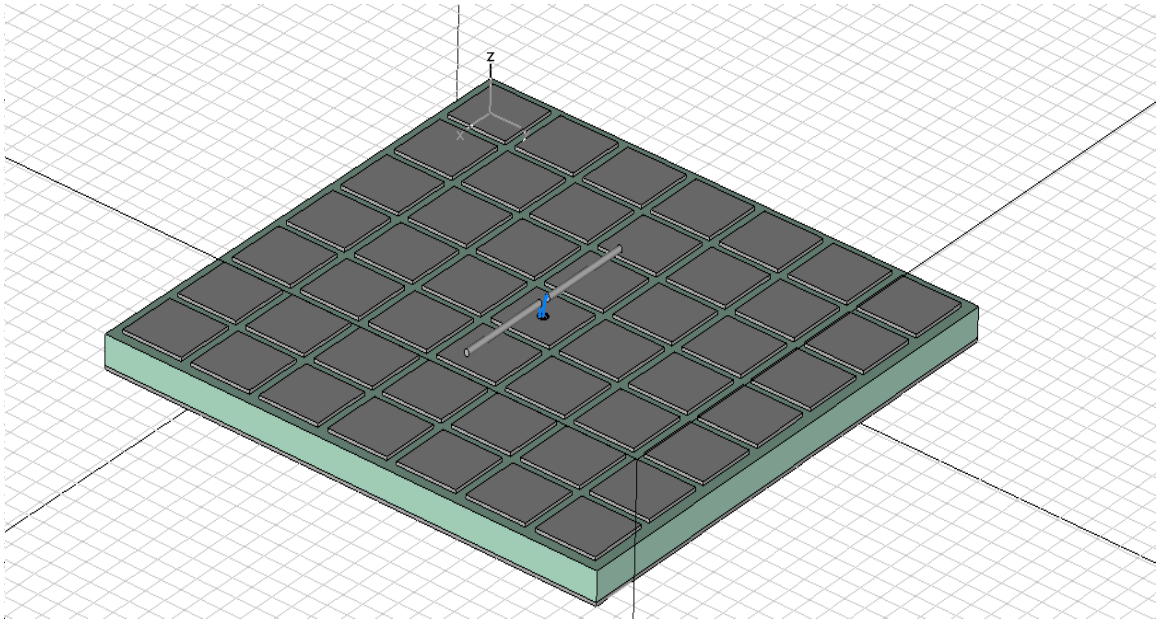

Figure 1. A mushroom type High-Impedance Ground Plane (HIGP) and dipole antenna design. (All the rectangular metal patches are connected to the bottom PEC plate by conductor vias.)

Another disadvantage of using a PEC as a ground plane is supporting the surface waves by a PEC surface. It is one of the most important problems while designing an antenna-ground plane system. Because all ground planes have finite sizes, when surface waves propagate until they reach an edge or a corner, they diffract. Diffracted waves interfere with the original antenna radiation and affect the overall antenna radiation pattern (Fig.5).

This interference can be reduced only by increasing the length of the dimensions of the ground plane or changing the properties of the surface material (Golla, 2001: 2-5).

Problem To Be Investigated

For the present needs of the Air Force, broadband high-impedance ground planes and surface mount antenna system designs are required to fill the gap in this area. There are many applications and studies in this area that are indicated in the following chapter, but the common characteristic of these previous designs is operating the designed and manufactured antennas in certain frequency bands, so the research question of this thesis is:

"Is it possible to design and optimize the parameters (patch geometry, patch width, gap width, substrate thickness and substrate material of a high-impedance ground plane and surface mounted antenna system that operates over a wide frequency band?"

Recent researches show that designing high impedance ground planes and antennas which operate in certain frequencies is possible (Sievenpiper and others, 1999: 2059-2074), (Yang and Rahmat-Samii, 2003: 2691-2703). Changing the geometry of the ground plane or the dimensions of the ground plane allows manipulation of the operating frequencies and bandwidths. Changing the substrate material (dielectric material) and the thickness of this material also gives us the opportunity to design and construct an unlimited number of structures (Linton and others, 2006).

To find satisfactory results to the research questions, the following methodology and investigative questions are indicated.

Scope/ Methodology

This thesis research is a computer based design and optimization of the antenna and ground plane system. It is complementary with the construction and testing part of the same design which is the subject of another thesis (Cakiroglu, 2008). In the design and optimization process, HFSS (High Frequency Structure Simulation) electromagnetic and antenna simulation software is used. HFSS software has been selected because it is one of the most commonly used programs to draw and simulate the fields of all kinds of 3-dimensional geometrical shape antennas and electromagnetic structures on computer. All the designs and simulations are done in an iterative fashion with concurrent thesis research on construction and testing of the designs.

The first step of the design process is to design and simulate the ground plane-antenna system which was presented in a previously related article (Yang and Rahmat-Samii, 2003: 2691-2703). It is necessary to confirm the results, because most of the simulations and designs were executed using Finite Difference Time Domain (FDTD) Method as the computational electromagnetics method where HFFS Simulation uses Finite Element (FE) Method. When using the different computational electromagnetics methods the results of the same designs in HFSS and the previous one should be consistent with each other. It confirms that the software is being used properly. It shows that all the excitations, boundaries and solution types are being assigned correctly.

The next step of the process is to design new HIGP surfaces. After designing the new surfaces, the following step is going to be designing the antennas. The next step is the optimization process of the HIGP. Combination of the antenna and ground plane system will be the next step. All of the process is executed in the frequency region of 0-20 GHz, which is also a constraint for the construction and testing part because of the limitations of the microwave lab equipment.

In this thesis research the following investigative questions are observed:

1. *Is it possible to design a surface that does not allow surface waves to propagate over this surface within a wide frequency band?*

Previously accomplished studies indicate such potential. The ways to improve the bandwidth will be investigated by changing the parameter values and geometries.

2. *Which geometrical shapes of patches are used in the HIGP design and which of them are more efficient than the others?*

Most of the basic geometrical shapes (square, triangle, hexagon and circle) are used in the design of the patches. Performed simulation results give the best solution in the choice.

3. *How do the dimensions (patch width, gap width, substrate thickness, radius of the vias) of the HIGP structure affect the bandgap (operating frequency) and bandwidth of the system?*

Every dimensional change of the structure affects the bandgap frequency and bandwidth of the operating system. Some of them increase the bandgap frequency while decreasing the bandwidth. Simulations show the best acceptable results in the choise of the dimensions.

4. Is it reasonable to use this HIGP and antenna system on aircraft and UAVs?

There are many antennas over the surface of an aircraft which work in different certain frequencies. If the ground plane designs include these frequencies (if the band gap of the structure includes these certain frequencies) then it is going to be possible to combine them into unique low profile antennas which can be mounted on an aircraft or UAV. The feasibility of this part will be remained as a future research.

Organization

This thesis is organized as previous researches, concepts, new designs and optimizations. Chapter two provides the literature review part of the thesis and gives a background on what was done so far in this research area. Chapter three is the validation part of the HFSS software that is used in this thesis with the previously published results. Chapter four and five explore the simulation of different types of new HIGP and surface mount antenna designs. The results show the development concepts and how they were applied to design a wide band HIGP solution. The conclusions present the major important points and results and provide a way for future work.

II. Literature Review

Overview

The purpose of this chapter is to review the relevant published sources and to explore the previously accomplished studies. In this chapter, metamaterials, photonic bandgap structures, previous high impedance ground plane designs, high impedance surface lumped-element approximation and antenna applications over some HIGP designs are described and presented.

Description and Relevant Research

Metamaterials

"Metamaterials are new artificial materials with unusual electromagnetic properties that are not found in naturally occurring materials. All natural materials, such as glass and diamonds have positive electrical permittivity, magnetic permeability, and an index of refraction. In these new artificially fabricated materials, all of these material parameters are negative. With these unusual material parameters, new kinds of miniaturized antennas and microwave devices can be created for the wireless communications and the defense industries." (Kshetrimayum, 2004:44)

Photonic Bandgap (PBG) Structures

A photonic bandgap (PBG) is defined as a band of frequencies in which electromagnetic waves do not propagate. A material with a complete photonic bandgap is characterized as

a three-dimensional metamaterial structure that does not allow electromagnetic wave propagation in any direction within certain frequency stop-bands.

Yablonovitch first explored taking photonic band gap technology out of the optical spectrum into the microwave spectrum in 1987. Multi-layer optical coatings are based on periodic boundaries between materials of alternating high and low indexes of refraction spaced at quarter-wavelength intervals. The quarter-wave stack exhibits very high reflectance for light within a limited frequency band dictated by the thickness of the layers and the materials used. But the greatest limitation of the quarter-wave stack is that the light must enter the structure at normal incidence (Golla, 2001:6-7). Yablonovitch sought a periodic three dimensional optical crystal structure that could prohibit electromagnetic wave propagation for all angles of incidence. The research in this area developed rapidly after that (Yablonovitch, 1987:2059-2062).

Mushroom type structures as high-impedance ground plane PBG materials were first developed by Sievenpiper in 1999. He created a two dimensional surface which had characteristics of suppressing surface waves and the image currents being in phase with the incident wave. He developed the mathematical description of the impedance of the mushroom type periodic structure. He then explored the frequency bandgap and reflection characteristics of the high-impedance ground plane (Sievenpiper and others, 1999: 2059-2074).

In the following years Broas et al. developed HIGP designs in the area of cell phone technology (Broas and others, 2001: 1262-1265). They designed and experimentally characterized such a high-impedance surface designed to operate at a certain frequency.

They described an antenna built on such a surface, integrated into a printed circuit board that was designed for the form factor of a portable handset. They showed high radiation occurred near that certain frequency. They also studied phased array antennas in the same area (Broas and others, 2005: 1377-1381). The high-impedance surface was used as the antenna ground plane between two radiator elements to reduce the inter-element coupling between them. Their measurement revealed the optimum performance occurred at the bandgap due to the suppression of surface currents in the ground plane.

In 2003 Yang and Rahmat-Samii studied the reflection phase characterization of the HIGP for low profile wire antenna applications. They created a HIGP design that is made up of square patches. They examined some of the radiation properties of the low profile dipole antenna mounted over this surface (Yang and Rahmat-Samii, 2003: 2691-2703).

One of the recent studies in this novel subject is currently being developed in The Quenn's University, Belfast, UK, where a continuously conformable antenna element for advanced wearable communications is being developed. Their study contains the design of a body-worn HIGP and an antenna system for communications under hostile channel conditions. They are searching an optimum square patch HIGP design by changing the parameters. They are looking for the bandwidth and band gap differences according to the changes in the parameter values. The objective of their research is to create technologies that can be used to communicate across the body, communicate to sensors embedded within the body, communicate to other combatants in the battle field, and communicate to airborne platforms (Linton and Scanlon, 2006).

High-Impedance Ground Planes (HIGPs)

High-Impedance Ground Plane (HIGP) is a metallic structure developed by Sievenpiper (Fig.2), which has the following interesting characteristics over a particular frequency band known as the electronic band-gap (EBG):

- It reflects waves in-phase
- It does not allow surface waves to propagate

These characteristics are novel, as a normal metal surface reflects waves with a 180° phase shift and permits the propagation of surface waves. Research using high impedance surfaces as ground planes for low-profile antennas has demonstrated the advantages of such surfaces (Sievenpiper and others: 1999). This mushroom type HIGP structure was made up of a flat thin metal layer, periodic hexagonal metal patches, a dielectric substrate between them, and conducting vias which connects patches to the metal layer.

A low-profile antenna such as a patch over a ground plane has some design limitations due to the metal ground plane. First, if the patch is brought too close to the ground plane, the image current induced in the metal ground cancels the current in the radiating element. Because the waves are reflected 180 degrees out of phase. The distance between radiating element and ground plane should be at least a quarter of a wavelength to avoid that. This distance limits the reduction in height of the antenna that can be achieved. Also it creates a resonant condition that limits bandwidth. Secondly, when the surface waves propagating along the ground plane reach the edge of the metal, they will radiate from the metal causing interference with the intended radiated wave. These two problem areas can

be addressed by replacing the metal ground plane with a high-impedance surface. (Sievenpiper and others, 1999: 2059)

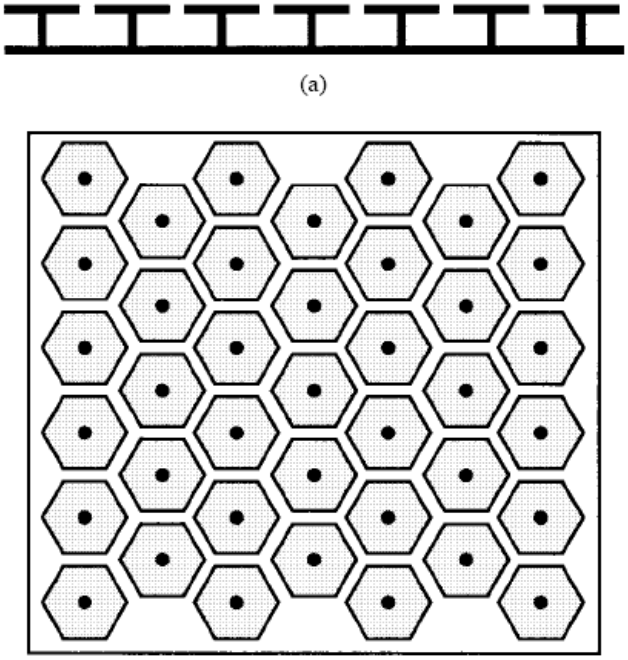

Figure 2. (a) Cross section of a high-impedance surface. (b) Top view of a high-impedance surface. (Sievenpiper and others, 1999: 2059)

"In the frequency range where the surface impedance is very high, the tangential magnetic field is small, even with a large electric field along the surface. Such a structure is sometimes described as a "magnetic conductor." Due to this unusual boundary condition, the high-impedance surface can function as a unique new type of ground plane for low-profile antennas. The image currents are in-phase, rather than out-of-phase, allowing radiating elements to lie directly adjacent to the surface, while still radiating efficiently. For example, a dipole lying flat against a high-impedance ground plane is not

shorted out as it would be on an ordinary metal sheet. Furthermore, in a forbidden frequency band, the high impedance ground plane does not support propagating surface waves, thus, the radiation pattern is typically smooth, and free from the effects of multipath interference along the ground plane." (Sievenpiper and others, 1999: 2060)

High-Impedance Surface Lumped-Element Approximation

When the dimensions of the lattice are small compared to the wavelength of the illuminating energy, the surface can be modeled as a parallel LC circuit (Fig. 3-4).

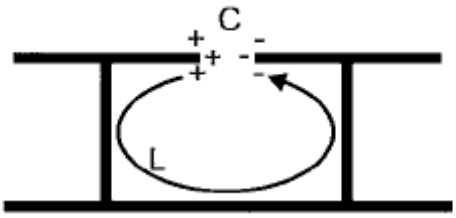

Figure 3. Origin of the capacitance and inductance in the high-impedance surface (Sievenpiper and others, 1999:2062).

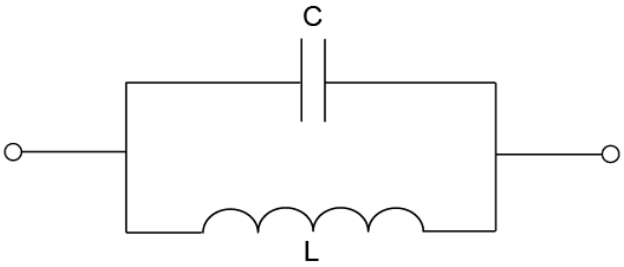

Figure 4. Lumped-Element Equivalent Circuit of HIGP (Sievenpiper and others, 1999:2060).

The mathematical derivation of the structure (Sievenpiper and others, 1999) begins with the surface impedance,

$$Z_s = \frac{E_z}{H_y} = \frac{1+j}{\sigma\delta} \tag{1}$$

Where E_z and H_y are tangential electric and magnetic field components to the surface, σ is the conductivity of the metal, and δ is the skin depth of the metal. For transverse magnetic (TM) fields surface impedance becomes,

$$Z_s = \frac{j\alpha}{\omega\varepsilon} \tag{2}$$

and for transverse electric (TE) fields surface impedance becomes,

$$Z_s = \frac{-j\omega\mu}{\alpha} \tag{3}$$

$$\alpha \approx \frac{\omega}{c}\sqrt{\frac{\omega\varepsilon}{2\sigma}}(1-j) \tag{4}$$

where ω is the frequency in rad/sec, ε is the permittivity constant of the dielectric substrate, c is the free space speed of light in m/sec, and σ is the conductivity of the metal layer. An inductive surface with a positive reactance can only support TM waves, while a capacitive surface with a negative reactance can only support TE waves (Sievenpiper and others, 1999: 2063). Below resonance, TM surface waves are supported, and above resonant frequency TE waves are supported.

The inductance arises from the current flowing between patches through the vias and the capacitance arises from the proximity of adjacent patches. At resonance, the impedance of a parallel LC circuit is

$$Z = \frac{j\omega L}{1 - \omega^2 LC} \tag{5}$$

Where L is the inductance, C is the capacitance, and ω is the frequency in rad/sec. And the resonant frequency is determined by

$$\omega = \frac{1}{\sqrt{LC}} \tag{6}$$

"At the resonant frequency, the impedance of the surface becomes very high. Over the bandwidth of the surface, centered at the resonant frequency, both TE and TM surface waves are suppressed. At frequencies below the lower band-edge the surface impedance is inductive and TM surface waves can propagate, and at frequencies higher than the upper band-edge the surface impedance is capacitive and TE surface waves can propagate. The bandwidth of the HIGP is the frequency range over which the reflected wave is in-phase with the incident wave. This occurs when the phase of the reflected wave is approximately between 90° and –90°. The bandwidth is also the frequency range over which surface currents are suppressed" (Linton and others, 2006: 35). It is defined as

$$BW = \frac{1}{\eta_0}\sqrt{\frac{L}{C}} \tag{7}$$

where η_0 is the impedance of the incident wave (usually the impedance of free-space). Approximate values of the capacitance and inductance for the HIGP structure shown in Fig. 3. and Fig 4. are

$$C = \frac{w\varepsilon_0(1+\varepsilon_r)}{\pi}\cosh^{-1}\left(\frac{2w+g}{g}\right) \tag{8}$$

$$L = \mu_0 h \tag{9}$$

where w is the patchwidth, g is the gapwidth, h is the substrate thickness and ε_r is the substrate permittivity.

Antenna Characteristics Over HIGP

"Using high-impedance ground planes, antennas have been demonstrated that take advantage of both the suppression of surface waves and the unusual reflection phase. An antenna on a high-impedance ground plane produces a smoother radiation profile than a similar antenna on a conventional metal ground plane, with less power wasted in the backward direction." (Sievenpiper and others, 1999: 2068) (Fig. 5). Because HIGP reflects the waves in phase and does not permit the surface waves to propagate. So that, diffracted waves do no occur. "Furthermore, radiating elements can lie directly adjacent to the high-impedance surface without being shorted out. These antennas can take on a variety of forms, including straight wires to produce linear polarization, or various other shapes to generate circular polarization. Patch antennas are also improved if they are

embedded in a high impedance surface." (Sievenpiper and others, 1999: 2068)

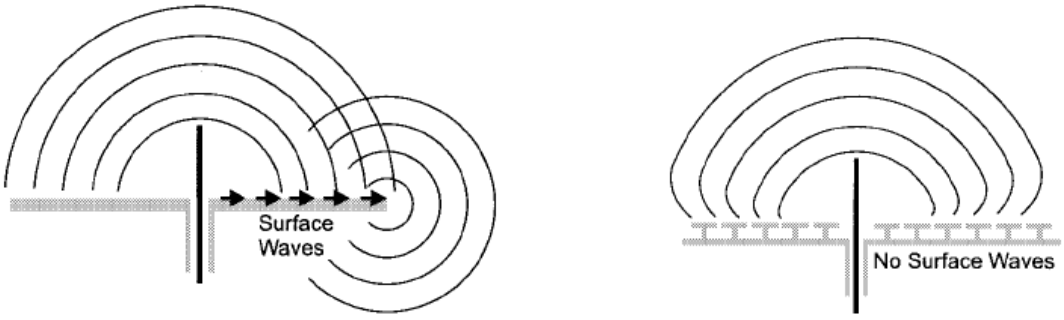

(a) (b)

Figure 5. (a) Antenna on a flat metal ground plane generates propagating surface currents, which cause multipath interference and backward radiation. (b) Surface waves suppressed on a high-impedance ground plane (Sievenpiper and others, 1999:2068).

Sivenpiper also showed that surface waves could be suppressed by embedding the patch in a high impedance ground plane. He measured the return loss of two patch antennas over ordinary metal and HIGP. Less return loss occurred when the antenna is embedded into the HIGP. Also radiated waves in the backward direction significantly reduced in comparison with the ordinary metal.

In addition array antenna coupling characteristics were investigated by Broas et al. They designed two element cell phone antenna array over HIGP. They found that in the band gap of the HIGP, coupling between the array elements was minimized. Because there was a suppression of surface waves in the band gap of the HIGP (Broas and others, 2005: 1377-1381).

Frequency Band Selection For Low Profile Antenna Designs (Comparison of The PEC, PMC, and HIGP)

In Yang and Rahmat-Samii's study, a dipole antenna was horizontally positioned over a ground plane. The PEC, PMC, and EBG (electronic band gap or HIGP) surfaces are each used as the ground plane to compare their capabilities for low profile antenna designs (Fig. 6).

(a) (b)

Figure 6. Dipole antenna over (a) the PEC or PMC ground plane or (b) the EBG ground plane. (Yang and Rahmat-Samii, 2003).

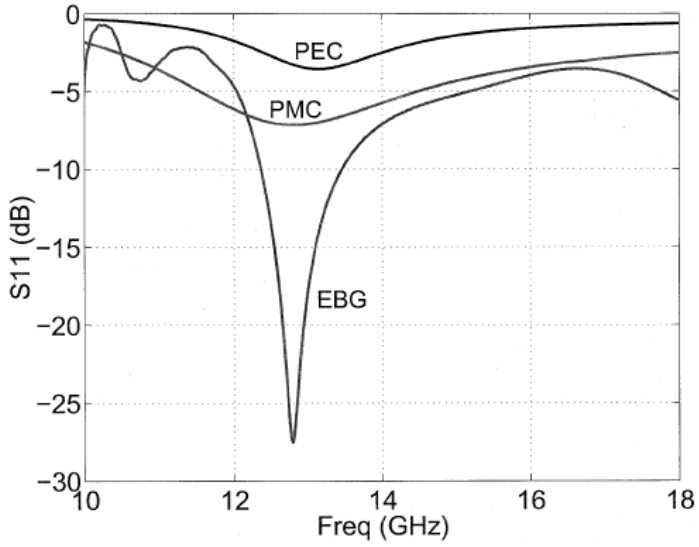

Figure 7. Simulated return loss results of the dipole antenna over PEC, PMC and HIGP. The dipole length is 0.40 $\lambda_{12\ GHz}$ and the overall antenna height is 0.06 $\lambda_{12\ GHz}$ (Yang and Rahmat-Samii, 2003).

The best (minimum) return loss is achieved by the dipole antenna over the EBG ground plane (Fig. 7). The reflection phase of the EBG surface varies with frequency from -180^{o} to 180^{o}. In a certain frequency band, the EBG surface successfully serves as the ground plane of a low profile dipole, so that the dipole antenna can radiate efficiently. From this comparison it can be seen that the EBG surface is a good ground plane candidate for a low profile wire antenna design.

Summary

Sub-wavelength textures can be applied to metal surfaces to change their electromagnetic properties. Thin coatings containing mushroom type grounded metal plates can behave as a high impedance surface and can be analyzed using a simple lumped-circuit parameter model. These surfaces have two important features: (1) they suppress the surface waves within a band gap and (2) they provide a reflection phase of zero at the resonance frequency. Return loss results in the previous researches discussed above show that antennas over or embedded in HIGP provide less return loss than antennas over the metal ground planes because of the surface wave suppression band gap of the HIGP.

Next chapter discusses the methodology and the usage of the HFSS(High Fequency Structure Simulation) software that is used to design and optimize the new HIGP and antenna designs in the following parts of the thesis.

III. Methodology

Chapter Overview

The purpose of this chapter is to provide the information of the methodology that was used to design and optimize the HIGP and HIGP-antenna combinations.

This chapter first outlines the general usage of the software that is used in the majority part of the thesis "High Frequency Structure Simulation (HFSS)", and secondly gives the information about the computational electromagnetics method (Finite Element (FE) Method) that is used in this software. Next, the comparison of a previously studied design which was designed by using Finite Difference Time Domain (FDTD) Method with FE method is presented. After that, the HIGP and HIGP-antenna designs are explained starting with the basic geometry and continuing with more complex geometries in the following chapter.

High Frequency Structure Simulation (HFSS)

In order to design and optimize three dimensional antenna-ground plane and electromagnetic applications, it was required to determine the software tool before starting the designs. The High Frequency Structure Simulation (HFSS) software is one of the most commonly used and capable software in this area. Structures which are made up of multiple types and shapes of materials (such as the structures generated in this thesis) can be designed and simulated with HFSS accurately. All the 3-dimensional electromagnetic and antenna simulations can be created and simulated in this software. Desired solution results can be plotted in 2D or 3D graphs.

General view of the HFSS window is presented in Fig. 8. The software includes post-processing commands for analyzing this behavior in detail. For example the following properties:

• basic electromagnetic field quantities and, for open boundary problems, radiated near and far fields,

• characteristic port impedances and propagation constants,

• generalized S-parameters and S-parameters renormalized to specific port impedances,

• the eigenmodes, or resonances of a structure,

can be calculated and animated (HFSS v.10 User Manual).

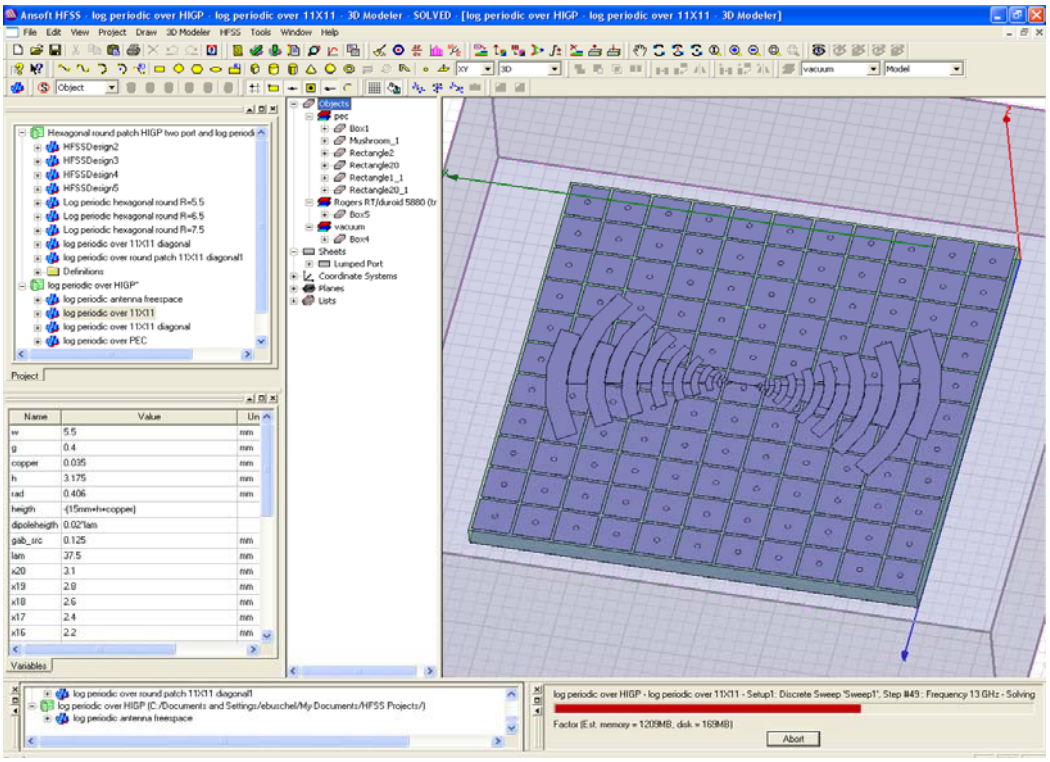

Figure 8. General view of HFSS window

The user is required to draw the structure, specify material characteristics for each object, and identify ports and special surface characteristics. HFSS then generates the necessary field solutions and associated port characteristics and S-parameters.

Creating Design steps:

1. Parametric model generation: create the geometry, boundaries and excitations,
2. Analysis setup: define solution setup and frequency sweeps,
3. Results: create 2D and 3D reports and field plots,
4. Solve loop: full automate the solution process.

To understand how these processes co-exist, Figure 9 illustrates the relationships.

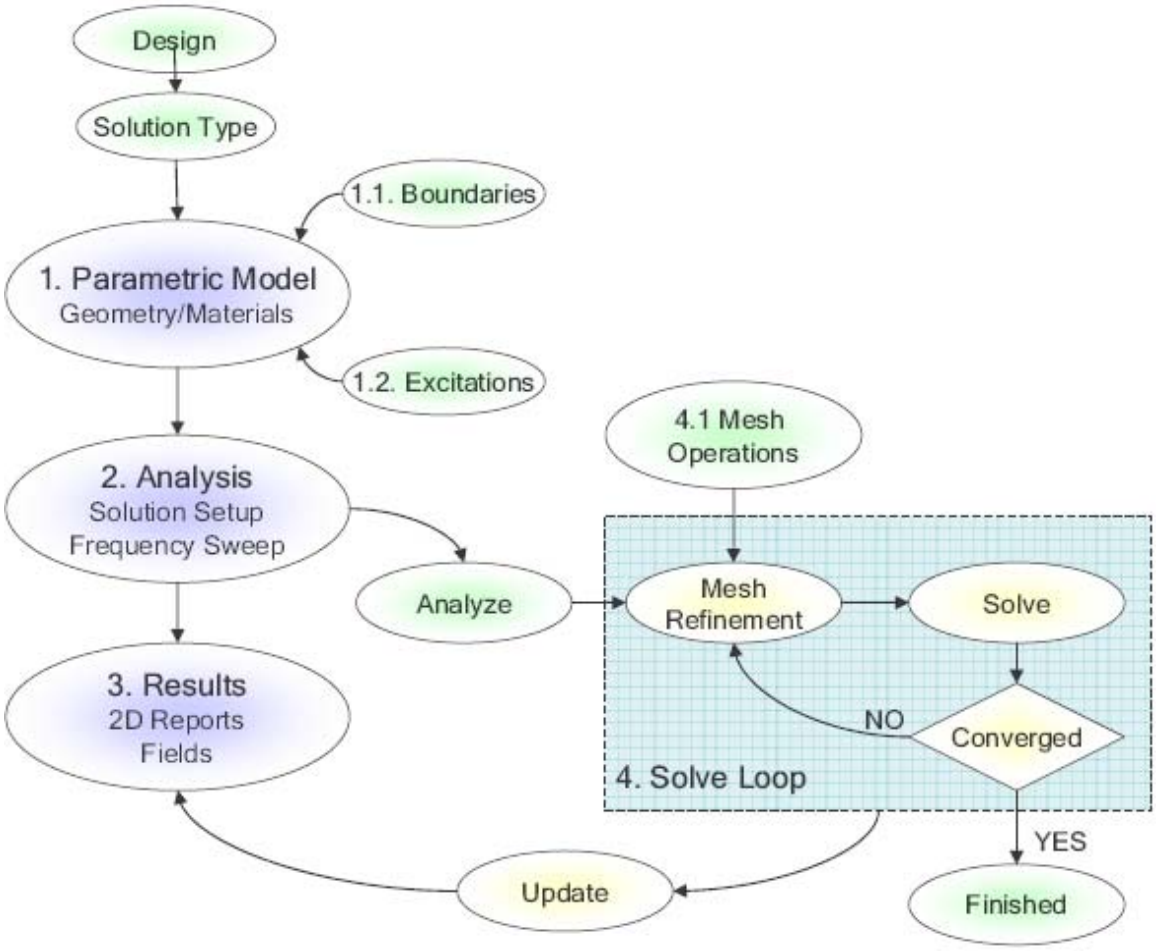

Figure 9. Solution Process of HFSS (HFSS v.10 User Manual)

Finite Element (FE) Method

The simulation technique used to calculate the full 3D electromagnetic field inside a structure is based on the Finite Element Method. Although its implementation is largely transparent, a general understanding of the method is useful in making the most effective use of HFSS.

"In order to generate an electromagnetic field solution, HFSS employs the finite element method. In general, the finite element method divides the full problem space into thousands of smaller regions and represents the field in each sub-region (element) with a local function. In HFSS, the geometric model is automatically divided into a large number of tetrahedra, where a single tetrahedron is a four-sided pyramid. This collection of tetrahedra is referred to as the finite element mesh." (HFSS v.10 User Manual)

Solution Type

There are three types of solutions in HFSS: Driven Modal Solution, Driven Terminal Solution and Eigenmode Solution. In this research, Driven Modal Solution was used as the solution type.

Driven Modal Solution: This solution type is used to calculate the S-parameters of high-frequency structures such as microstrips, waveguides, and transmission lines, which are driven by a source.

Creating Geometry and Assigning Materials

In order to generate the designs, the first step is to create the geometrical shape of the structure. Any three dimensional structure (cylinder, box, polyhedron, cone, sphere or torus) can be drawn in HFSS. Any type of materials that are used in the construction phase of the research in the lab can be assigned to this structure. Multiple types of shapes and materials are combined to form the HIGP structure (Fig. 10). For example in HIGP designs, the bottom level of the ground plane, the two components of mushroom structure (patch, and via that is in the middle of this patch) are assigned as Perfect Electric

Conductors (PEC). Copper is used as PEC in the construction phase of this research. Since the electromagnetic characteristics of the copper are very close to PEC, PEC material is assigned instead of copper in order to run the simulations faster. A dielectric substrate is assigned between the metal patch and bottom metal plate. The substrate materials that are used:

Table 1. Substrate Materials

Material	Relative Permittivity
Rogers RT/ duroid 5870	2.33
Rogers RT/ duroid 5880	2.2
Rogers RT/ duroid 6002	2.94
Rogers RT/ duroid 6010	10.2

Duroid 5880 is mostly used, since it has the lowest relative permittivity of all. It is desirable for the substrate material permittivity be as close as free space permittivity. Because the simulation results in the following chapter shows that widest surface wave suppression band gap occurs if the lowest permittivity material is used.

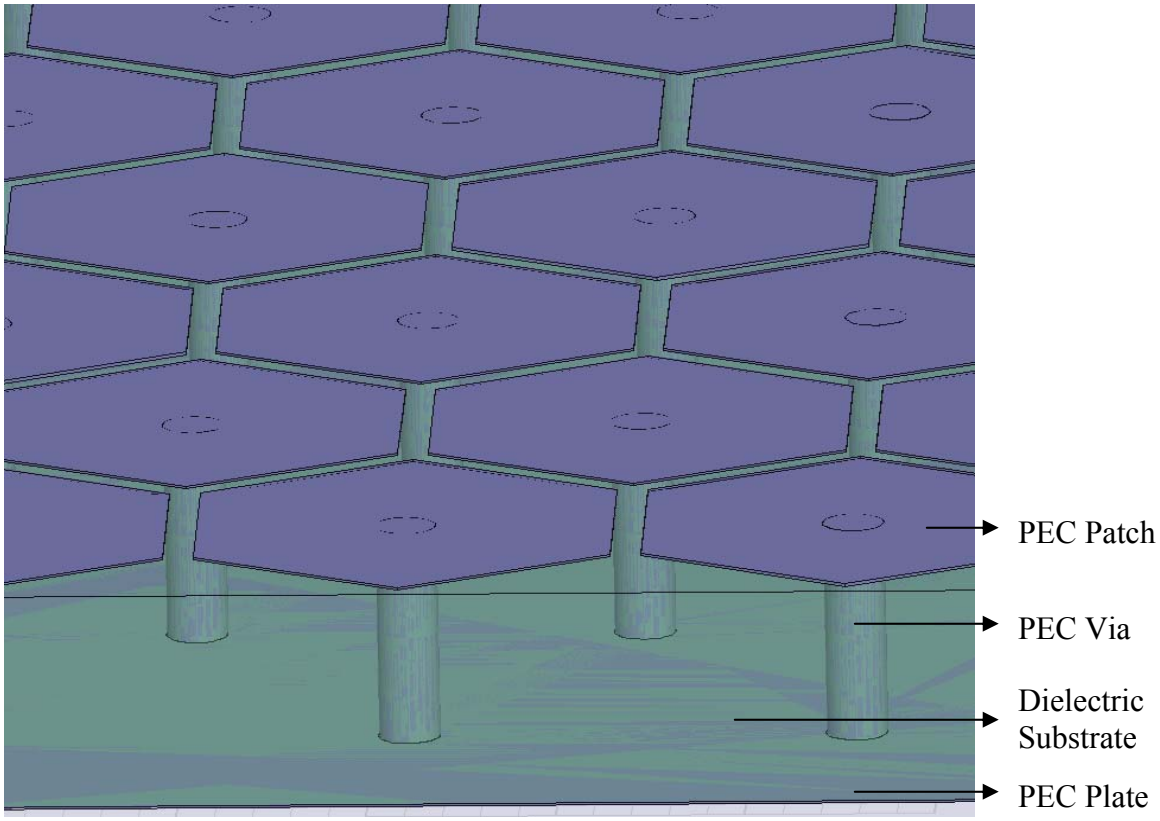

Figure 10. General Structural Shape and Material Assignments

Creating Excitations

In order to run a simulation in driven modal solution type, a source excitation must be defined. Excitation types in the HFSS are: Wave port, lumped port, incident plane wave, voltage excitation, current excitation and magnetic bias. In this research, wave port and lumped port excitations are generally used.

In the design of the HIGPs, to find the structure's electromagnetic surface wave suppression bandwidth by way of S_{21} parameters, two patch elements on two opposite edges or corners are fed by coaxial cables. Coaxial cables are made up of outer conductor cylinder, inner conductor cylinder and a dielectric between these conductors. Excitation for the coaxial cable is defined as wave port on the bottom surface of the conductor

cylinders. And integration line is defined from outer conductor wall to inner conductor wall.

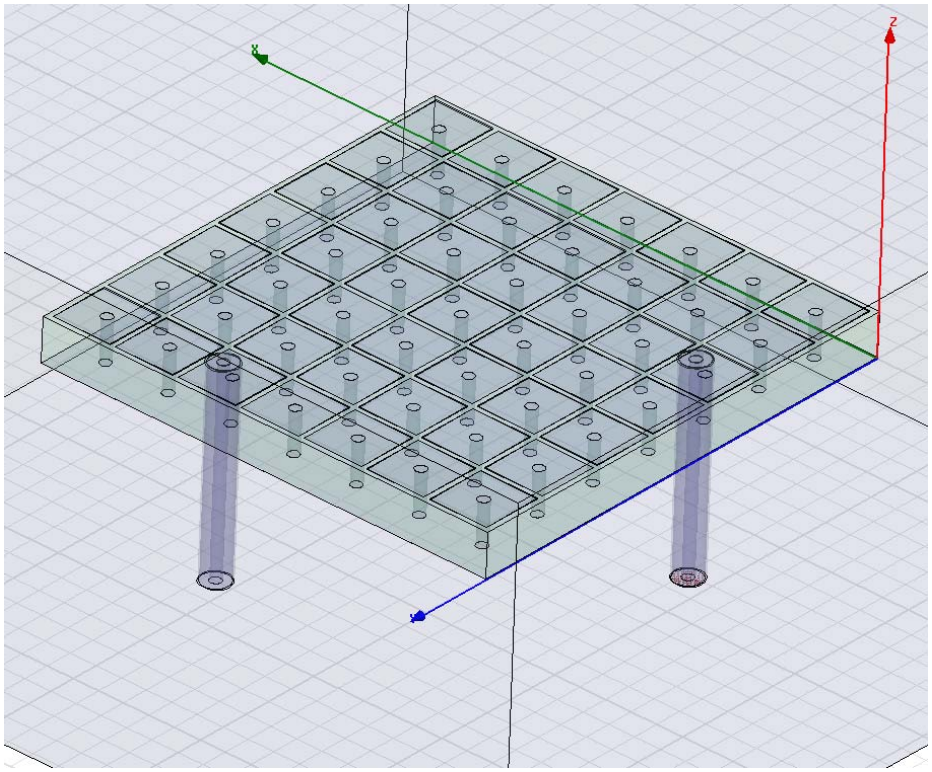

Figure 11. An Application of HIGP fed by two coaxial cables ports

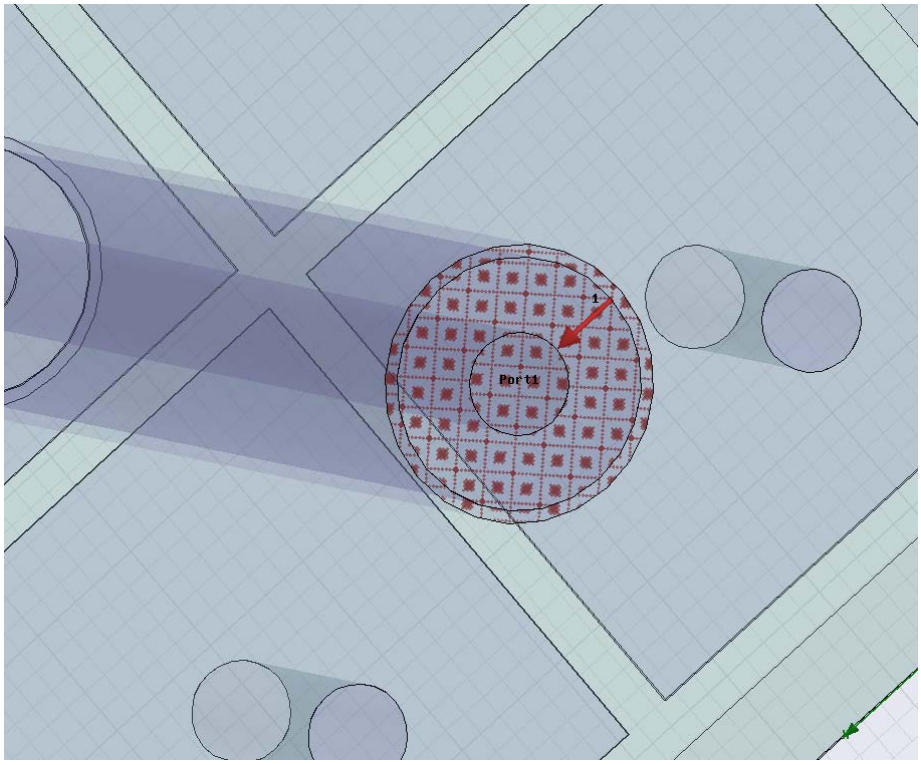

Figure 12. Wave port excitation on a coaxial cable

Another excitation type which is used in two arm antenna simulations, such as dipole antenna, is lumped port. Lumped ports are similar to traditional wave ports, but can be located internally and have a complex user-defined impedance. Lumped ports compute S-parameters directly at the port. First, a 2D rectangle is placed connecting the inner edges of the arms, then an integration line is defined on this rectangle (Fig. 13).

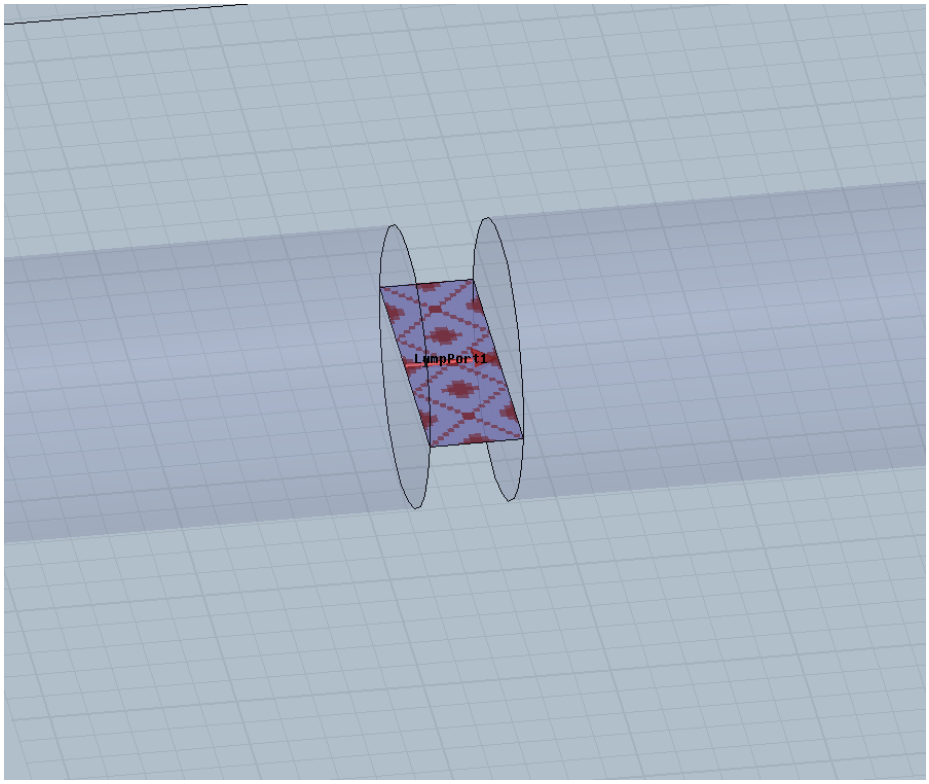

Figure 13. Lumped port excitation on a dipole antenna

Boundary Conditions

The last step of finishing the drawing phase is to define a box which has radiation boundaries on all faces of the box. The whole structure is put inside this box. A radiation boundary is used to simulate an open problem that allows waves to radiate infinitely far into space, such as antenna designs. HFSS absorbs the wave at the radiation boundary, essentially ballooning the boundary infinitely far away from the structure. A radiation surface does not have to be spherical, but it must be exposed to the background, convex with regard to the radiation source, and located at least a quarter wavelength from the radiating source (Fig. 14).

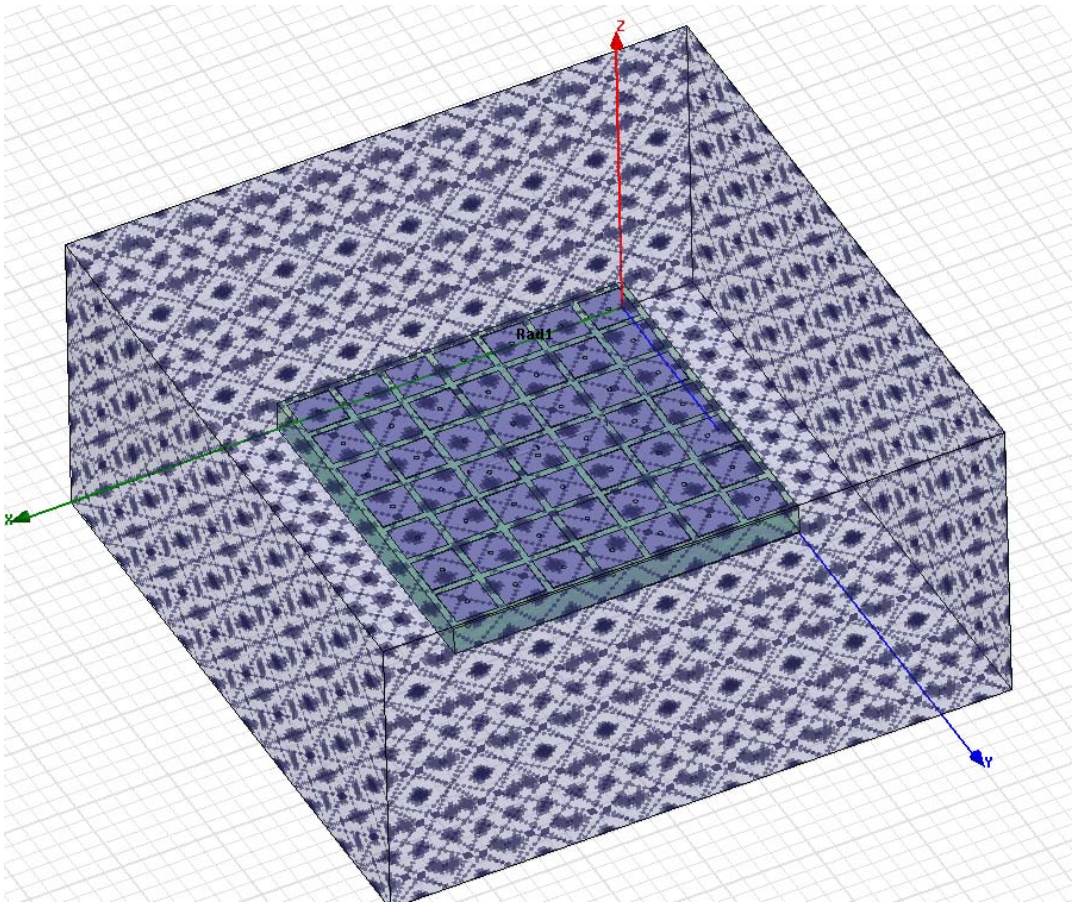

Figure 14. Radiation Boundaries

All the PEC boundary conditions are assigned as PEC materials itself, so no further process is needed. While simulating PMC boundaries, the surface that is desired to be PMC is assigned as “perfect H” surface (Fig. 15).

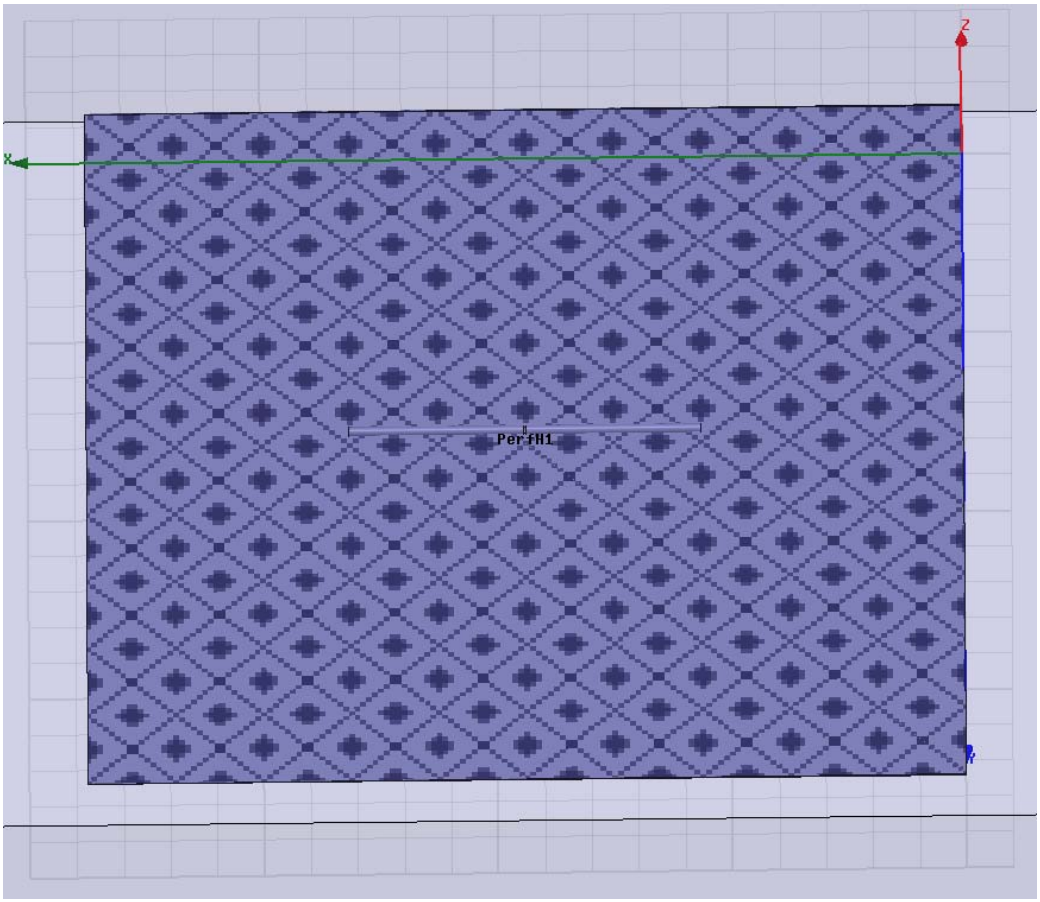

Figure 15. PMC surface boundary (A dipole antenna over it)

Solution Setup, Analyzing and Creating Reports

After drawing the 3D structure, assigning excitations and boundary conditions, the last step before running the simulation is entering the solution setup information. Solution frequency is entered as center frequency of the expected results along with the operating bandwidth. Maximum number of passes are entered generally as 20, maximum delta S is entered as 0.01-0.2 (related to the complexity of the structure, if it is a relatively more complex geometry then smaller delta S is chosen in order not to excess the memory and run time) (Fig.16). For example, increasing the number of the patch elements makes the

structure more complex. So it takes more time and memory to complete the simulation run.

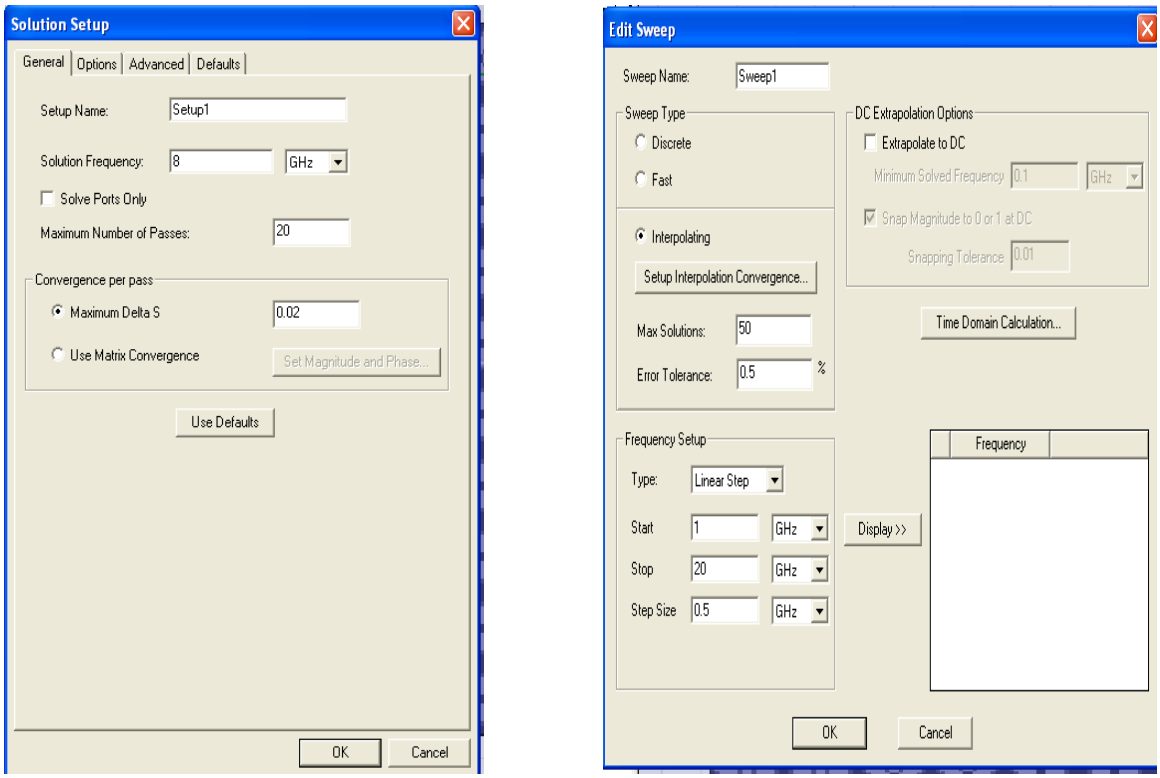

Figure 16. Solution and Sweep Setup

After solution setup, sweep setup is entered. In sweep setup, frequency sweep is entered beginning from 1 to 20 GHz in all designs. Generally discreet or interpolating sweep is chosen. An interpolating sweep estimates a solution for an entire frequency range. HFSS chooses the frequency points at which to solve the field solution so that the entire interpolated solution lies within a specified error tolerance. The sweep is complete when the solution meets the error tolerance criterion or generates the maximum number of solutions. An interpolating sweep's time requirement is much less than a discrete sweep's

because a solution for the entire frequency range is interpolated based on solutions for a minimal number of frequency points. Sweep interval is entered as 500 MHz or 250 MHz again related to the complexity of the structure. Other values are left as default. Validation is executed to check the errors before each run. Validation gives the errors of the drawing such as intersections, errors of the defined boundaries and excitations. Encountering these kinds of errors before running the simulation saves time that would be lost in the run time. It gives opportunity to correct the errors before running the simulation.

When the simulation run is completed, 2D and 3D reports are created from the results menu. In this research S_{11} and S_{21} 2D results are generally used to analyze the characteristics of the HIGP and antenna designs. S_{11} parameter is used to see the return loss of the antenna, and S_{21} parameter is used to define the surface wave suppression bandwidth of the HIGP.

Confirmation Of The HFSS Software With The Previous Research

For an HIGP structure various frequency band definitions have been defined. A frequency band gap was defined in (Sievenpiper and others, 1999: 2059-2074) using the dispersion diagram. However in (Yang and Rahmat-Samii, 2003: 2691-2703), they noted that this definition only refered to the surface waves that propagate in the horizontal plane. In low-profile wire antenna applications, such a band gap definition is not applicable because complicated interactions occur between the antenna and the HIGP surface, and electromagnetic waves are not restricted to propagate in the horizontal plane.

To ensure that resulting designs will meet the criteria for low-profile antenna applications, an operational frequency band of an HIGP surface is defined as the frequency region inside which a low profile wire antenna radiates efficiently with a good return loss and acceptable radiation patterns.

In this research HIGPs are designed and then two opposite elements are fed by coaxial cables. S_{21} results are used to find the suppression bandwidth (also operating band) of the HIGP designs. And antenna-HIGP designs are tested in the simulation by using the S_{11} parameter, which is the return loss of the antenna.

To confirm the simulation software and setup are working properly, previous research is taken as starting point (Yang and Rahmat-Samii, 2003: 2691-2703).

In their research a dipole antenna was simulated horizontally over an HIGP, a PEC and a PMC (Fig 6), and the results are compared by evaluating S_{11} (return loss) parameters of each. They used the Finite Difference Time Domain (FDTD) Method simulation and in this research HFSS software uses the Finite Element (FE) Method. Since the computation methods are different, a confirmation of the results is required for consistency before exploring new designs.

The dipole length is $0.40\,\lambda_{12\,GHz}$ and its radius is $0.005\ \lambda_{12\,GHz}$, while $\lambda_{12\,GHz}$ is the free space wavelength at 12 GHz. A finite ground plane with $1\,\lambda_{12\,GHz}$ x $\lambda_{12\,GHz}$ size is used in the analysis. And the EBG structure has the following parameters:

$$W = 0.12\,\lambda_{12\,GHz}$$

$$g = 0.02\,\lambda_{12\,GHz}$$

$$h = 0.04\,\lambda_{12\,GHz} \qquad (10)$$

$$r = 0.005\,\lambda_{12\ \mathrm{GHz}}$$

$$\varepsilon_r = 2.20$$

where W is the patch width, g is the gap width, h is the substrate thickness, r is the radius of the vias, and ε_r is the substrate permittivity. The height of the dipole over the top surface of the EBG ground plane is $0.02\,\lambda_{12\ \mathrm{GHz}}$. Thus the overall height of the dipole antenna from the bottom ground plane of the EBG structure is $0.06\,\lambda_{12\ \mathrm{GHz}}$. The input impedance is matched to a 50Ω transmission line. And the lowest return loss of the dipole is obtained on EBG structure at 13 GHz. The same simulation is run in the HFSS and the results are compared with the FDTD results (Figs. 17, 18, 19 and 20). The results are quite close to each other. The differences (all the results are shifted 1GHz to the higher frequencies and the return loss of the dipole over HIGP in HFSS (-20 dB) is 7dB more than the dipole over EBG in FDTD result (-27dB)) between the results occur because of the usage of the different computational EM technique of the software. The results are consistent with each other.

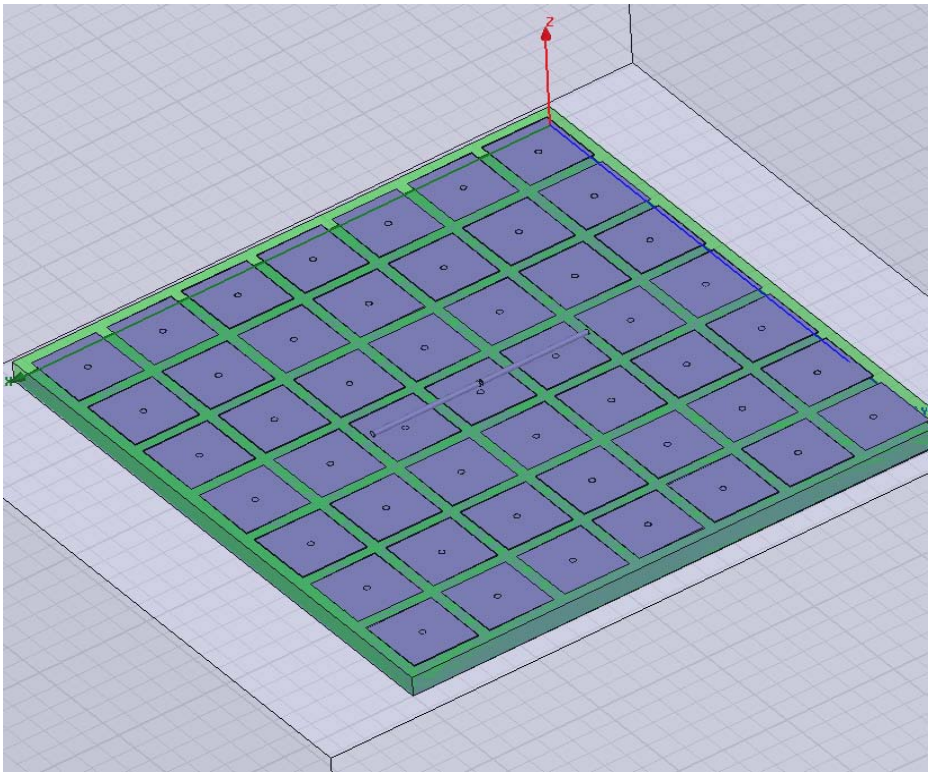

Figure 17. HFSS design of the dipole over EBG

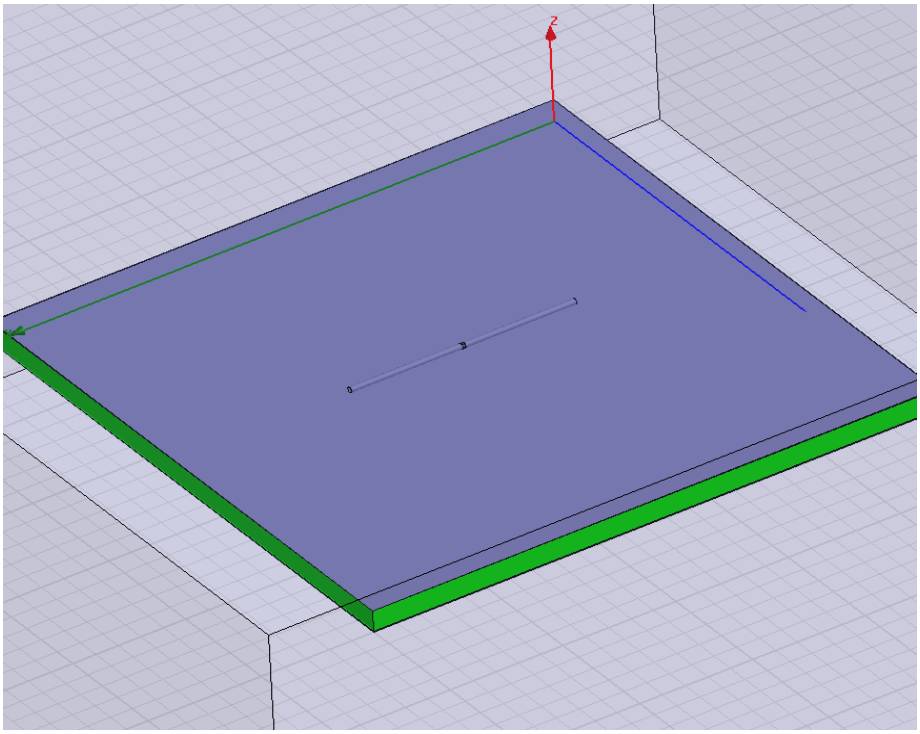

Figure 18. HFSS design of the dipole over PEC and PMC

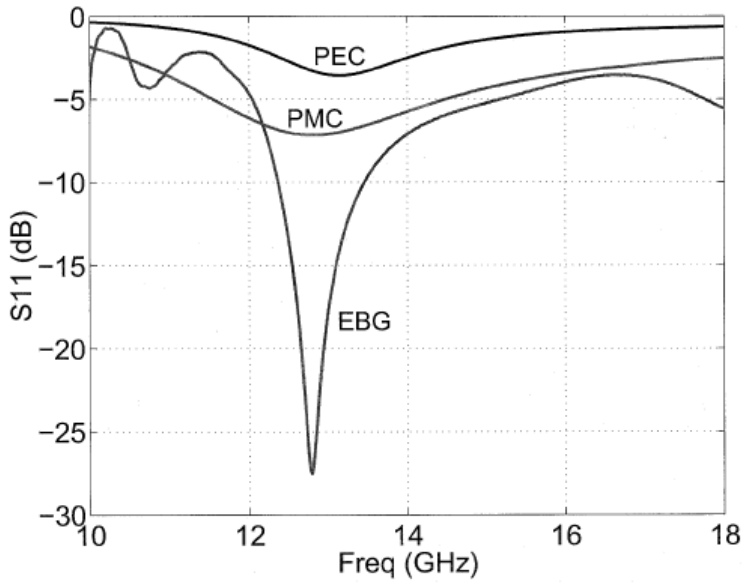

Figure 19. FDTD Simulation Results (Yang and Rahmat-Samii, 2003: 2693)

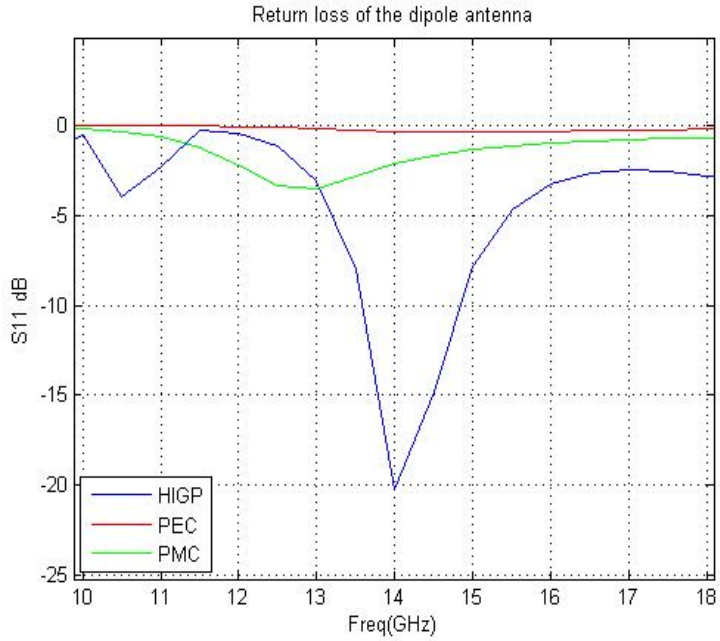

Figure 20. HFSS FE Method Simulation Results

Summary

In this chapter, the HFSS software that is used to design the antennas and the HIGPs and general usage areas of this software are mentioned. The solution process and "Finite Element Method" is discussed. Next, creating a structure geometry; assigning the materials, boundary conditions and excitations are presented. The information about solution setup, analyzing and creating reports is provided. Lastly, the confirmation of the design setups of the HFSS with previous research is mentioned.

The following chapter will discuss new HIGP and antenna designs to find the optimum geometry, and optimum surface wave suppression frequency bandwidth.

IV. Design, Analysis and Results

Chapter Overview

In this chapter new HIGP designs and Antenna-HIGP combinations are presented. The goal of all the designs is to obtain the maximum surface wave suppression frequency band gap for HIGPs, and to obtain minimum return loss in the suppression band gap of the HIGP for the Antenna-HIGP combinations.

In order to achieve this goal, some variables of the HIGP designs such as patch width, gap width, etc. are changed. After that different geometrical patch shapes (square, round, triangle and hexagon) are tried to reach the optimum results. Different antenna types (narrowband and wideband) are mounted over these HIGP designs and looked for the best return loss and radiation. Antenna-HIGP results are compared with the same type of Antenna-PEC, Antenna-PMC and antenna free space results.

Square Patch HIGP Designs

The following 3 designs are created as 7X7, 9X9 and 11X11 square patch HIGPs. While designing these HIGPs patch width(w) and gap width(g) dimensions are chosen from equation (10) (Yang and Rahmat-Samii, 2003: 2692). w is chosen as 0.12 times, g is chosen as 0.02 times the wavelength of the center operating frequency of the HIGP design. Substrate thickness (h) and via radius(r) are changed as 3.175mm and 0.406mm to get a consistent comparison between the simulation and measurement results (Cakiroglu, 2008).

7X7 Square Patch HIGP Design

The first design is simulated using the parameters of the multiples of 8GHz wavelength:

$$w = 4.5\text{mm } (0.12\,\lambda_{8\text{ GHz}})$$

$$g = 0.75\text{mm } (0.02\,\lambda_{8\text{ GHz}}) \quad (11)$$

$$h = 3.175\text{mm}$$

$$r = 0.406\text{mm}$$

where w is the patch width, g is the gap width, h is the substrate thickness and r is the radius of the vias. Total dimension of the HIGP is fixed to $1\,\lambda_{8\text{ GHz}}$ X $1\,\lambda_{8\text{ GHz}}$ (Figs. 21 and 22). The second elements in the two opposite corners are fed by coaxial cables (these two patch elements are used as antennas) as mentioned in the previous chapter. S_{21} results are computed and plotted to see the suppression frequency band gap (Fig.23).

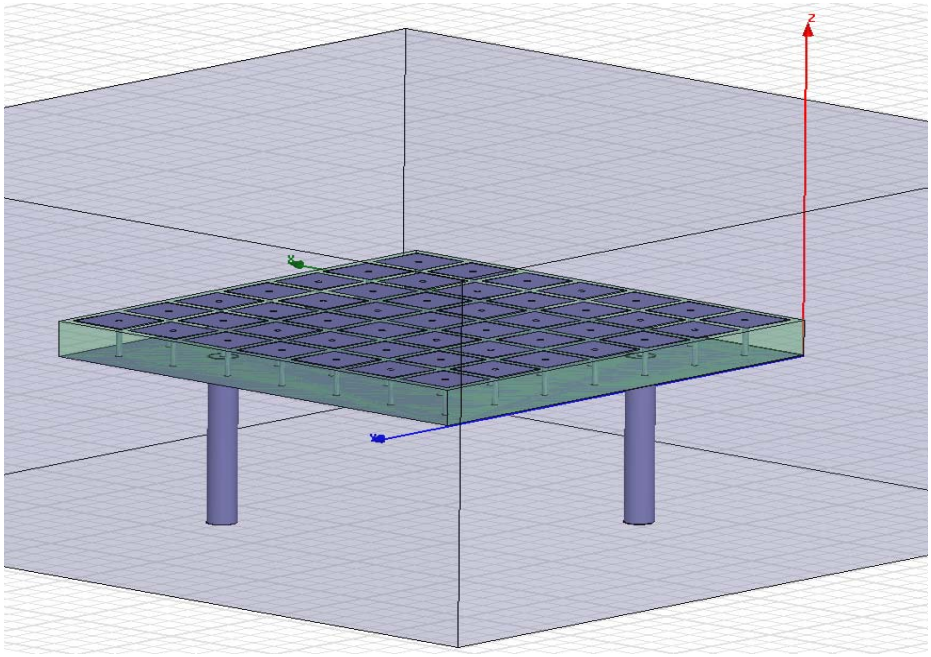

Figure 21. 7x7 HIGP Design

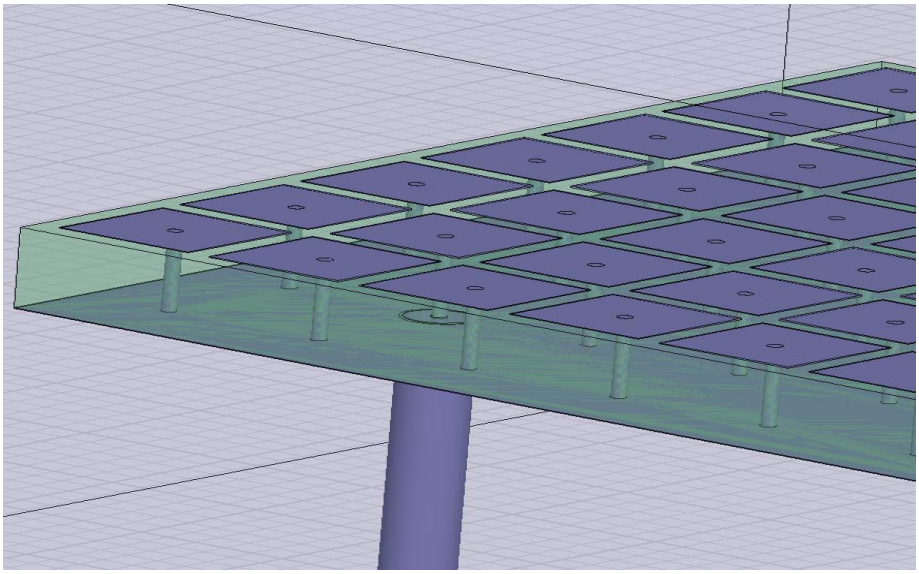

Figure 22. Port of the 7x7 HIGP

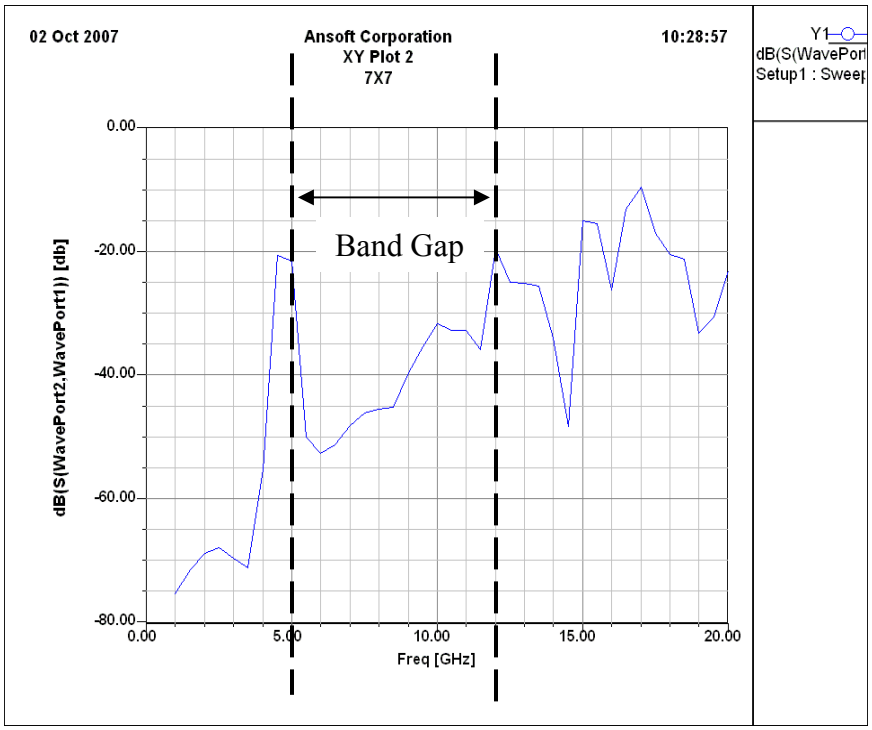

Figure 23. S_{21} simulation result of the 7x7 HIGP (Band Gap=5-12 GHz)

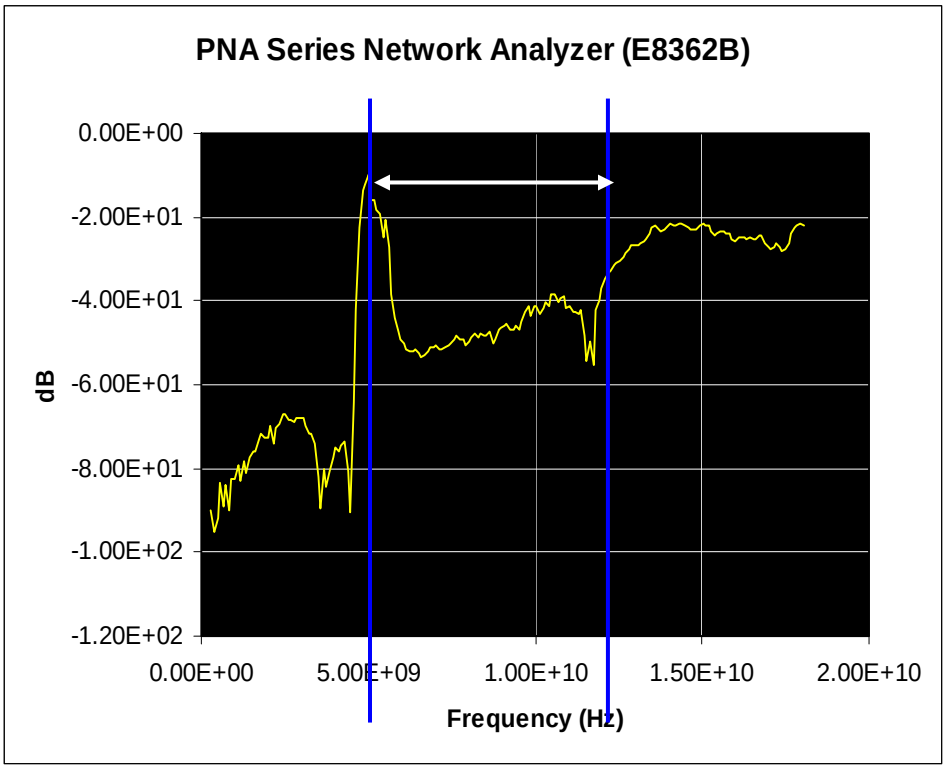

Figure 24. S21 measurement result of the 7x7 HIGP (Cakiroglu, 2008)

Both the simulation and measurement results show that there is a suppression band gap between 5 and 12 GHz (20-40dB drop occurs).

In order to confirm the band gap of the structure, parallel corner elements and middle elements of two edges are fed by coaxial cables in the second and third simulations (Figs. 25 and 28). If all of these feeding configurations give the same results, then it can be accepted that the HIGP has a band gap in that frequency band. And the results of the simulation and measurements are shown in Figs. 26, 27 and 29.

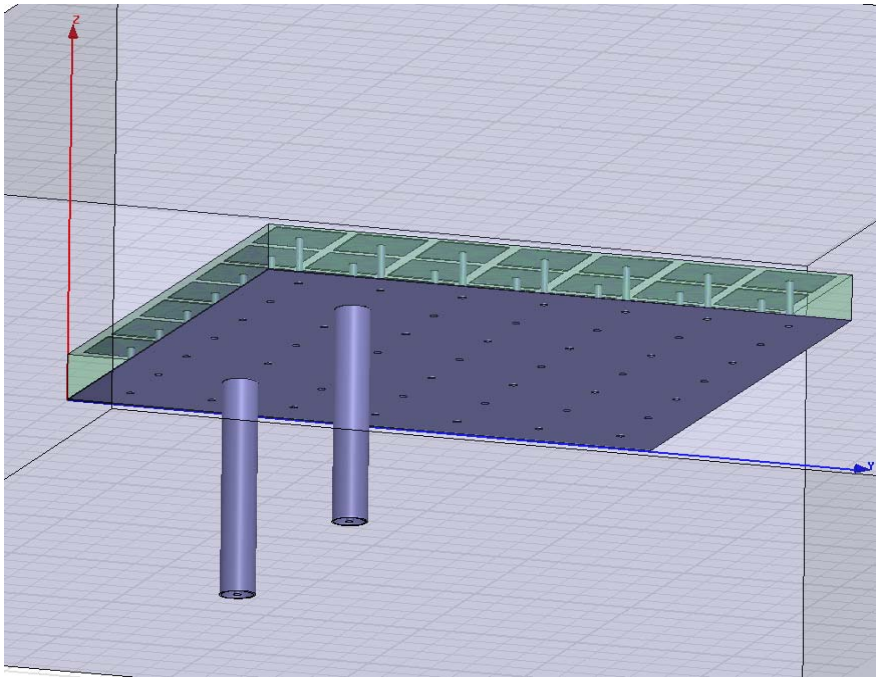

Figure 25. Parallel Feed 7x7 HIGP

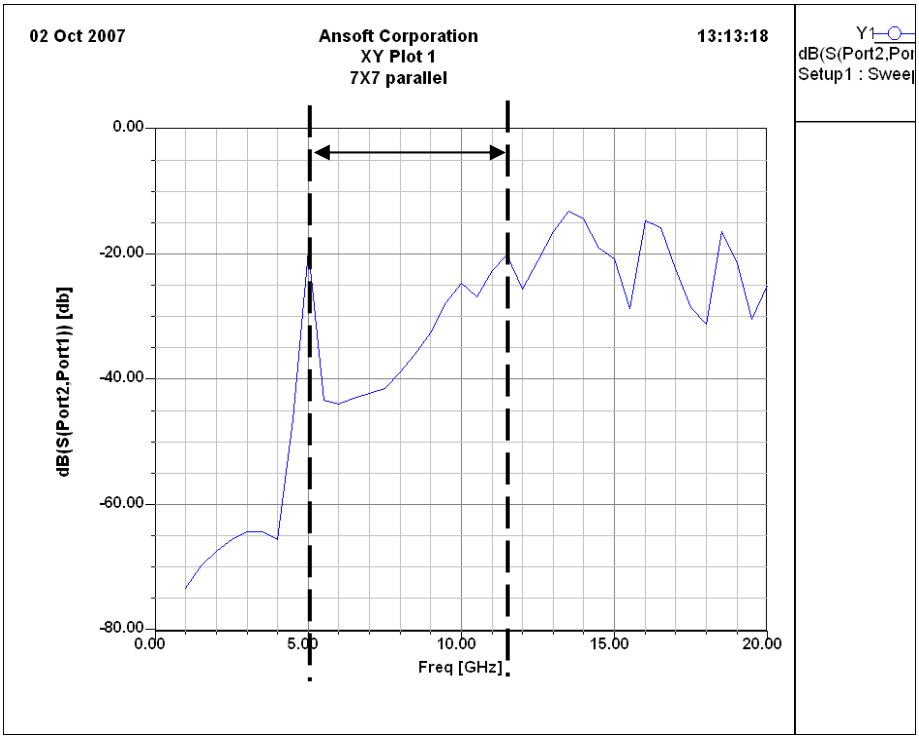

Figure 26. S_{21} simulation result of the parallel feed 7x7 HIGP (Band Gap=5-11.5 GHz)

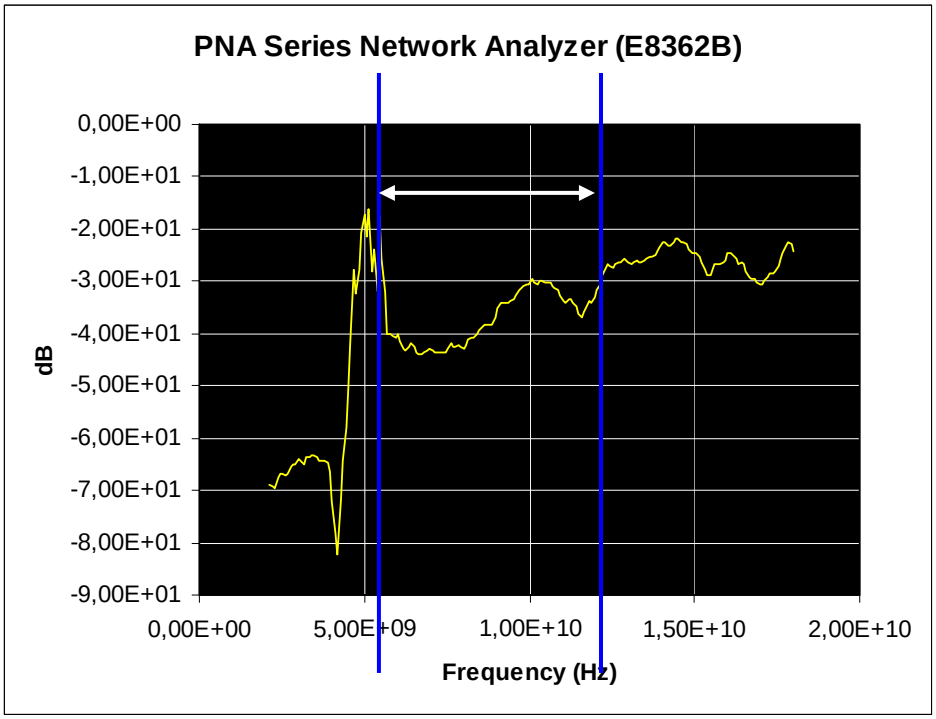

Figure 27. S_{21} measurement result of the parallel feed 7x7 HIGP (5.5-12GHz) (Cakiroglu, 2008)

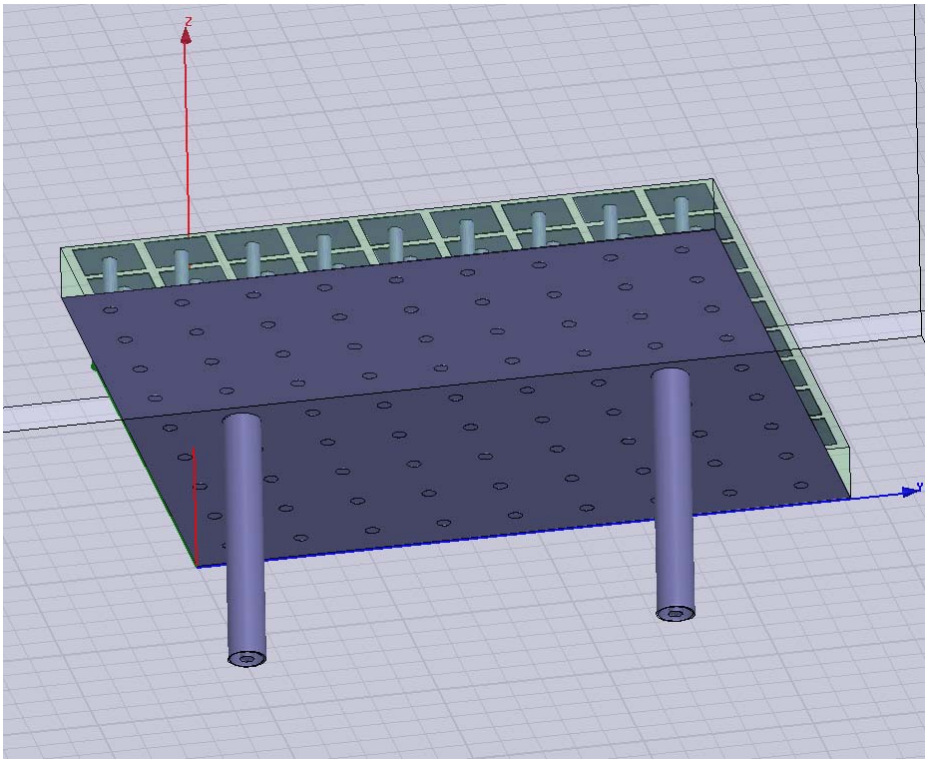

Figure 28. Parallel feed from opposite edges 7x7 HIGP

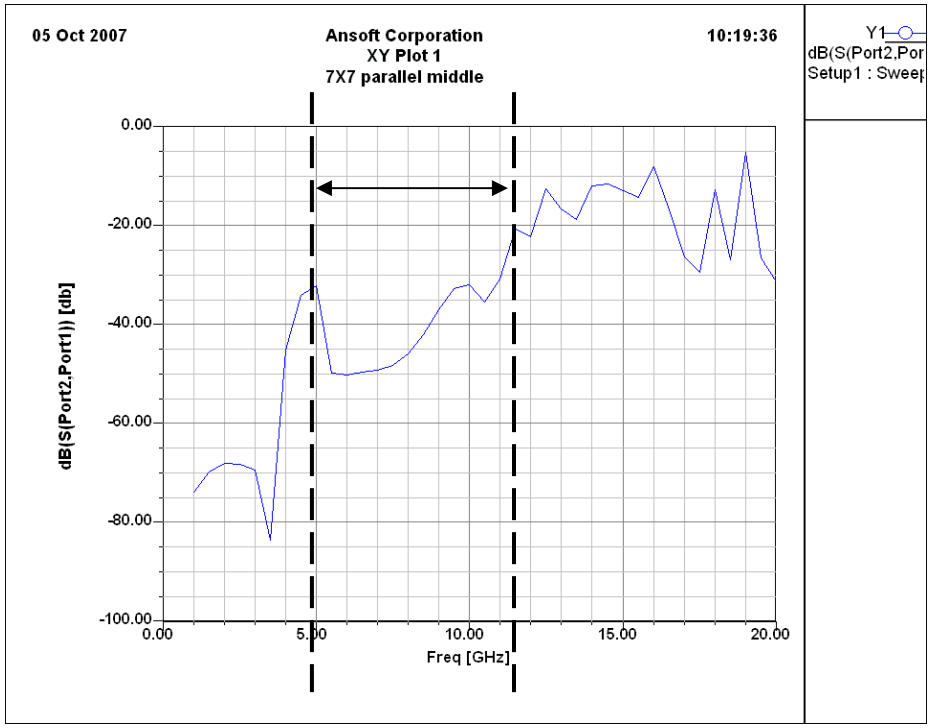

Figure 29. S_{21} simulation result of the parallel feed from opposite edges 7x7 HIGP (Band Gap=5-11.5 GHz)

Next, two rows are added in both directions without changing the patch width, gap width and the places of the coaxial cables (diagonal feed) to see if any diffraction occurred and effected the result of the previous design (Fig 30 and 31).

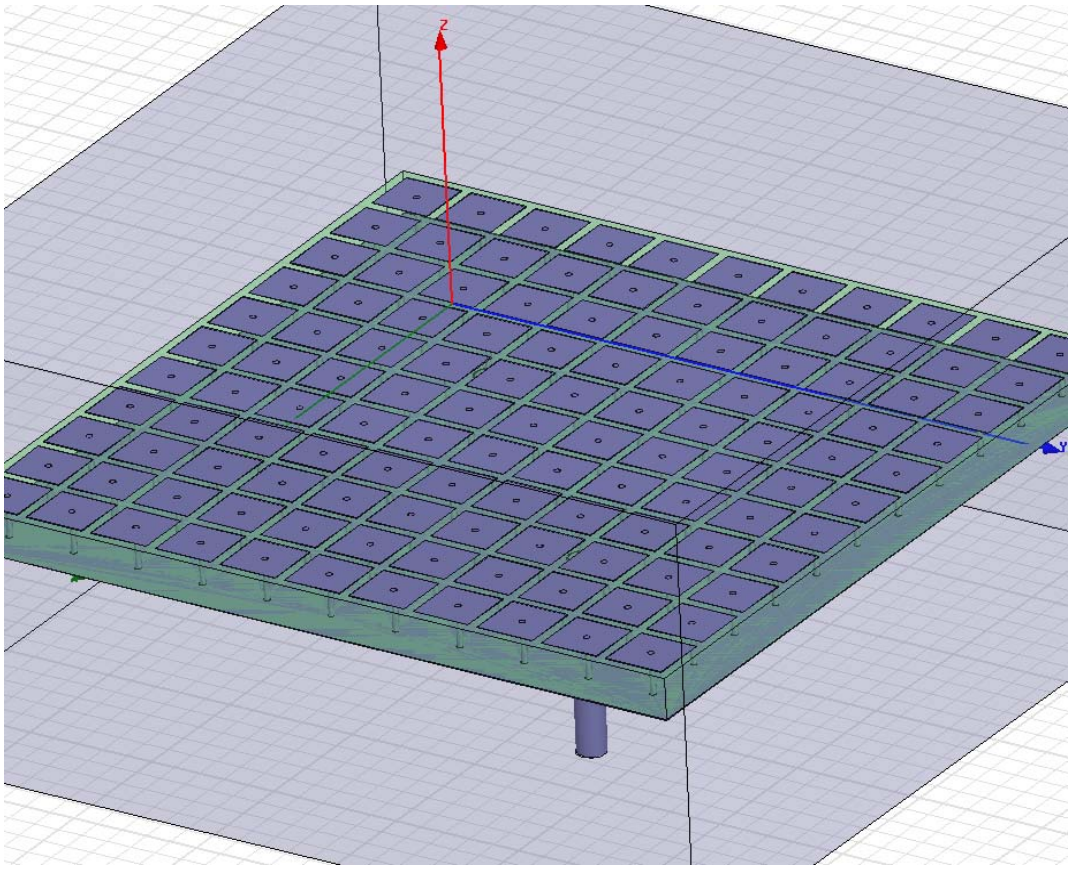

Figure 30. Two rows added 7x7 HIGP (becomes 9x9) (diagonal feed)

Next, vias are removed from the patches and no via S_{21} results are observed to see the function of the vias (Fig. 32). And lastly all the simulation results are combined in one graph to see the differences (Fig 33).

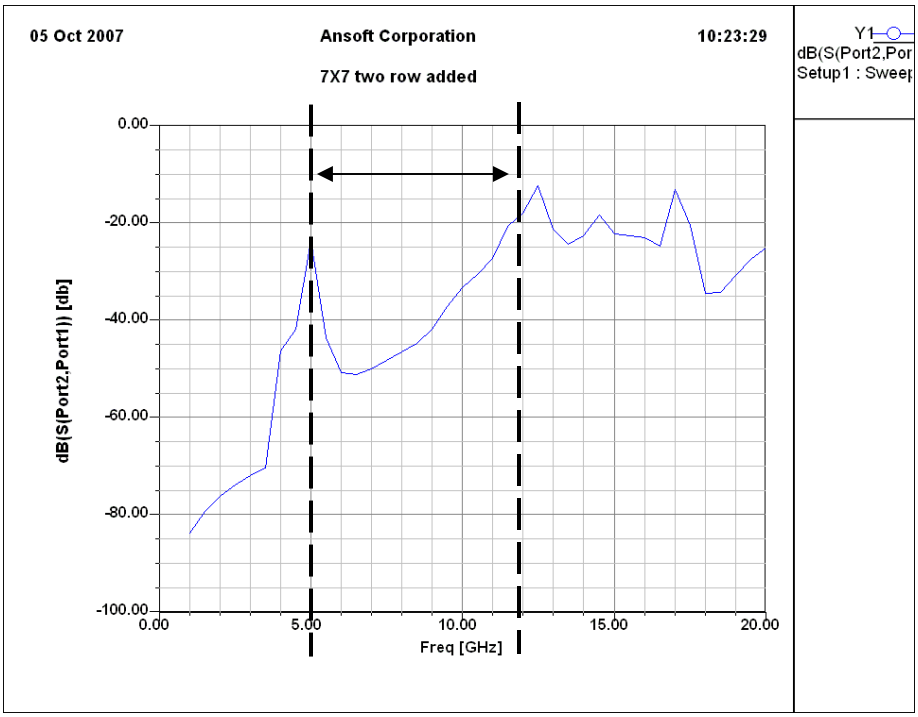

Figure 31. S_{21} simulation result of the two rows added 7x7 HIGP (Band Gap=5-12 GHz)

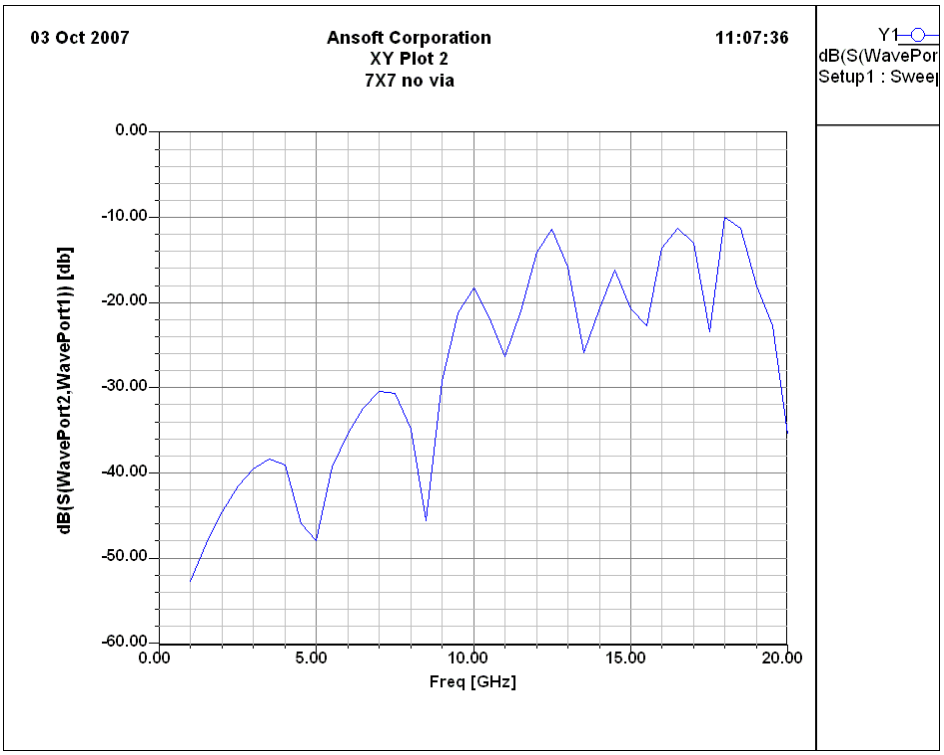

Figure 32. S_{21} simulation result of the "no via" 7x7 HIGP (There is no Band Gap)

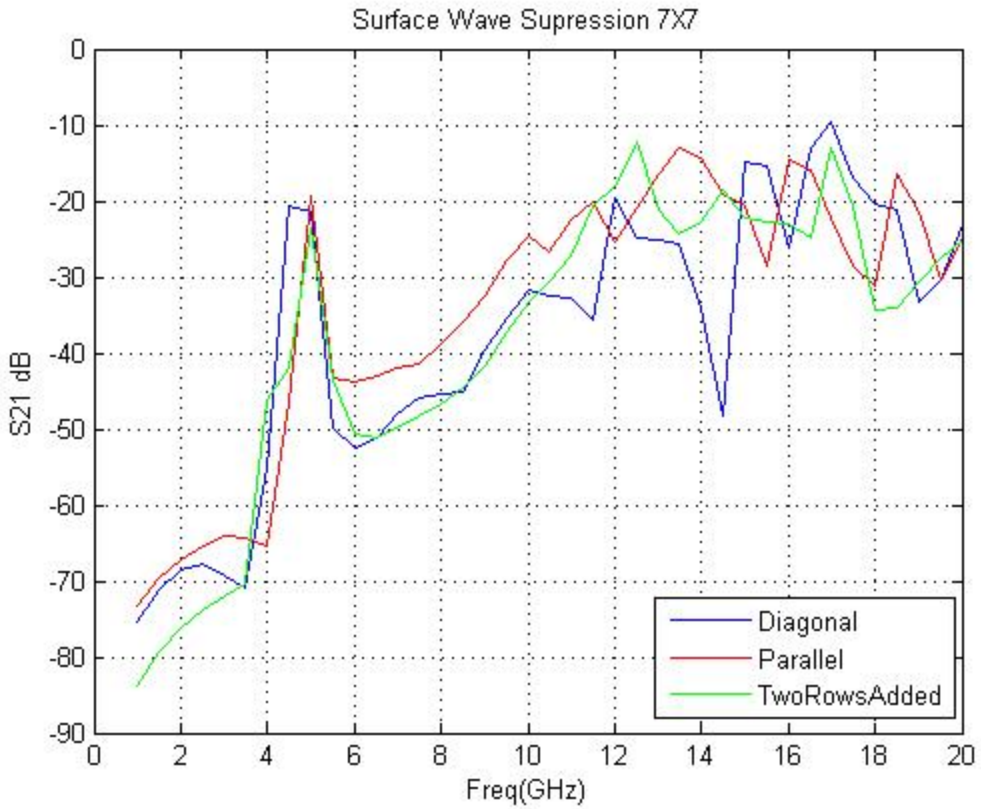

Figure 33. Diagonal, parallel and two rows added S_{21} results.

All of the three designs above (diagonal feed, parallel feed and two rows added feed), give almost the same band gap for 7x7 HIGP design. Measurement results also confirm the simulation results. When vias are removed, surface wave suppression band gap disappears because LC circuit behavior no longer exists.

9X9 Square Patch HIGP Design

This design is simulated using the parameters of the multiples of 10GHz wavelength:

$$w = 3.6\text{mm } (0.12\,\lambda_{10\text{ GHz}})$$

$$g = 0.6\text{mm } (0.02\,\lambda_{10\text{ GHz}}) \quad (12)$$

$$h = 3.175\text{mm}$$

$$r = 0.406\text{mm}$$

where w is the patch width, g is the gap width, h is the substrate thickness and r is the radius of the vias. Total dimension of the HIGP is fixed to $1\,\lambda_{10\text{ GHz}}$ X $1\,\lambda_{10\text{ GHz}}$ (Fig 34). S_{21} simulation and measurement results are plotted to see the suppression frequency band gap for different types of feed (Figs. 35, 36, 37, 38, 39, 40 and 41).

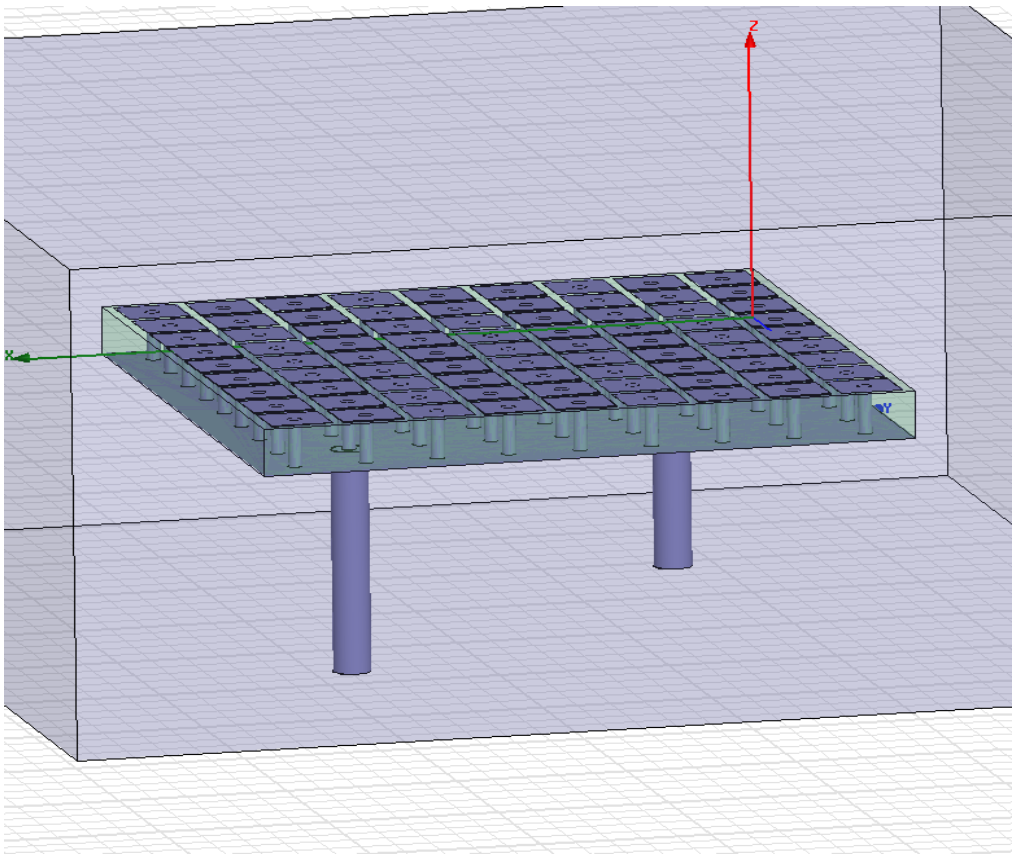

Figure 34. 9x9 HIGP Design (diagonal feed from corners)

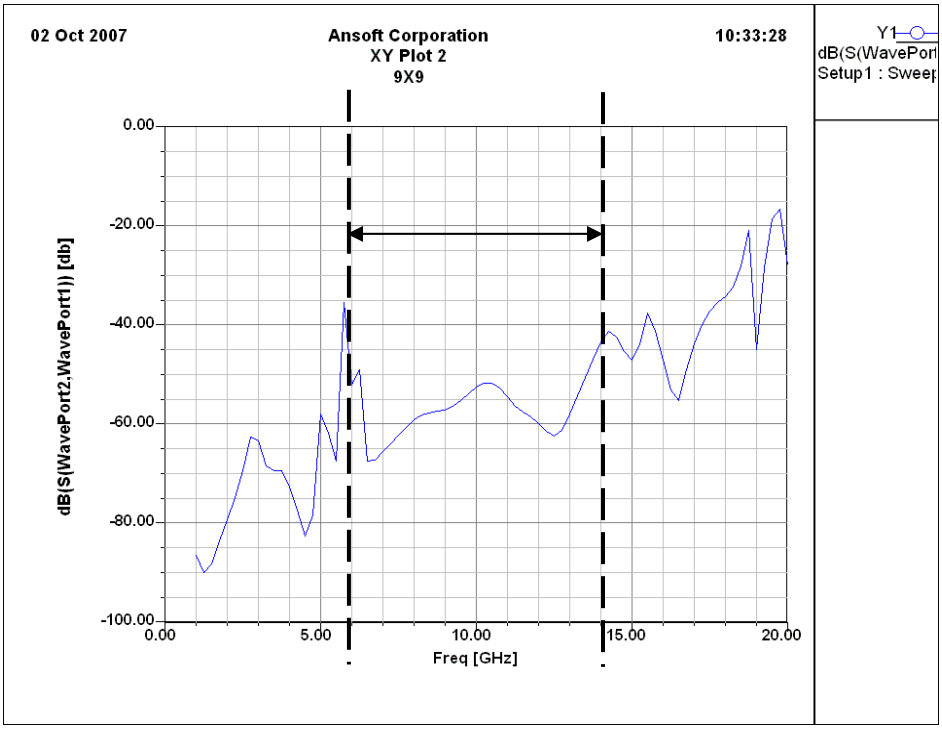

Figure 35. S_{21} simulation result of the 9x9 HIGP (diagonal feed) (Band Gap=6-14 GHz)

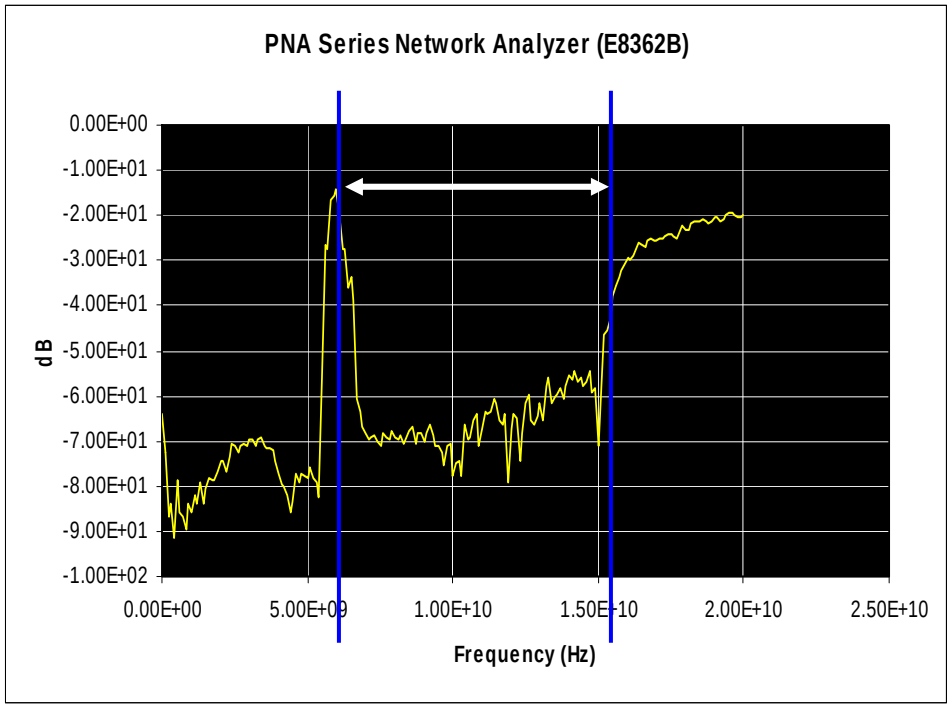

Figure 36. S_{21} measurement result of the 9x9 HIGP (diagonal feed) (Band Gap=6-15GHz) (Cakiroglu, 2008)

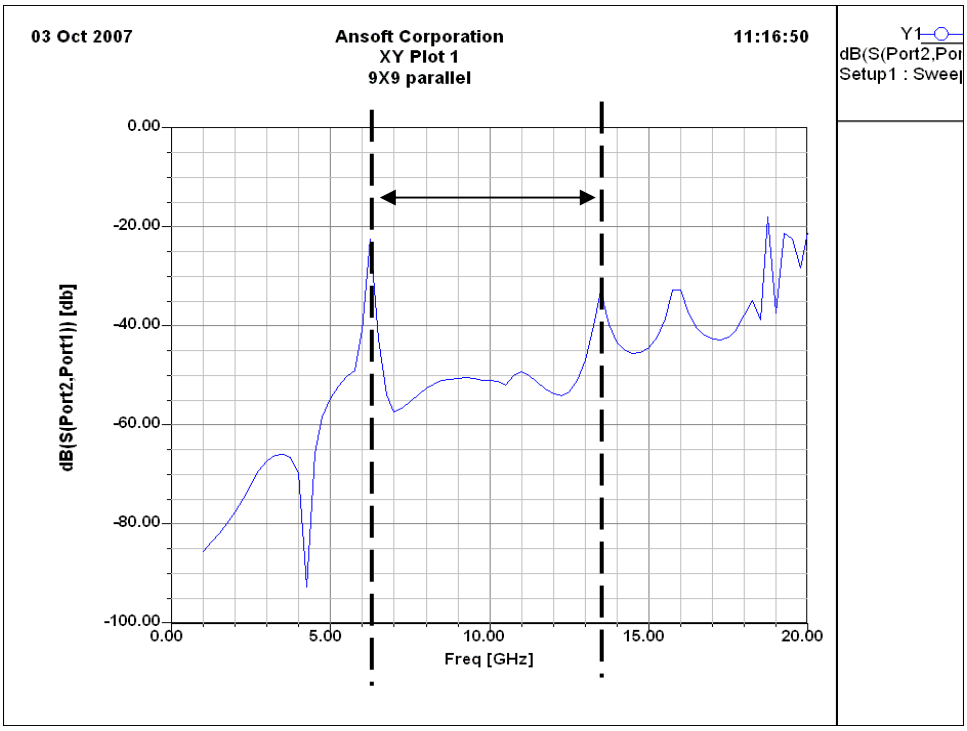

Figure 37. S_{21} simulation result of the 9x9 HIGP (parallel feed from corners) (Band Gap=6-13.5 GHz)

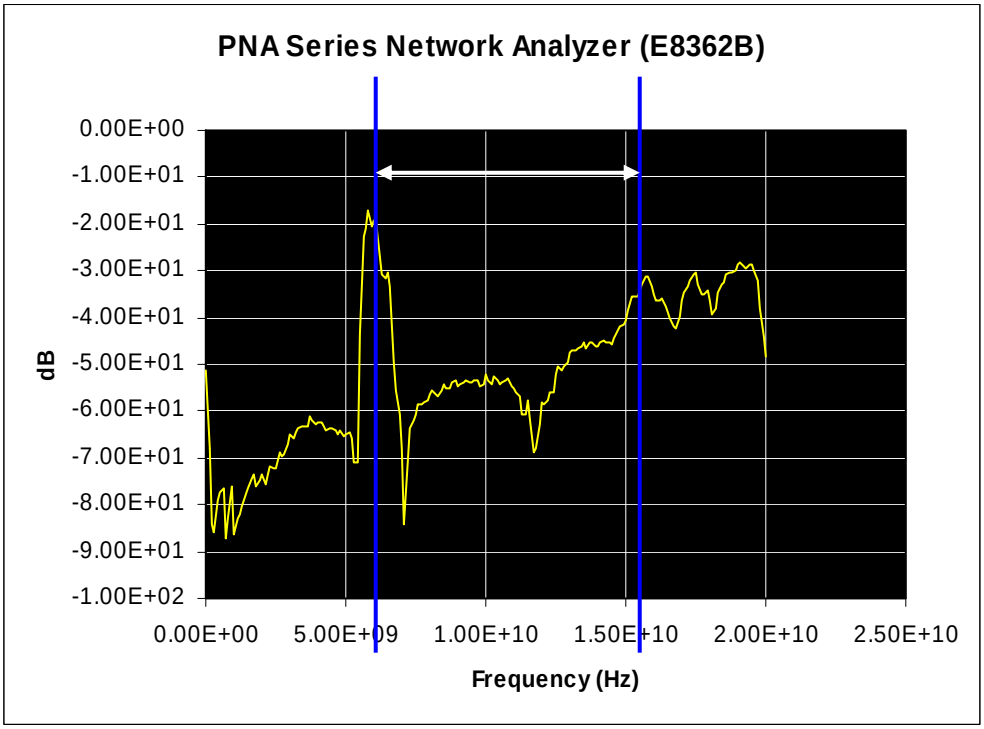

Figure 38. S_{21} measurement result of the 9x9 HIGP (parallel feed from corners) (Band Gap=6-15 GHz) (Cakiroglu, 2008)

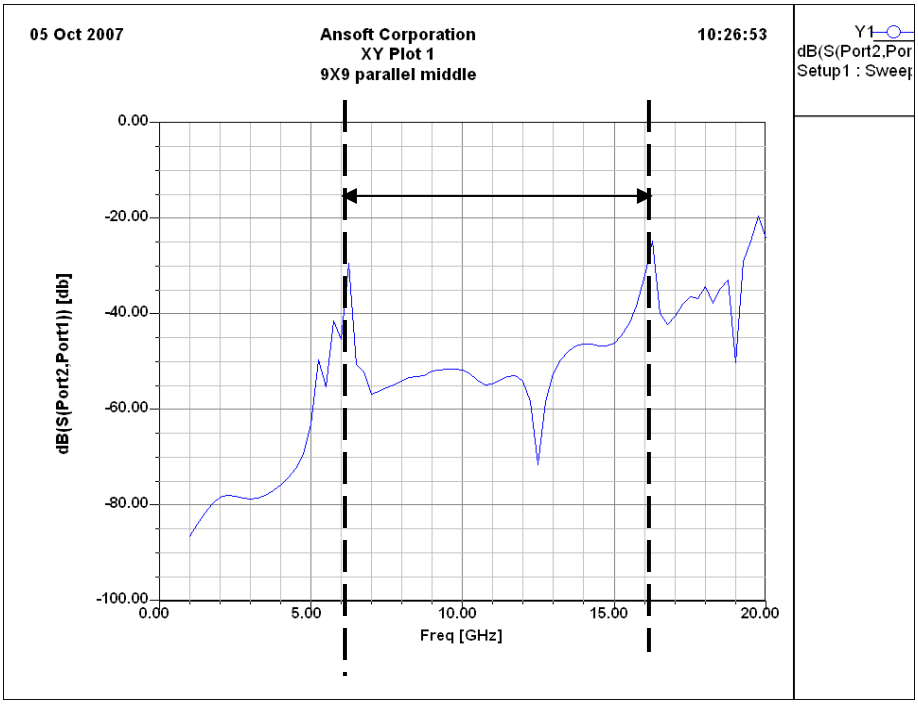

Figure 39. S_{21} simulation result of the 9x9 HIGP (parallel feed from middle) (Band Gap=6-16 GHz)

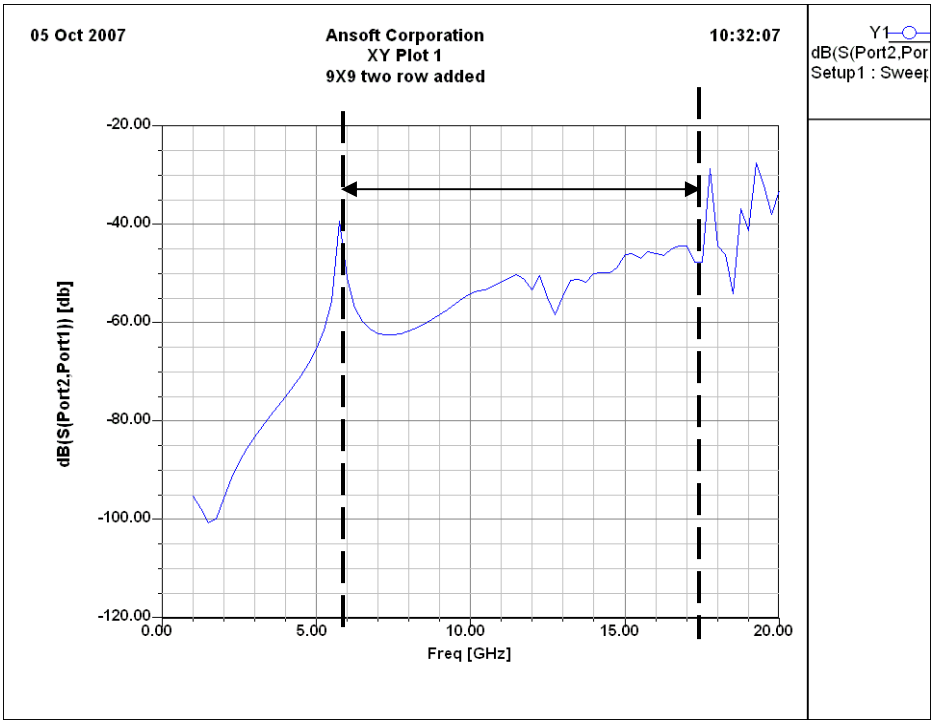

Figure 40. S_{21} simulation result of the 9x9 HIGP (diagonal feed two row added (11x11)) (Band Gap=6-17 GHz)

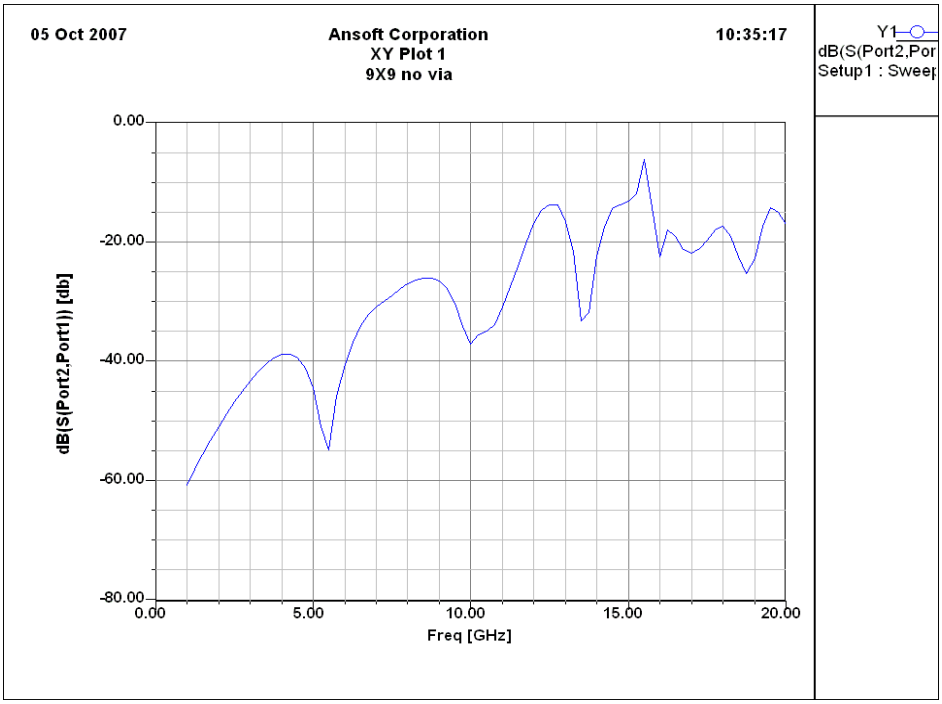

Figure 41. S_{21} simulation result of the 9x9 HIGP (diagonal feed "no via")
(Band Gap = there is no band gap)

In order to evaluate the results and determine the band gap exactly, all the S_{21} results are combined together and plotted (Fig. 42).

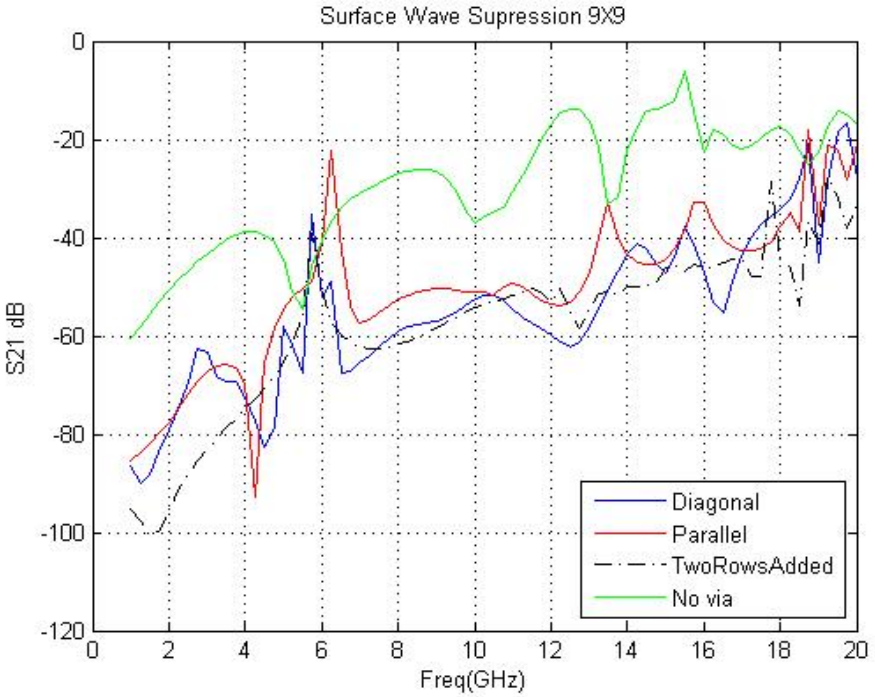

Figure 42. Diagonal, parallel, two rows added and "no via" S_{21} results

It is seen from the results that a clear surface wave band gap occurs between 6-14 GHz regardless of the feed position (approximately 20dB drop occurs). When vias are removed from the patches, S_{21} values increase and band gap disappears, since inductance (L) no longer exists.

11X11 Square Patch HIGP Design

This design is simulated using the parameters of the multiples of 12GHz wavelength:

$$w = 3 \text{ mm } (0.12 \lambda_{12\text{ GHz}})$$

$$g = 0.5 \text{ mm } (0.02 \lambda_{12\text{ GHz}}) \quad (12)$$

$$h = 3.175\text{mm}$$

$$r = 0.406\text{mm}$$

where w is the patch width, g is the gap width, h is the substrate thickness and r is the radius of the vias. Total dimension of the HIGP is fixed to $1\lambda_{12\,GHz}$ X $1\lambda_{12\,GHz}$ (Fig. 43). S_{21} simulation and measurement results are plotted to see the suppression frequency band gap for different types of feeds (Figs. 44, 45, 46, 47, 48 and 49).

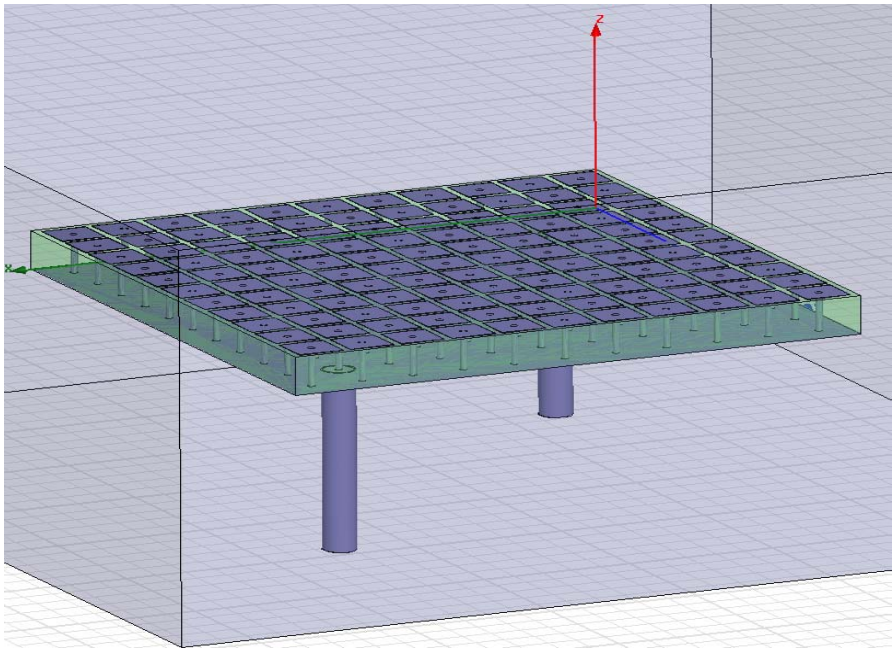

Figure 43. 11x11 HIGP Design (diagonal feed from corners)

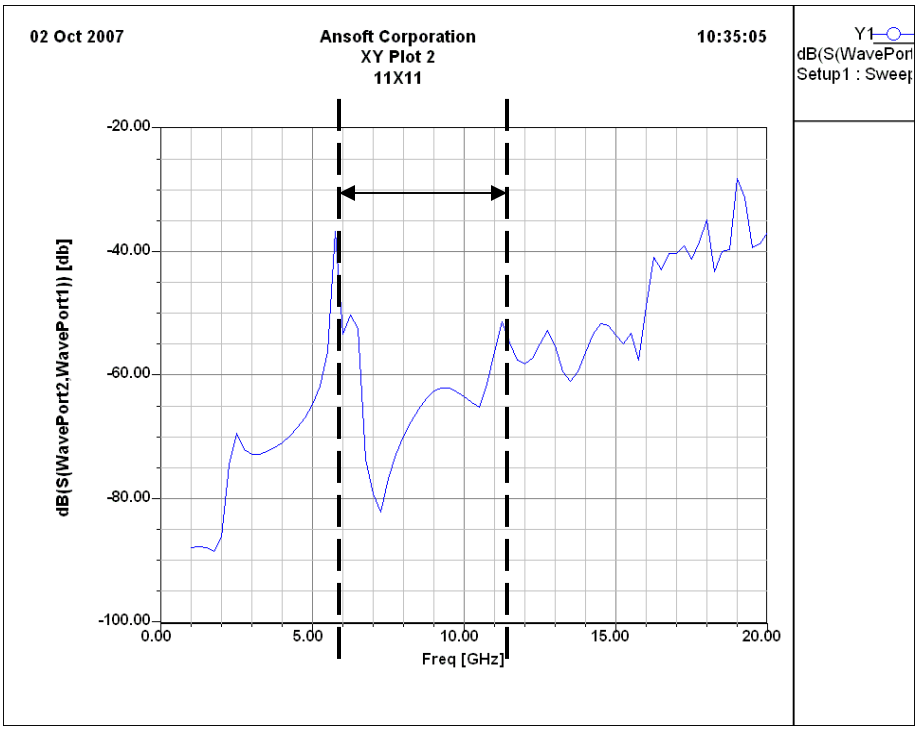

Figure 44. S_{21} simulation result of the 11x11HIGP (diagonal feed) (Band Gap=6-11 GHz)

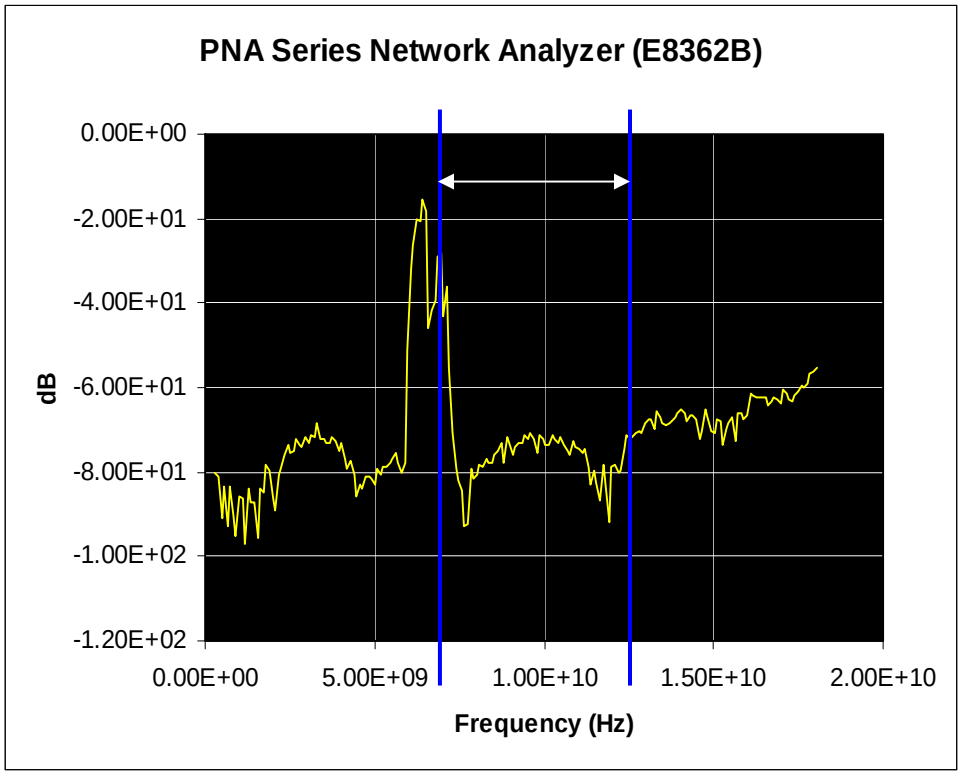

Figure 45. S_{21} measurement result of the 11x11HIGP (diagonal feed) (Band Gap=7-13 GHz) (Cakiroglu, 2008)

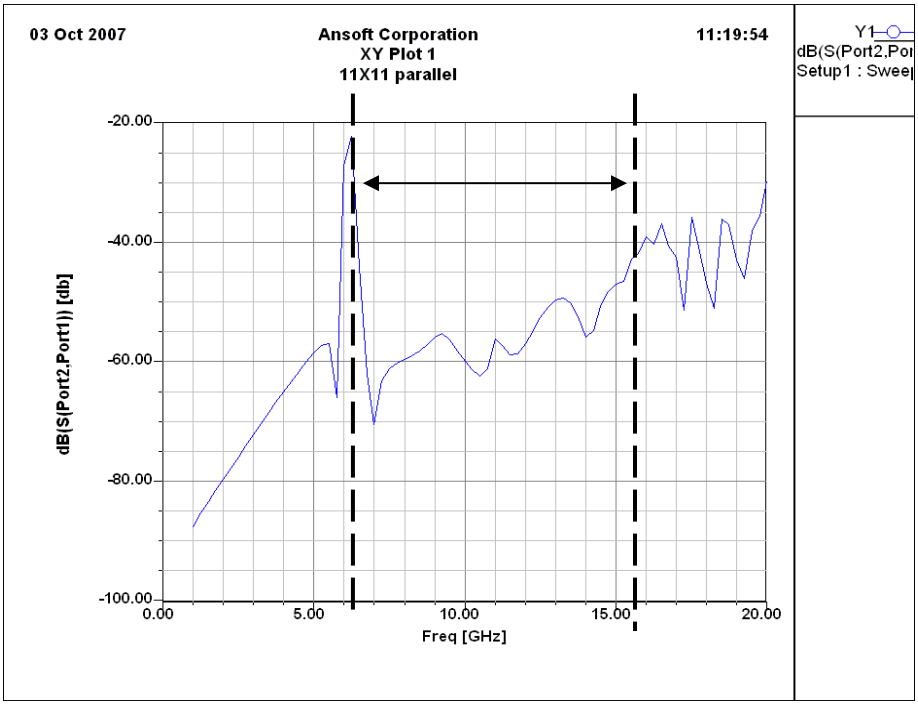

Figure 46. S_{21} simulation result of the 11x11HIGP (parallel feed from corners) (Band Gap=6-15 GHz)

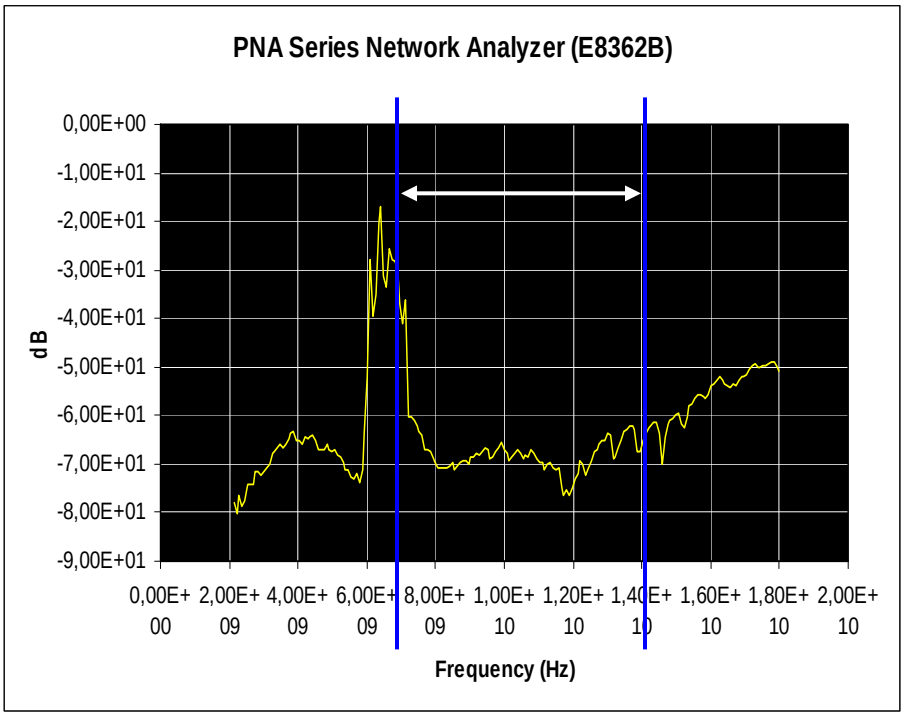

Figure 47. S_{21} measurement result of the 11x11HIGP (parallel feed from corners) (Band Gap=7-14 GHz) (Cakiroglu, 2008)

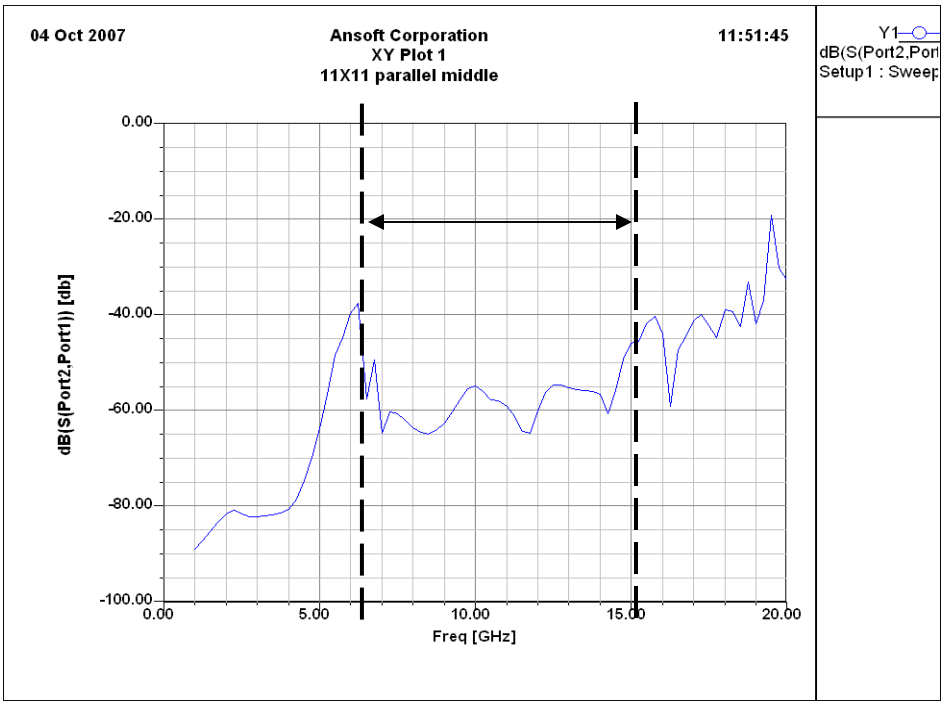

Figure 48. S_{21} simulation result of the 11x11HIGP (parallel feed from middle) (Band Gap=6-15 GHz)

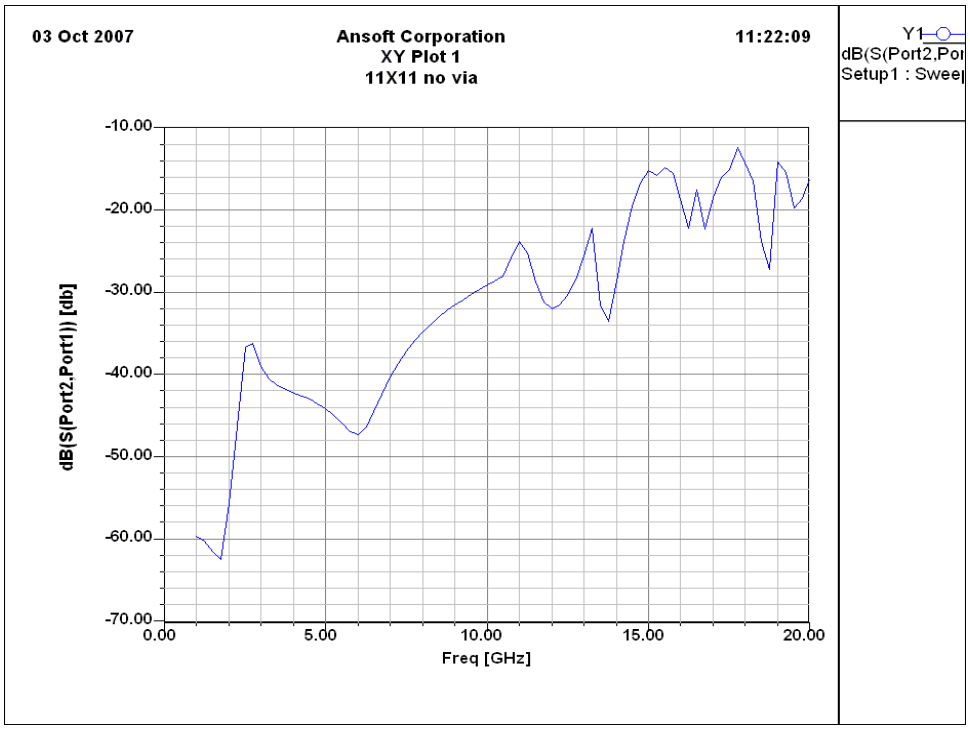

Figure 49. S_{21} simulation result of the 11x11HIGP ("no via") (Band Gap= there is no band gap)

When all the 11x11 results are evaluated together, a band gap is found between 6-15 GHz (20-40dB drop occurs) (Fig. 50). When vias are removed, band gap disappears and S_{21} values increase significantly.

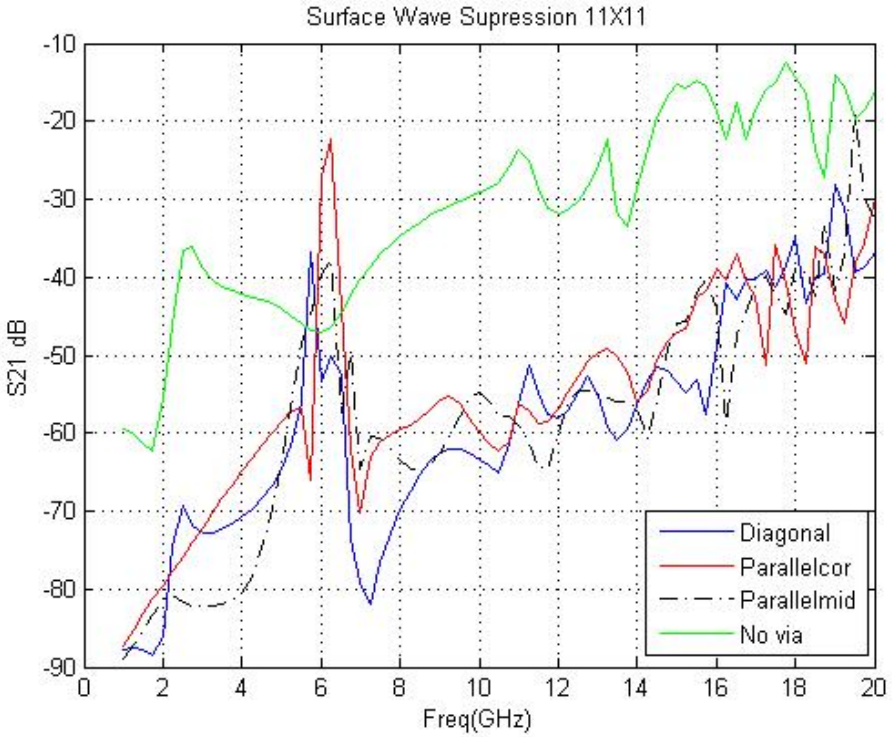

Figure 50. Diagonal, parallel, and "no via" S_{21} results

Optimization of 7X7 Square Patch HIGP Design

In this part, dimensions of the 7x7 square patch optimization is done by changing the patch width, gap width, substrate thickness andsubstrate material. In every part of the optimization process only one variable is changed at a time and the others are held constant. The goal of the optimization is to obtain the widest band gap for the HIGP. All the S_{21} parameter simulations are run by feeding two opposite corner elements with coaxial cables as shown in the previous part of this chapter (Figs. 21 and 22).

Patch Width (w) Optimization

For the first part of the optimization, patch width value is varied from 3.5mm to 7.5mm with an increment of 1mm. Gap width (g)= 0.75mm, substrate thickness (h)= 3.175mm, and duroid-5880 with a permittivity of 2.2 is used as a substrate material. Five different band gap behaviors occur for each of the w change (Figs. 51, 52, 53, 54 and 55).

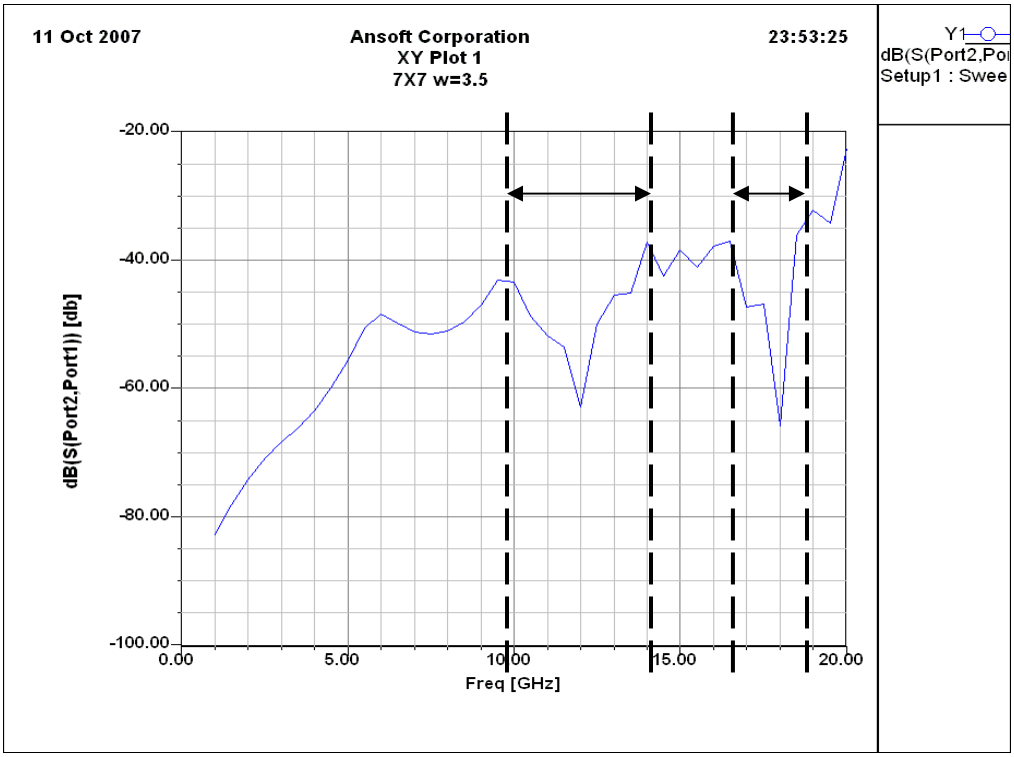

Figure 51. Patch width optimization w=3.5mm
(widest band gap occurs between 10-14 GHz)

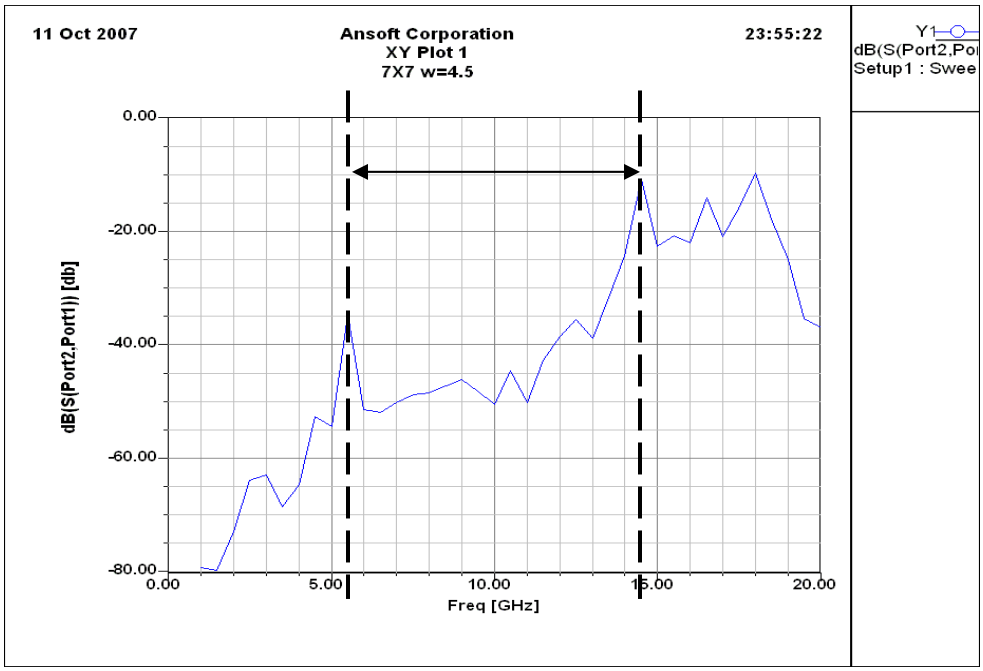

Figure 52. Patch width optimization w=4.5mm
(band gap occurs between 5.5-14.5 GHz)

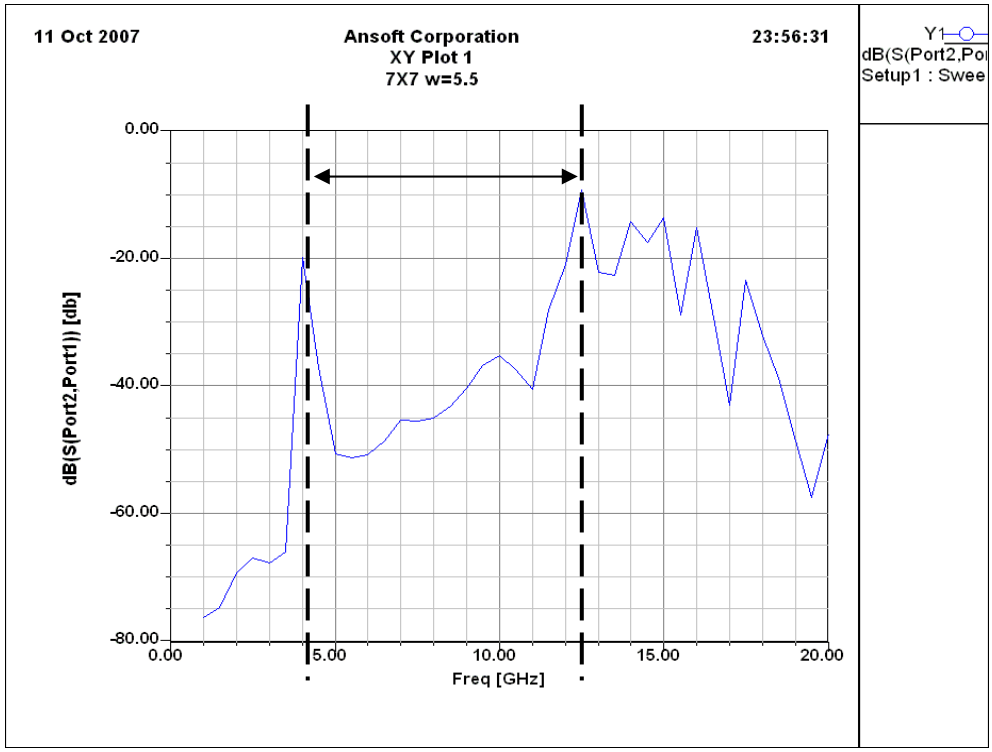

Figure 53. Patch width optimization w=5.5mm
(band gap occurs between 4-12.5 GHz)

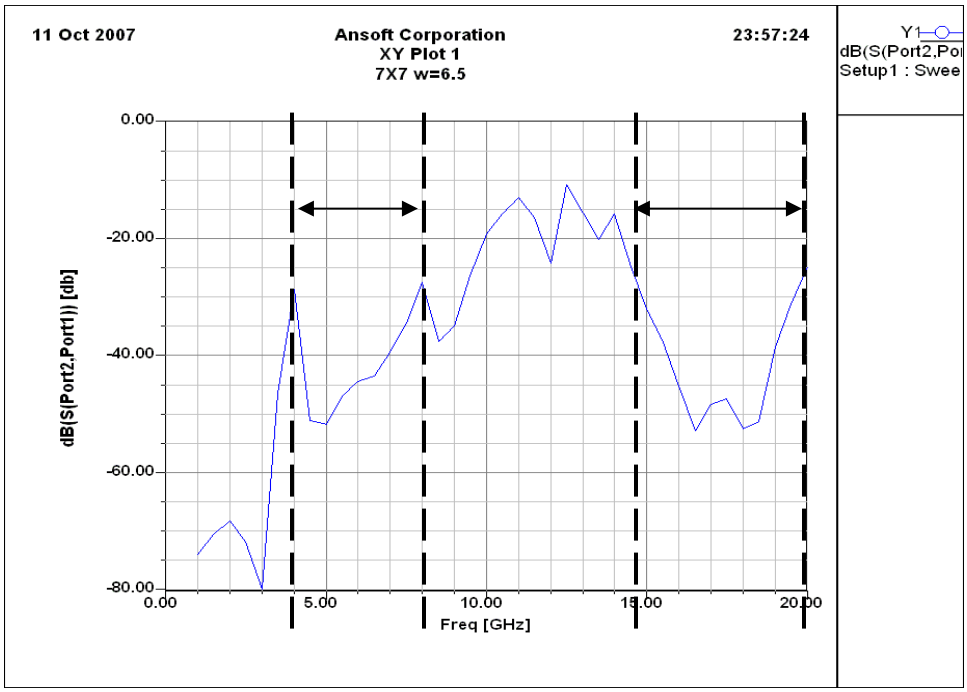

Figure 54. Patch width optimization w=6.5mm
(band gap occurs between 4-8 GHz and 15-20 GHz)

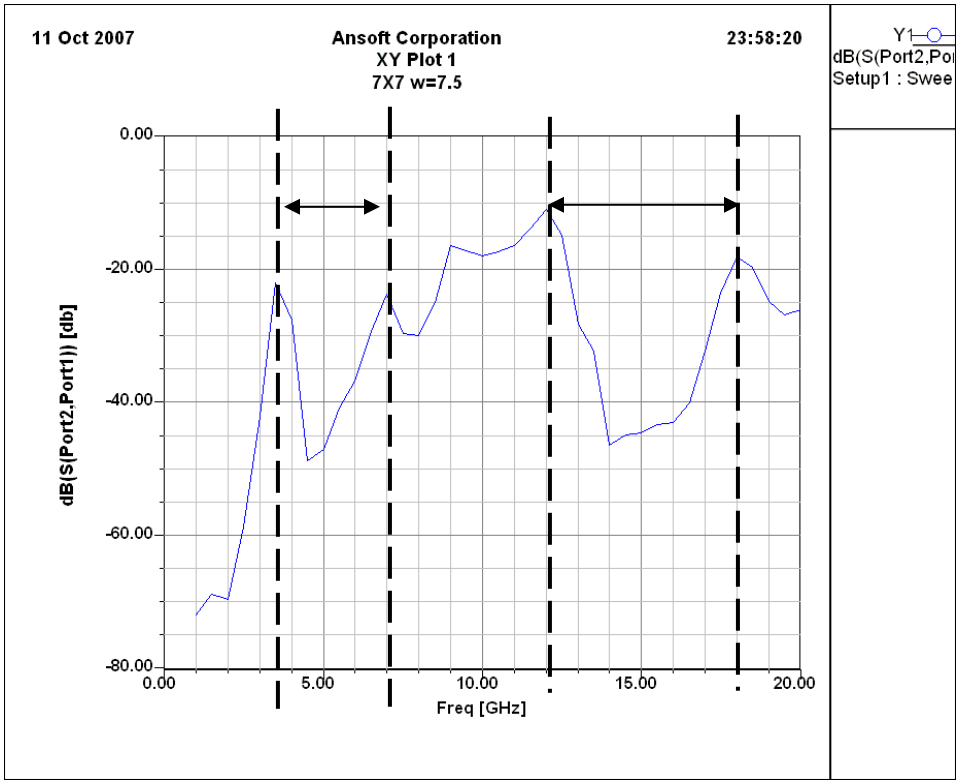

Figure 55. Patch width optimization w=7.5mm
(band gap occurs between 3.5-7 GHz and 12-18 GHz)

According to these results a patch width between 4.5-5.5 mm provides a smoother and wider band gap, and lower S_{21} that making these structures useful for broadband applications. Since w=4.5mm design gives the widest band gap, the following optimization steps will be taken by choosing the 4.5mm as a fixed value for patch width. Also, patch width optimization results show that band gap shifts to the left (to the lower frequencies) when patch width value is increased. Because, when the scale is made larger then the operating frequency becomes lower. And a second frequency band gap occurs at high frequencies (Figs. 54 and 55).

Gap Width (g) Optimization

In this part, gap width between patches is optimized by selecting w=4.5mm patch width. Gap widths of 0.4mm, 0.6mm, 0.75mm, 1.2mm and 1.5mm are used for each simulation (Fig. 56, 57, 58, 59 and 60). And S_{21}dB results are inspected.

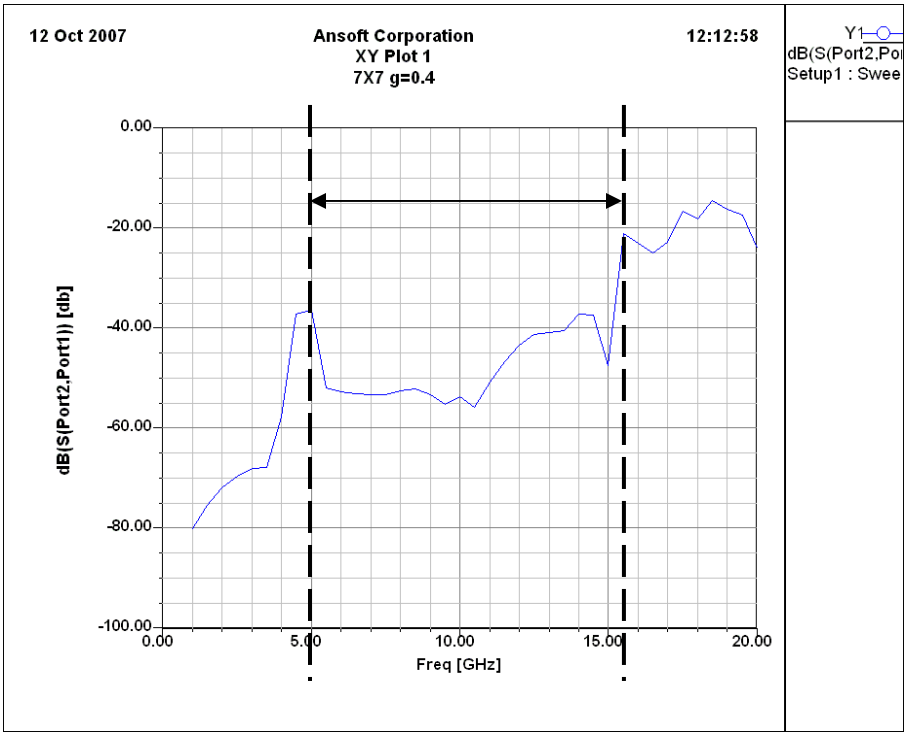

Figure 56. Gap width optimization g=0.4mm
(band gap = 5-15 GHz)

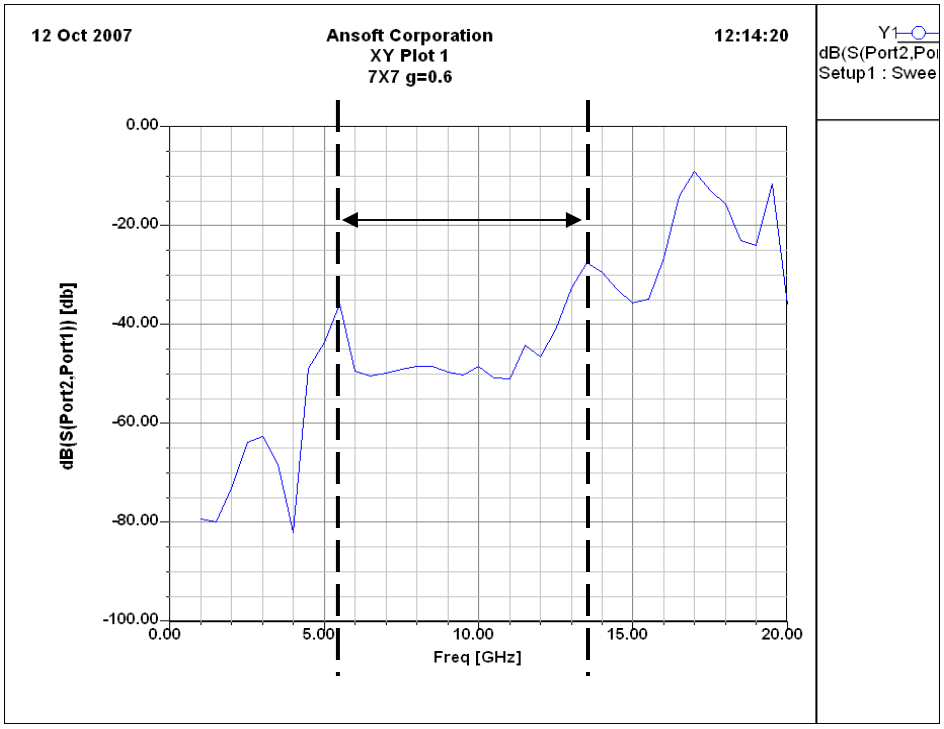

Figure 57. Gap width optimization g=0.6mm
(band gap = 5.5-13.5 GHz)

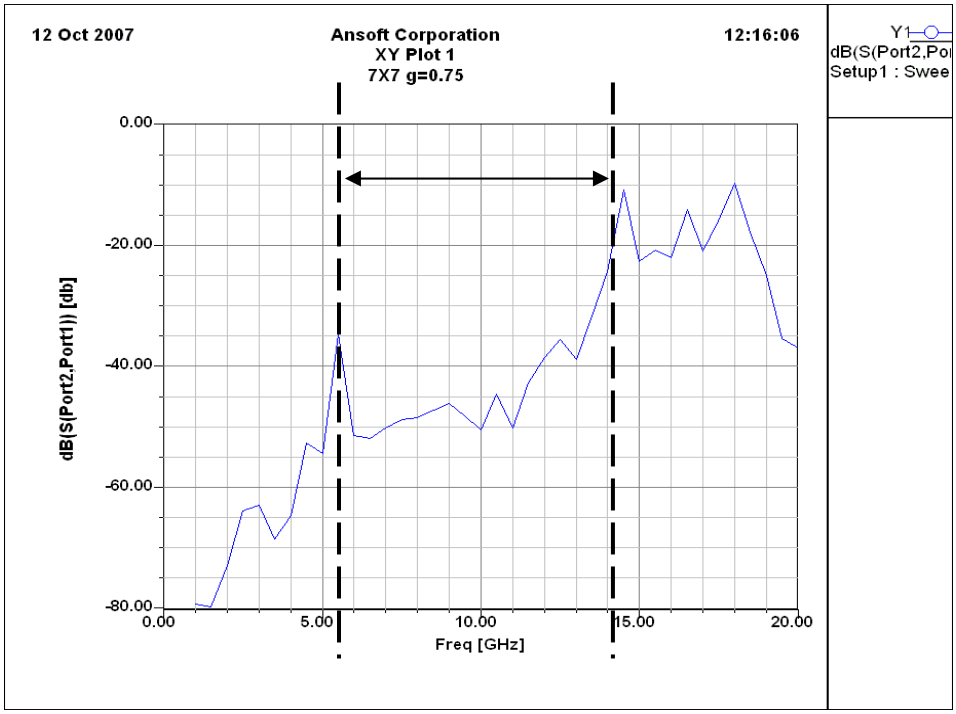

Figure 58. Gap width optimization g=0.75mm
(band gap = 5.5-14 GHz)

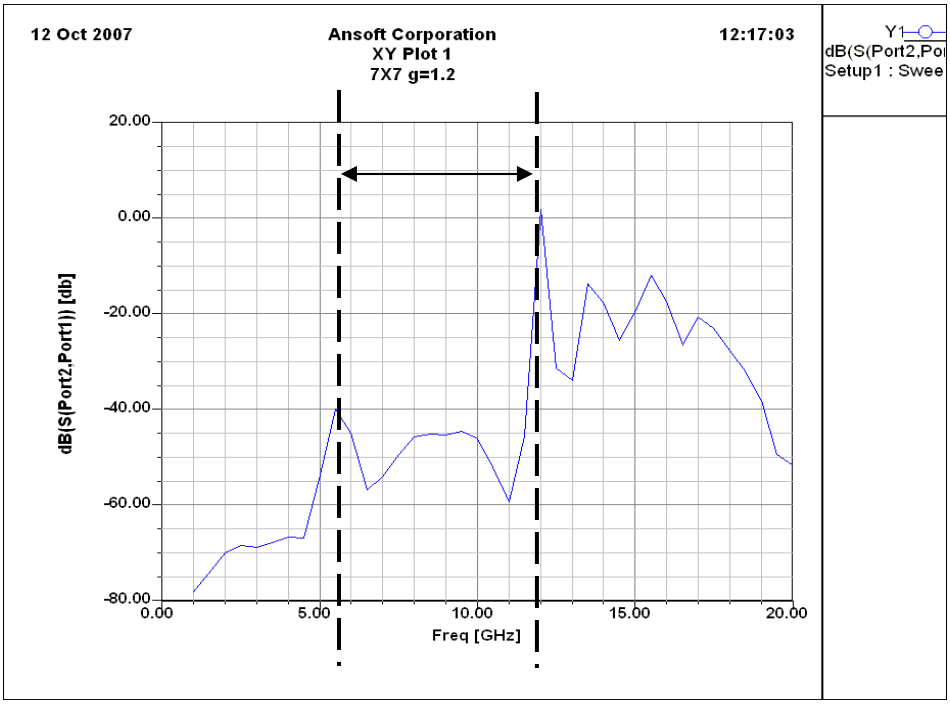

Figure 59. Gap width optimization g=1.2mm
(band gap = 5.5-12 GHz)

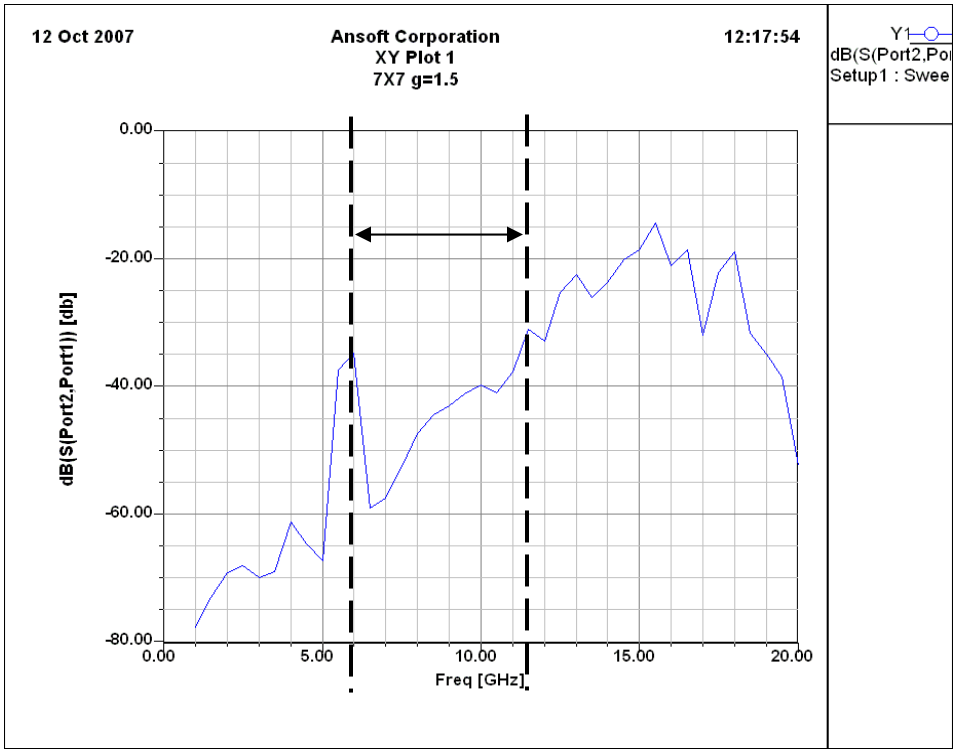

Figure 60. Gap width optimization g=1.5mm
(band gap = 6-11.5 GHz)

When the gap width value is increased, the suppression band gap becomes narrow. So the optimum “g” value for the widest band gap is 0.4mm. The widest band gap occurs when the gap width is left at minimum practical value. This practical value is 0.4mm for the construction of the structure. Next, optimization is made on the substrate thickness.

Substrate Thickness (h) Optimization

In this part, substrate thickness (h) is changed by the values of 3.175mm, 1.575mm, 0,787mm, 0.508mm, 0.381mm (Fig. 61, 62, 63, 64 and 65) . It is decided on these certain values because duroid materials (5870, 5880, 6002, 6010) are manufactured in these certain thicknesses which are also used in the construction part.

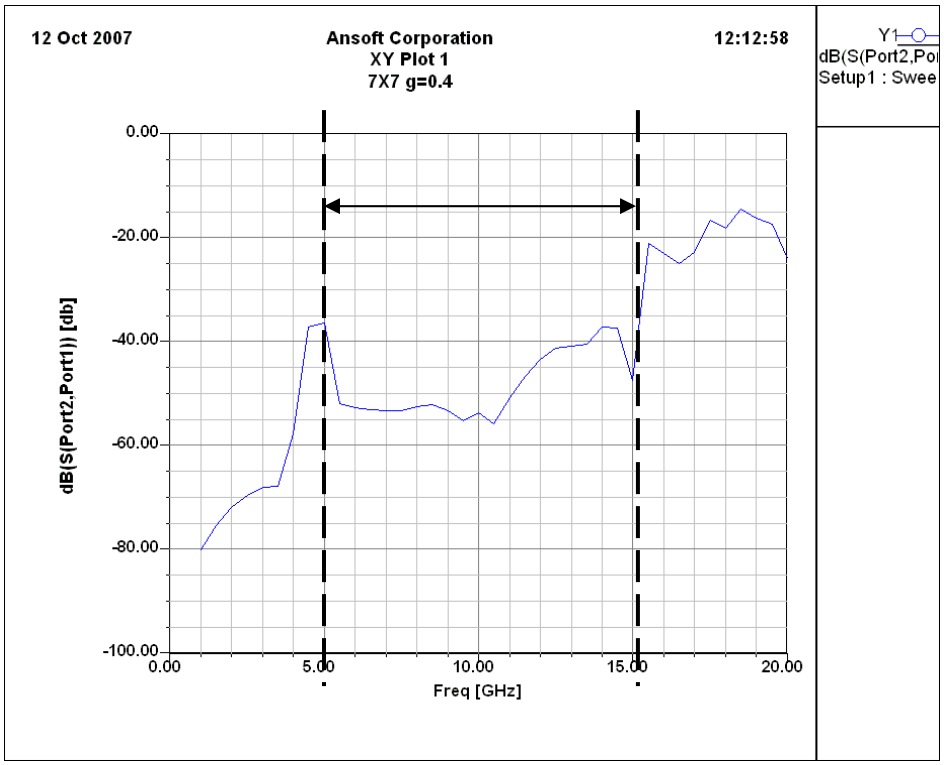

Figure 61. Substrate thickness optimization h=3.175mm (band gap = 5-15GHz)

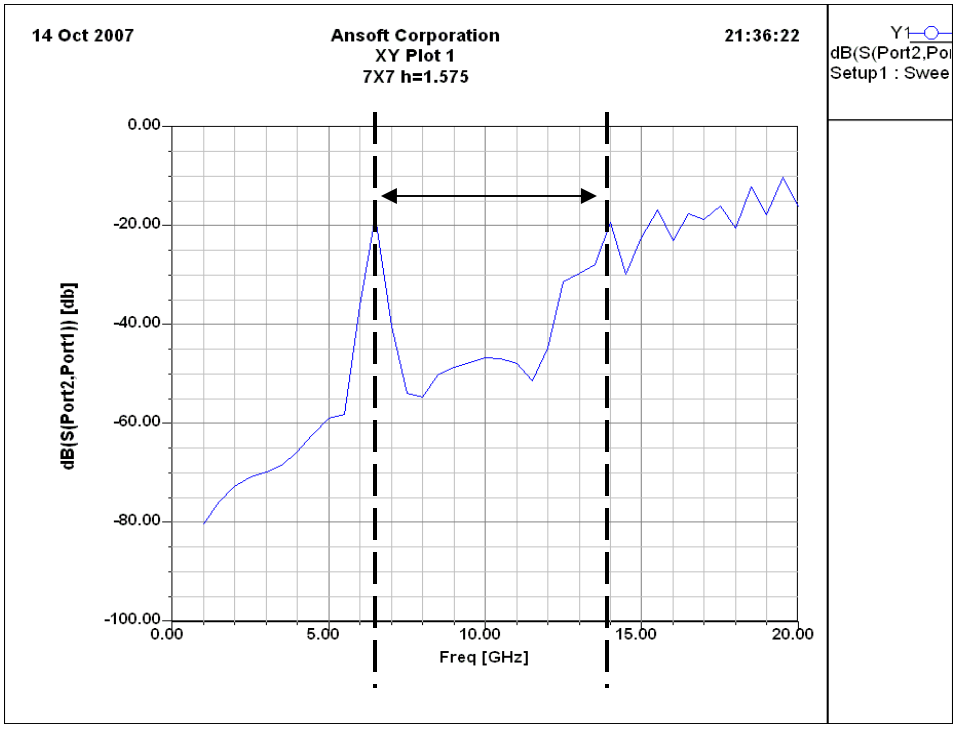

Figure 62. Substrate thickness optimization h=1.575mm
(band gap = 6.5-14GHz)

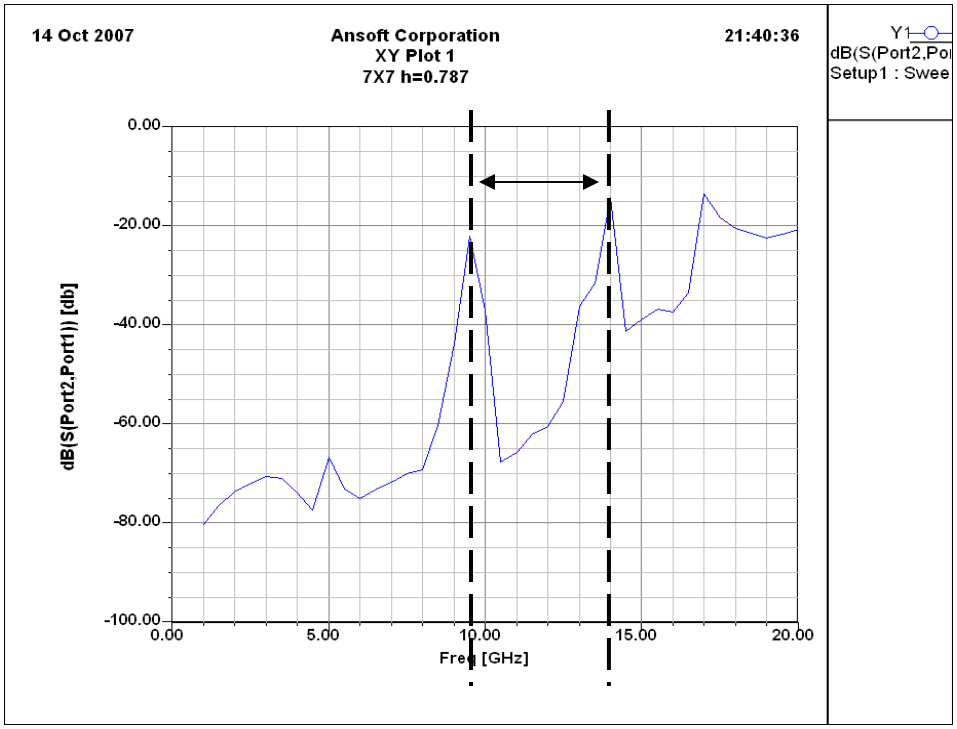

Figure 63. Substrate thickness optimization h=0.787mm
(band gap = 9.5-14GHz)

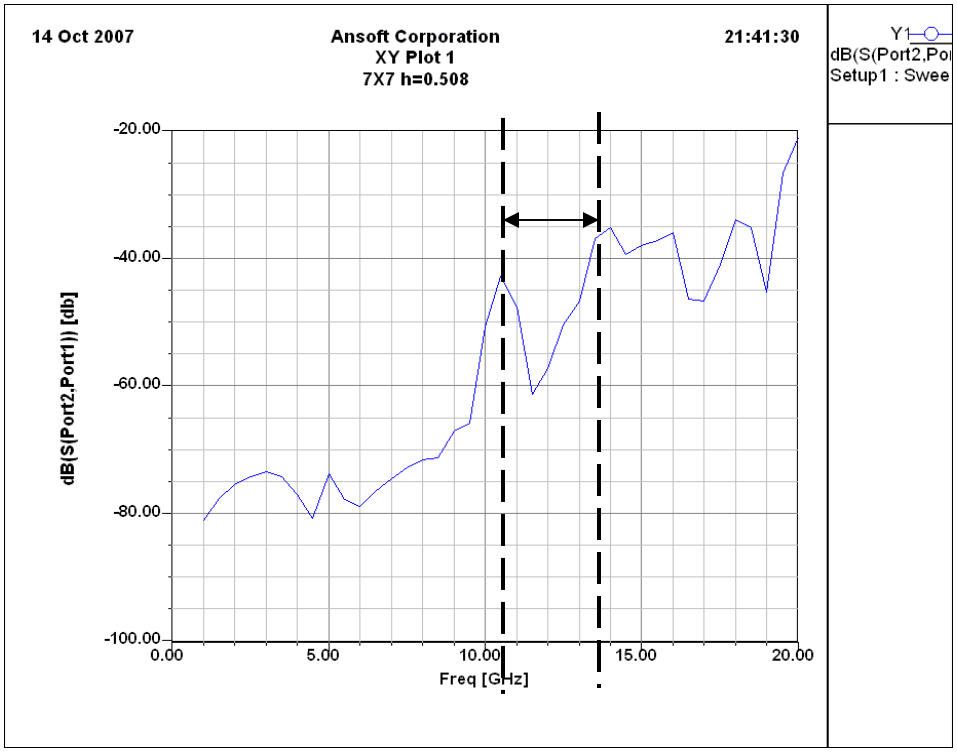

Figure 64. Substrate thickness optimization h=0.508mm
(band gap = 11.5-13GHz)

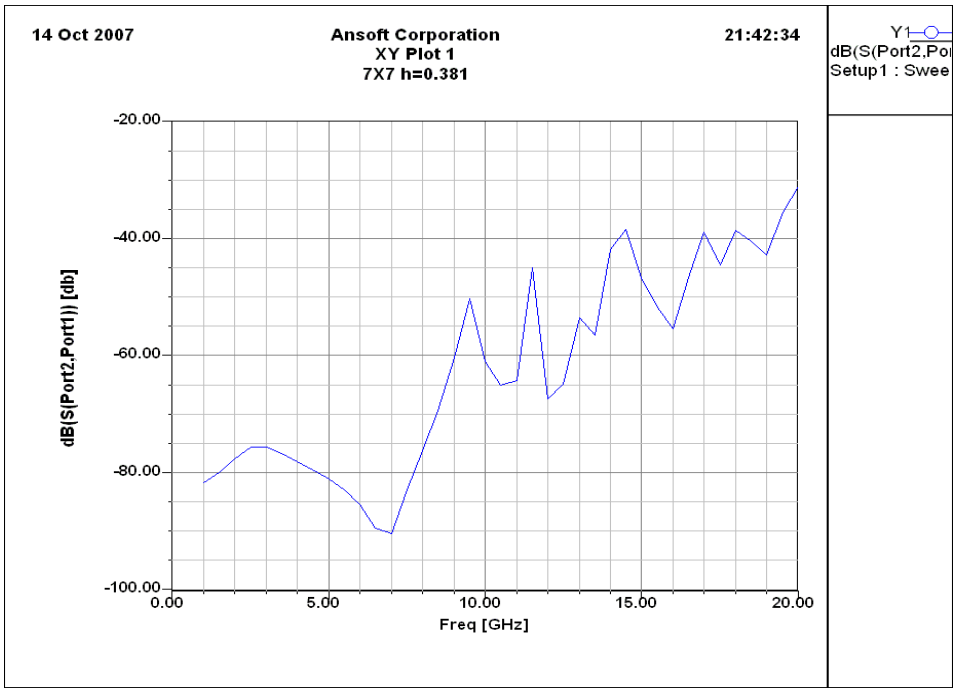

Figure 65. Substrate thickness optimization h=0.381mm
(there is no clear band gap)

These results indicate that choosing thicker substrate thickness provides wider surface wave suppression band gap. Because, inductance increases when the thickness of the substrate is increased. Since the inductance increases, bandwidth of the HIGP increases as well (Eqs.7 and 9). 3.175mm height is the optimum practical height for a HIGP design for the selected thickness values. Next optimization is run by changing the substrate material itself.

Substrate Material Optimization

This part of the optimization process is performed to investigate the effects of changing the substrate material. Since every material has a different permittivity and permittivity is one of the key parameters for the propagation of the electromagnetic waves, band gap characterization should change. Duroid 5880 (ε_r=2.2), Duroid 5870 (ε_r=2.33), Duroid 6002 (ε_r=2.94), Duroid 6010 (ε_r=10.2) are used as substrate materials and w=4.5mm, g=0.4mm, h=3.175 remain constant to see the effect of different materials (Figs. 66, 67, 68 and 69).

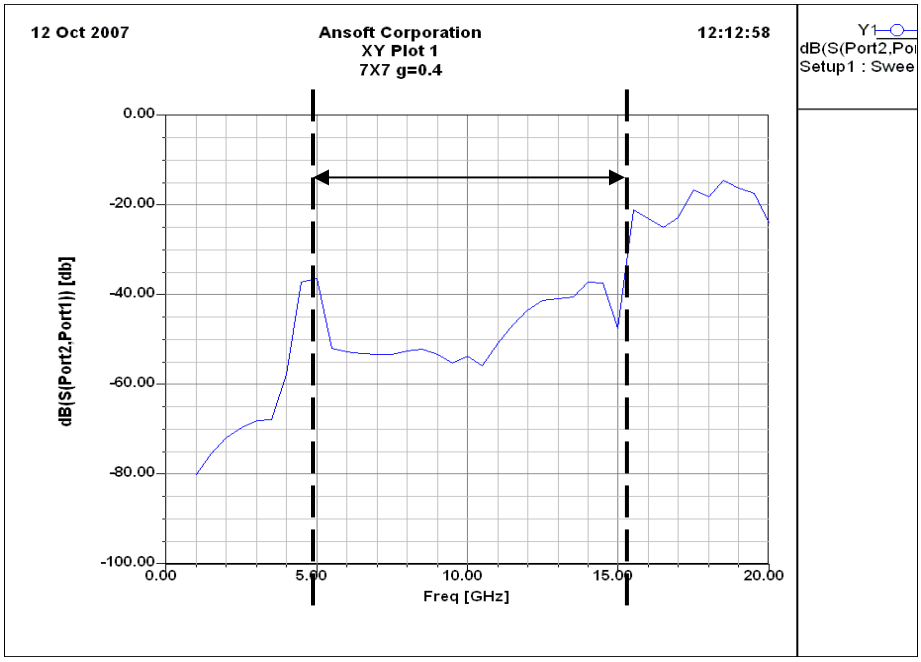

Figure 66. Substrate material optimization Duroid 5880 (ε_r=2.2)
(band gap = 5-15GHz)

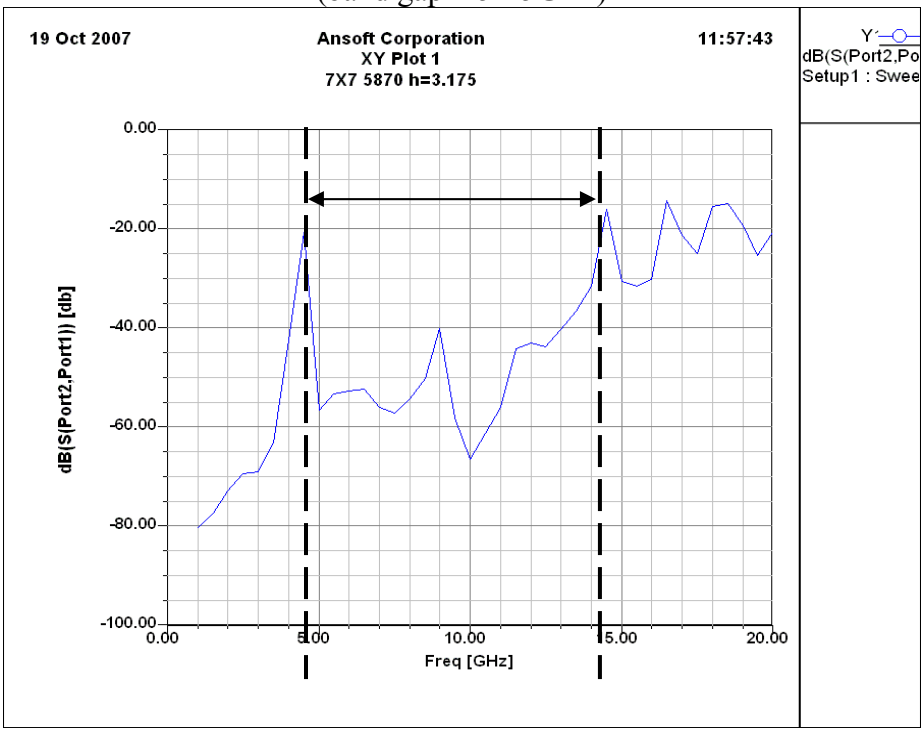

Figure 67. Substrate material optimization Duroid 5870 (ε_r=2.33)
(band gap = 4.5-14.5GHz)

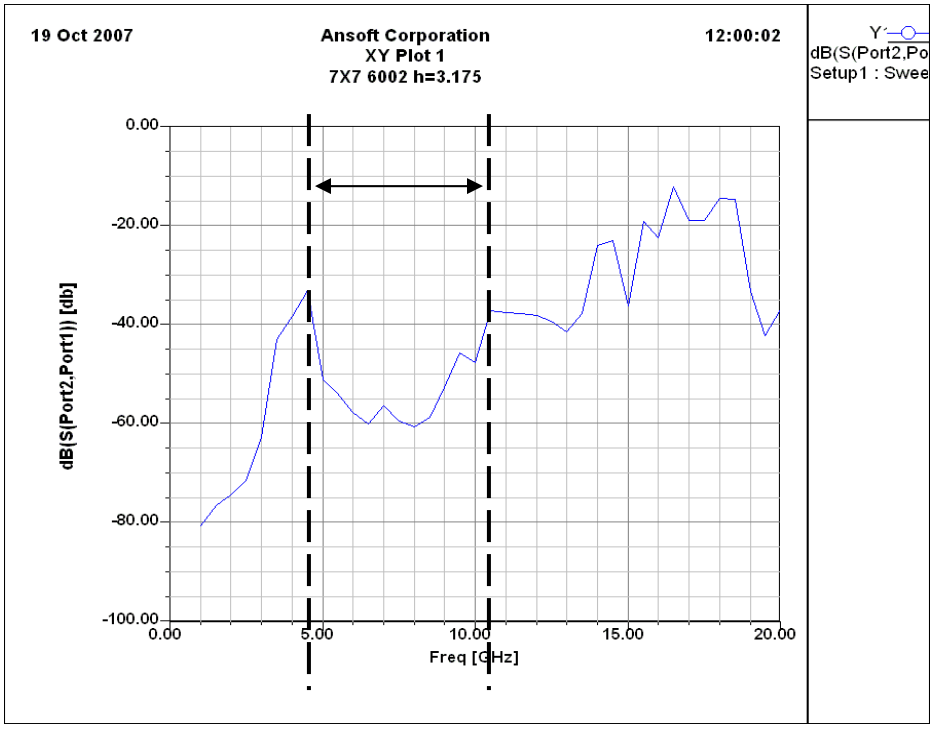

Figure 68. Substrate material optimization Duroid 6002 (ε_r=2.94) (band gap = 4.5-11.5GHz)

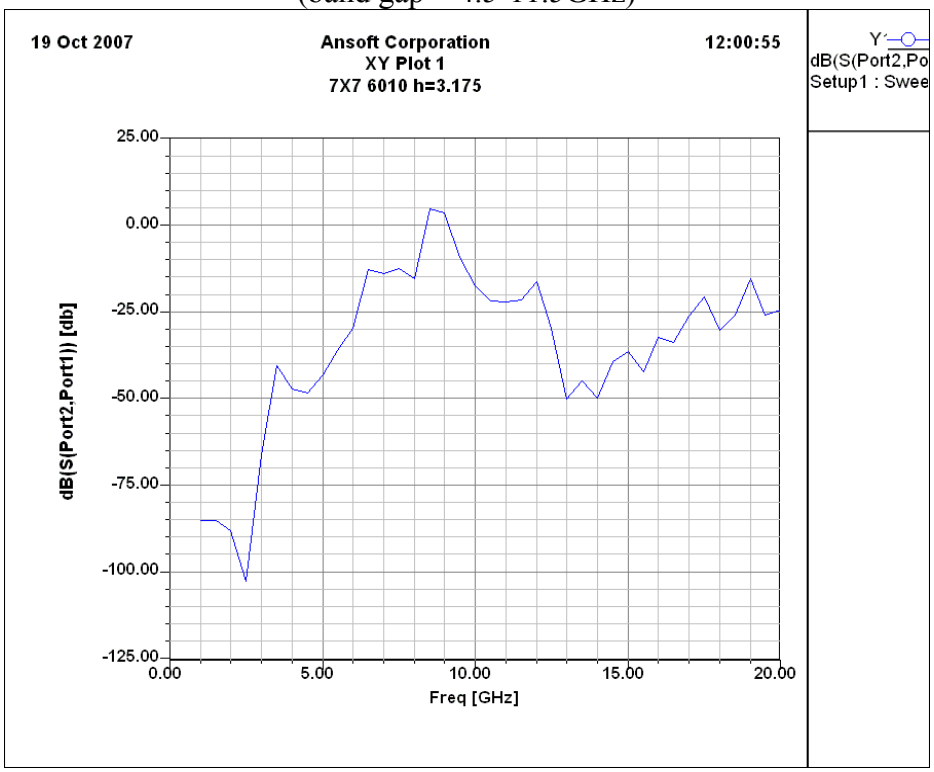

Figure 69. Substrate material optimization Duroid 6010 (ε_r=10.2) (there is no clear band gap)

Using a smaller permittivity material (relative to free space permittivity) as a substrate provides wider band gap behavior. Because using lower permittivity material causes lower capacitance, and lower capacitance causes narrower bandwidth (Eqs. 7 and 8). So that, 5880 and 5870 materials are suitable for HIGP designs with their lower permittivity. Since Duroid 6010 material has extremely higher permittivity in comparison with the other type of materials, the band gap disappears.

Conclusion of the Optimization of the 7x7 Square Patch HIGP:

For the widest band gap, the following parameters should be used in the construction phase:

Patch width (w) = 4.5mm (if 1GHz lower frequency is desired 5.5mm can be used)

Gap width (g) = 0.4mm

Substrate Thickness (h) = 3.175mm

Substrate Material = Duroid 5880 (which has the lowest permittivity)

Dipole Antenna Over Square Patch HIGP Applications

Dipole Antenna Over 7x7 (8GHz) HIGP

A dipole antenna is mounted over 7x7 HIGP design which was previously shown in Fig. 21. The parameters that are used:

$$w = 4.5\text{mm } (0.12\,\lambda_{8\text{ GHz}})$$

$$g = 0.75\text{mm } (0.02\,\lambda_{8\text{ GHz}})$$

$$h = 3.175\text{mm} \tag{13}$$

$$r = 0.406\text{mm}$$

$$L = 0.4\,\lambda_{8\text{ GHz}}$$

$$R = 0.005\,\lambda_{8\text{ GHz}}$$

where, w is the patch width, g is the gap width, h is the substrate thickness, r is the radius of the vias, L is the dipole antenna length and R is the radius of the dipole antenna. $0.02\,\lambda_{8\text{ GHz}}$ distance is left for the dipole antenna height over the surface of the HIGP (Figure 70). Simulation is run to see S_{11} return loss results of the antenna. The same antenna is mounted over PEC and PMC surfaces with the same antenna height. Also dipole antenna (has free space resonant frequency of 9GHz) free space return loss is investigated.

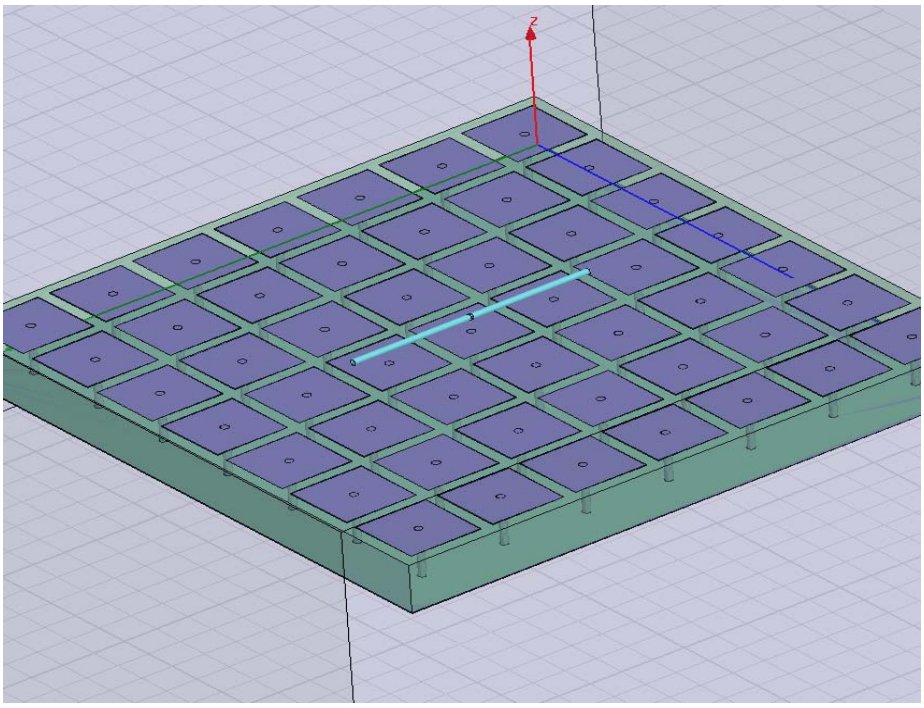

Figure 70. Dipole antenna over 7x7 square patch HIGP

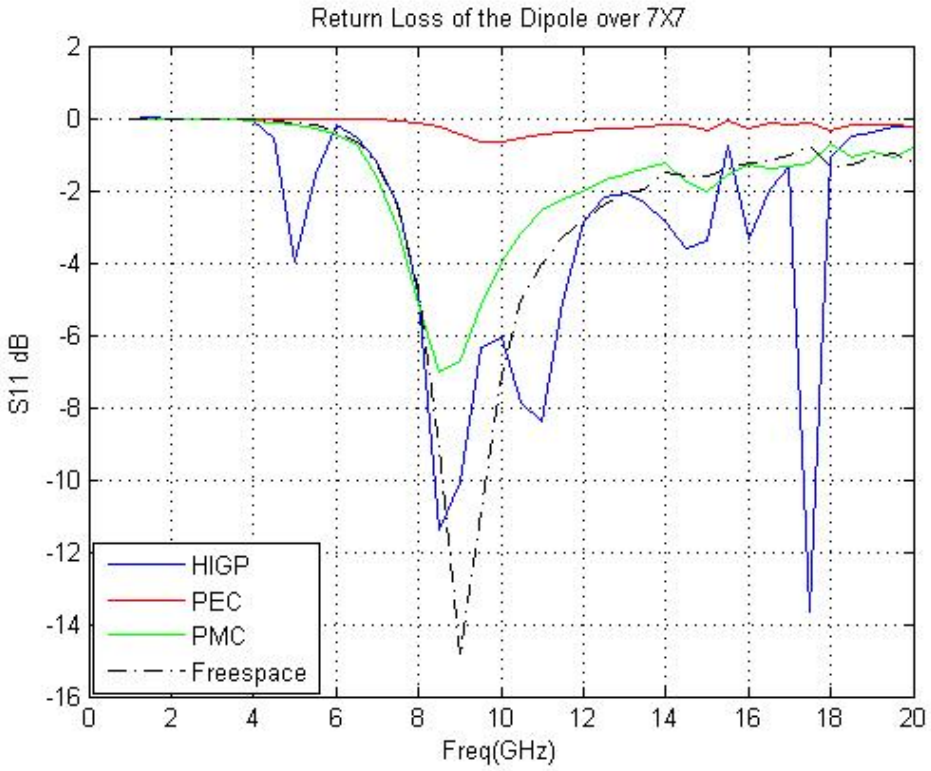

Figure 71. S_{11} Return Loss of the dipole antenna over 7x7 HIGP, PEC, PMC and in free space.

According to total results (Fig. 71), minimum return loss occurs on the antenna which is mounted over HIGP. It operates better than the antennas mounted over both PEC and PMC surfaces and it is very close to free space return loss.

Dipole Antenna Over 9x9 (10 GHz) HIGP

The same parameters of the 7x7 HIGP-antenna design (13) except $\lambda_{10\,\mathrm{GHz}}$ are used instead of $\lambda_{8\,\mathrm{GHz}}$ and number of patch elements are increased to 9x9 (Fig. 72).

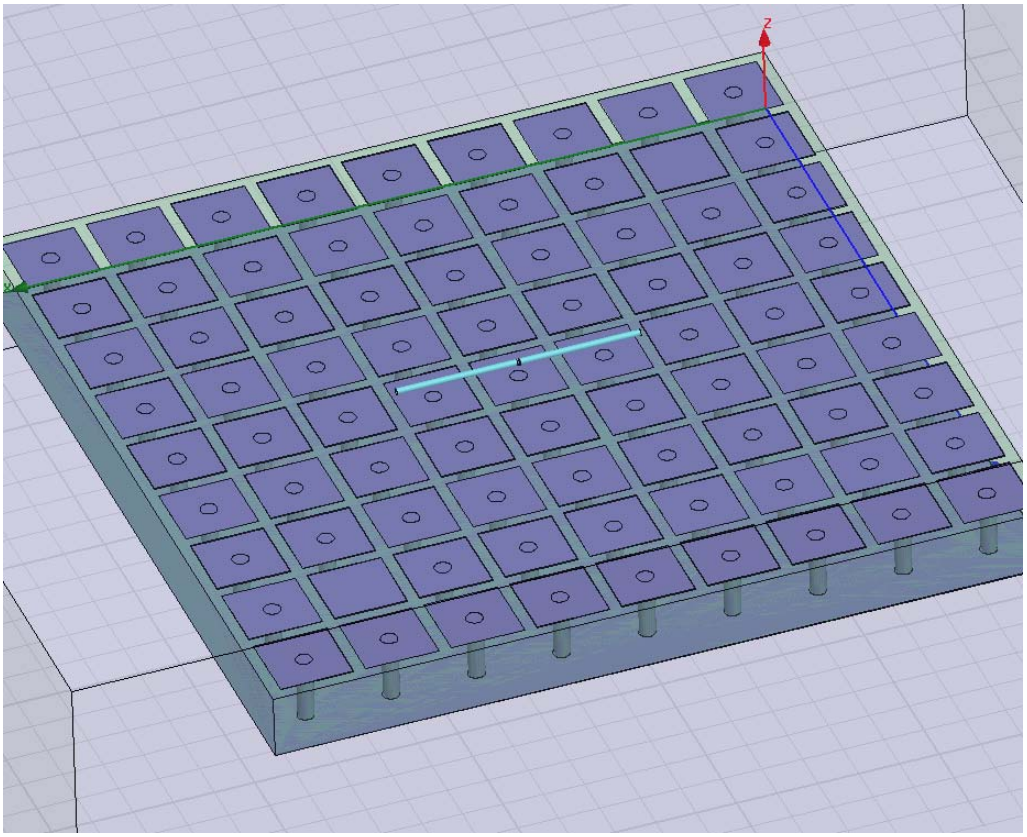

Figure 72. Dipole antenna over 9x9 square patch HIGP

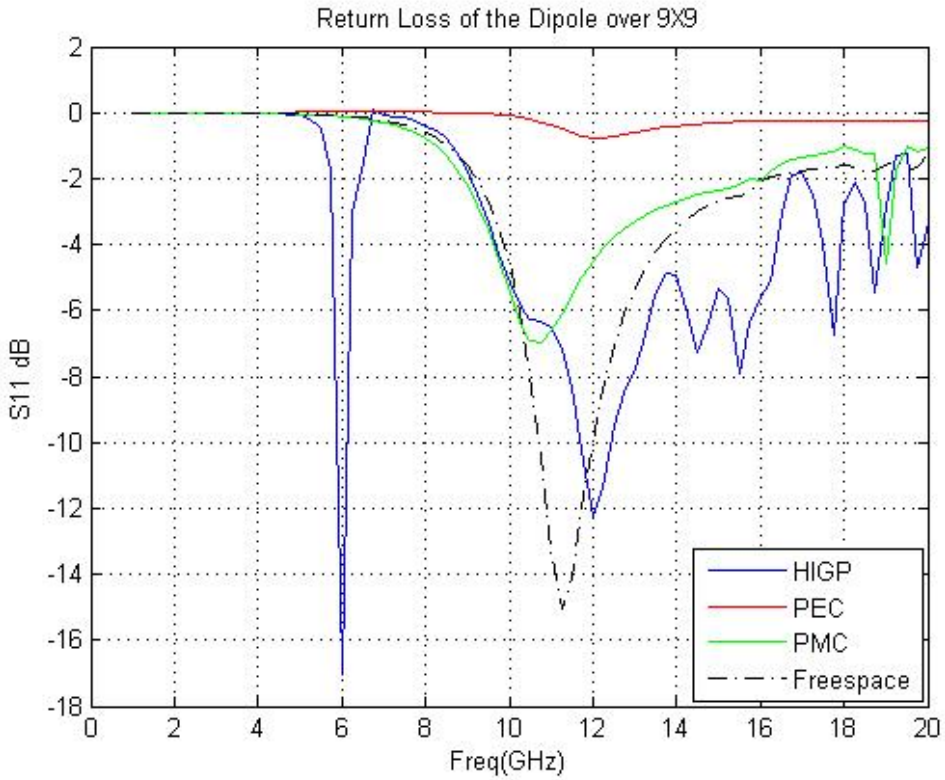

Figure 73. S_{11} Return Loss of the dipole antenna over 9x9 HIGP, PEC, PMC and in free space.

Return loss of the dipole over HIGP in the frequency band 8-16 GHz is lower than PEC and PMC return losses. It is known from Fig. 42 that 9x9 square patch HIGP has a band gap of 6-14 GHz. Since the free space resonant frequency (11 GHz) is inside this band gap, dipole antenna radiates well on this frequency band and gives very low return loss (Fig. 73). Also, another resonant frequency occurs at 6 GHz because of the coupling between the antenna and HIGP. Since this resonant frequency has a very narrow bandwidth, it can not be accepted as a good radiation frequency.

Dipole Antenna Over 11x11 (12 GHz) HIGP

In this application, the same parameters of the 7x7 and 9x9 HIGP-dipole antenna applications are used, except $\lambda_{12\,GHz}$ is used instead of $\lambda_{8\,GHz}$ and $\lambda_{10\,GHz}$ as the multiple for patch width and gap width, also number of the patches is increased to 11x11 (Fig. 74). A dipole antenna which has a free space resonant frequency of 9 GHz is used.

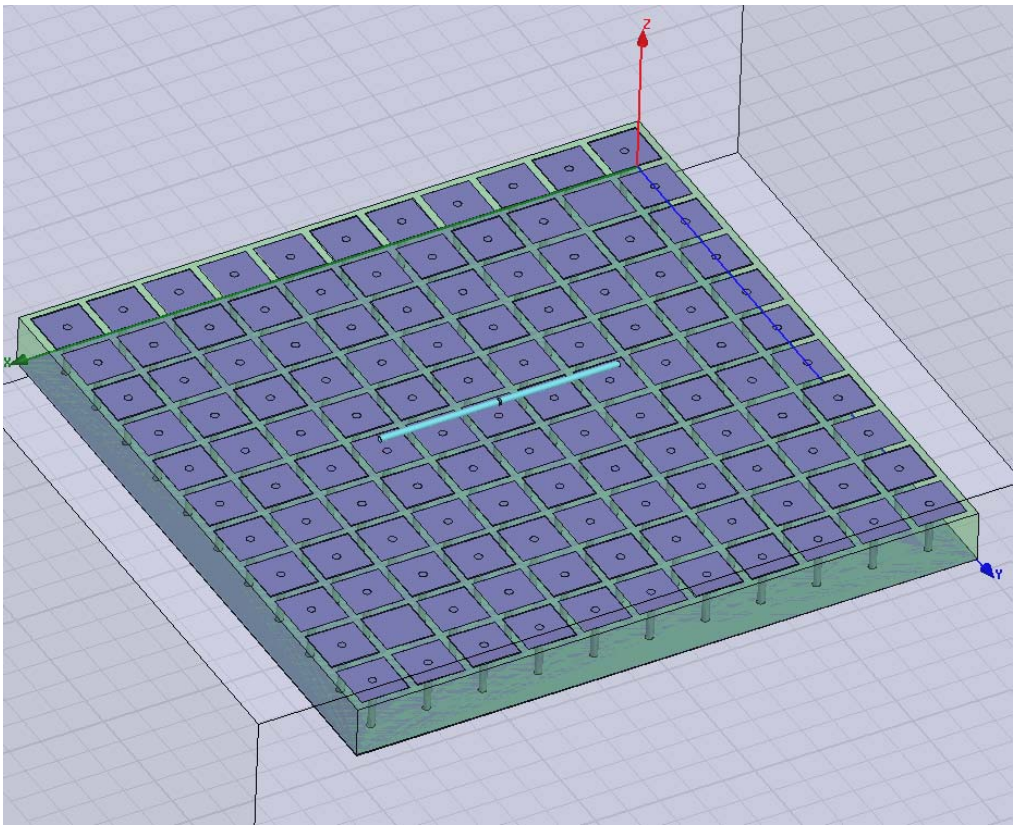

Figure 74. Dipole antenna over 11x11 square patch HIGP

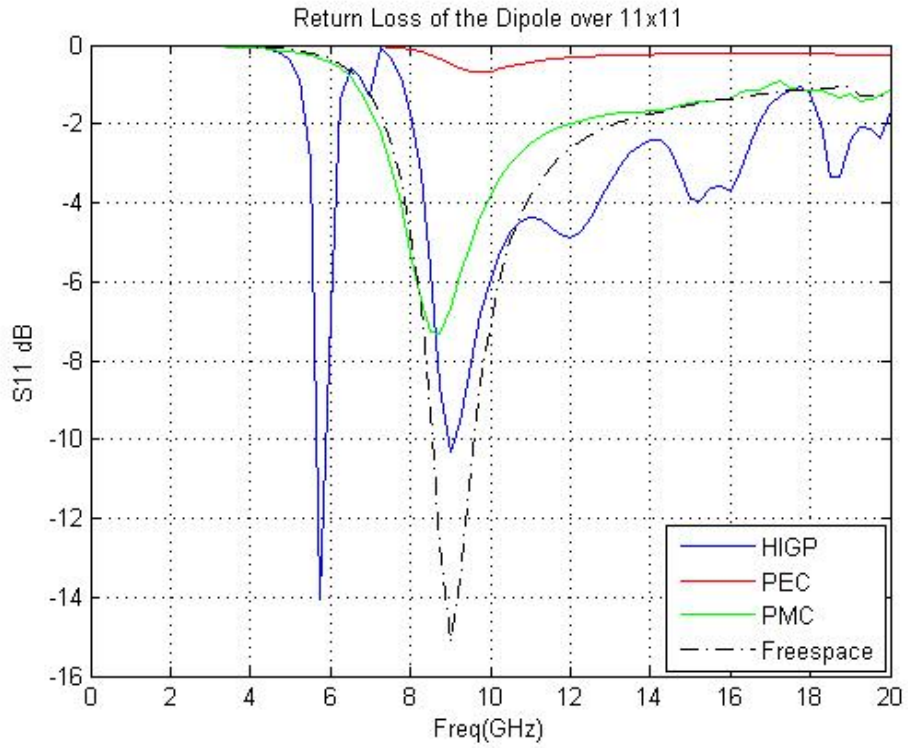

Figure 75. S_{11} Return Loss of the dipole antenna over 11x11 HIGP, PEC, PMC and in free space.

Since the HIGP in this application has a band gap between 6-15 GHz (Fig. 50) and the dipole antenna has a free space resonant frequency (9GHz) inside this band gap, HIGP gives minimum return loss in comparison with PEC and PMC. Dipole over PEC, again has a very high return loss which is very close to 0 dB, in other words it can not radiate. Also a resonant frequency at 6 GHz occurs because of the coupling between the antenna and HIGP. But it has a very narrow bandwidth, so it is not a good radiation frequency that we desire.

Round Patch HIGP Designs

In this application a round patch HIGP design is investigated to find the optimum patch width (diameter) (Fig. 76). Round patches are placed to leave minimum space between them. Two elements in the opposite corners are fed by coaxial cables, and S_{21} parameters are searched to see the band gaps. Gap width (g) is 0.4 mm, substrate thickness (h) is 3.175 mm and RT/duroid 5880 is used as the substrate material in all designs. Diameter of the patches is changed from 4.5mm, 5.5mm, 6.5mm and 7.5mm (Figs. 77, 78, 79 and 80).

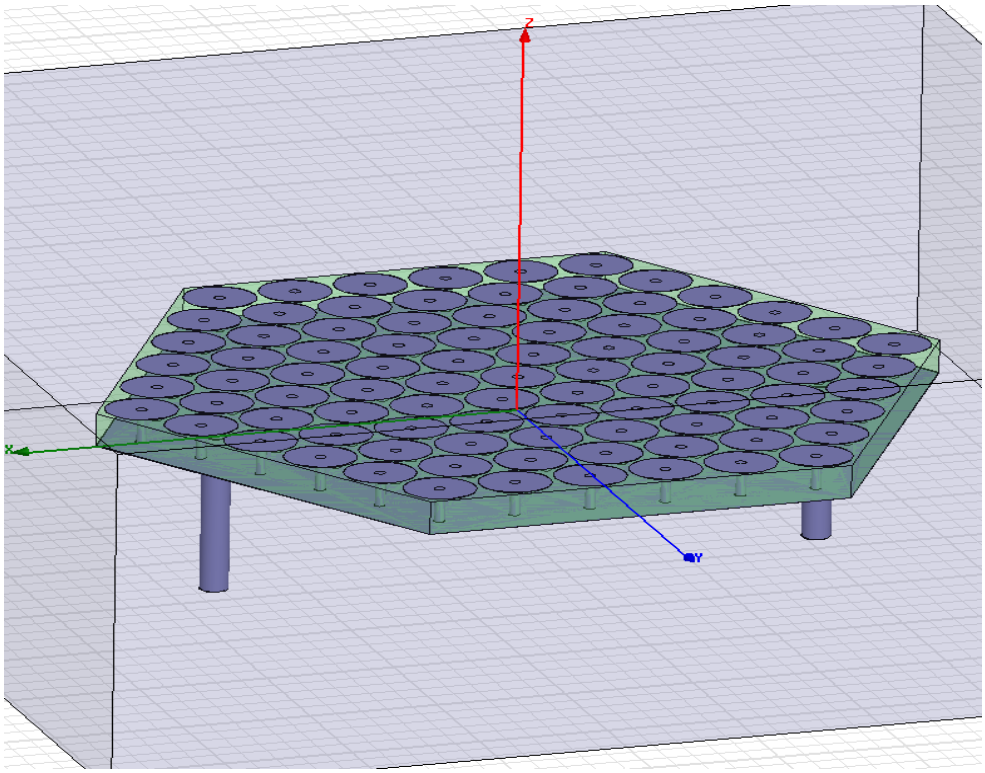

Figure 76. Round patch HIGP

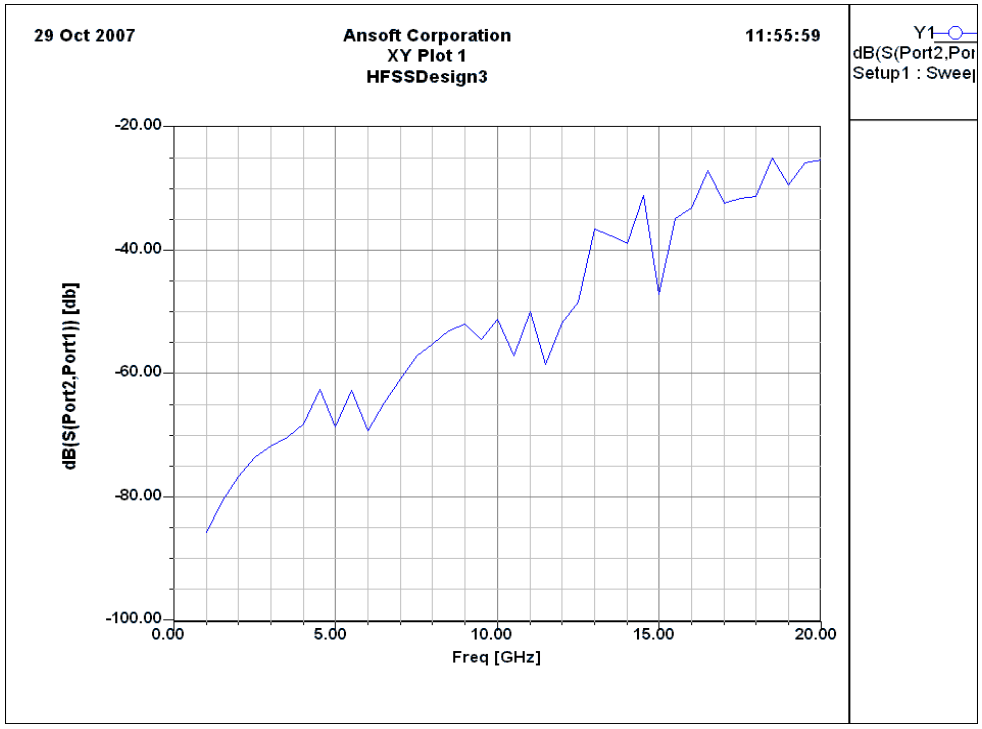

Figure 77. S_{21} Round patch w=4.5mm (no clear band gap)

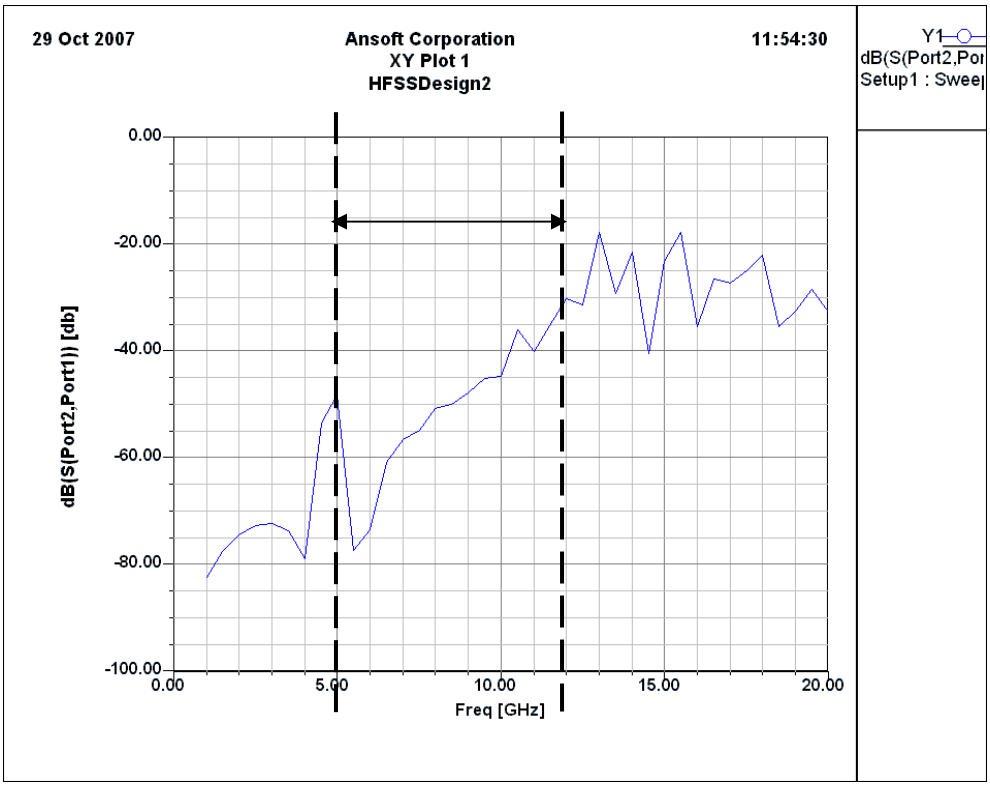

Figure 78. S_{21} Round patch w=5.5mm (band gap=5-12 GHz)

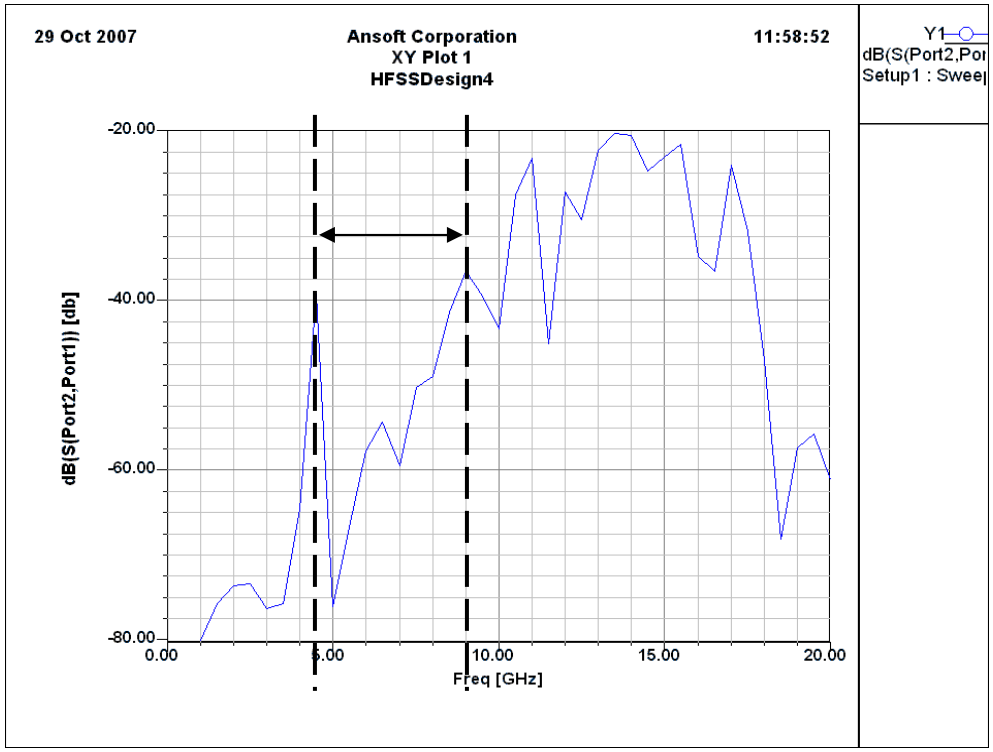

Figure 79. S_{21} Round patch w=6.5mm (band gap=4.5-9 GHz)

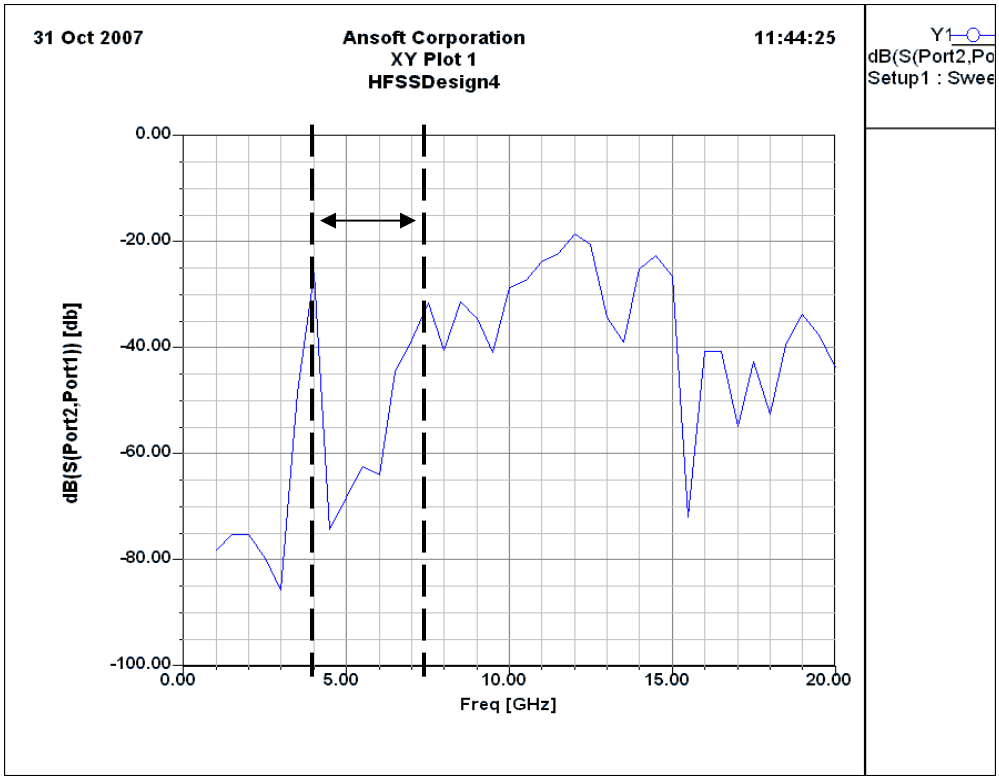

Figure 80. S_{21} Round patch w=7.5mm (band gap=4-7.5 GHz)

5.5mm patch width is the optimum diameter according to these results. 5.5-6.5mm range is the selectable diameter range. Widest band gap occurs in this patch width.

Log Periodic Antenna Applications

Background

A log-periodic antenna is an antenna having a structural geometry such that its impedance and radiation characteristics repeat periodically as the logarithm of frequency (Stutzman and Thiele, 1981: 288). In practice the variations over the frequency band of operation are minor, and log-periodic antennas are usually considered to be frequency independent antennas. One of the first log periodic antennas was the log periodic toothed planar antenna, introduced by DuHamel and Isbell shown in Fig. 81.

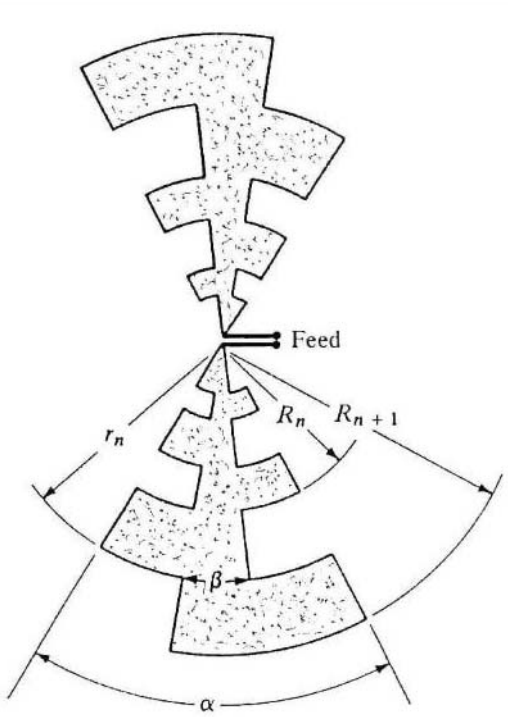

Figure 81. Log-periodic toothed planar antenna. (Duhamel and Isbell, 1957: 124)

Basic log-periodic structure can be defined by a set of ratios (Duhamel and Isbell, 1957). If the geometries of Fig. 80 use uniform periodic teeth, the geometric ratio of the log-periodic structure (τ) is defined by

$$\tau = \frac{R_n}{R_{n+1}} \tag{14}$$

and the geometric ratio of the width of the antenna slot (χ) is defined by

$$\chi = \frac{r_n}{R_{n+1}} \tag{15}$$

The geometric ratio (τ) defines the period of operation. If two frequencies f_1 and f_2 are one period apart, they are related to the geometric ratio (τ) by

$$\tau = \frac{f_1}{f_2}, f_2 > f_1 \tag{16}$$

The angular parameters α and β values found to have no strong requirements for broadband operation. The sum of the angular parameters α and β should be equal to 90^o in order to maintain a self complementary design (DuHamel and Ore, 1958: 139-152). However, DuHamel was able to create working designs where β went to zero. He also showed the shape of the antenna can change if the fundamental log-periodic structure is maintained.

Log-periodic Antenna Design for HIGP

In order to see the characteristics of a broadband antenna over HIGP, PEC and PMC, a log-periodic antenna with the following parameters was designed related to Fig. 81:

$$L = 58.9\text{mm}$$

$$G = 3\text{mm}$$

$$\tau = 0.775$$

$$\chi = 0.885 \qquad (17)$$

$$\alpha = 67.5^{o}$$

$$\beta = 22.5^{o}$$

where L is the total antenna length, G is the gap between two antenna elements. Free space, over PEC, over PMC and over different type of HIGP return losses of the designed antenna are shown in Figures 82, 82, 83, 84, 85, 86 and 87.

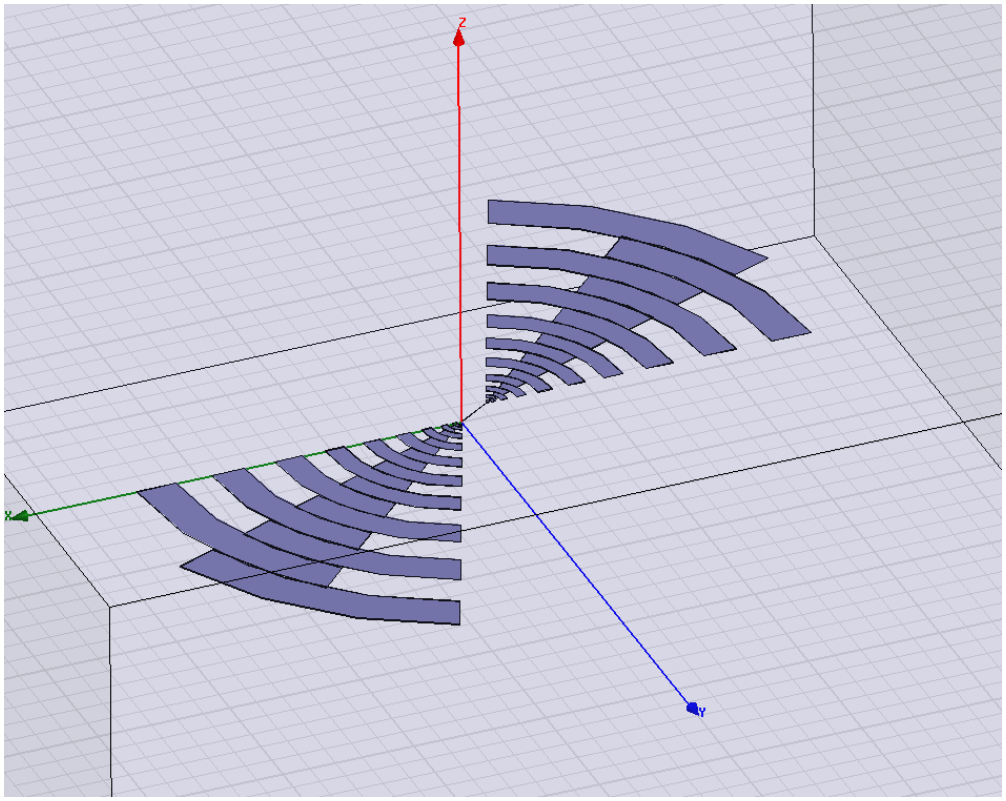

Figure 82. Log-periodic antenna in free space

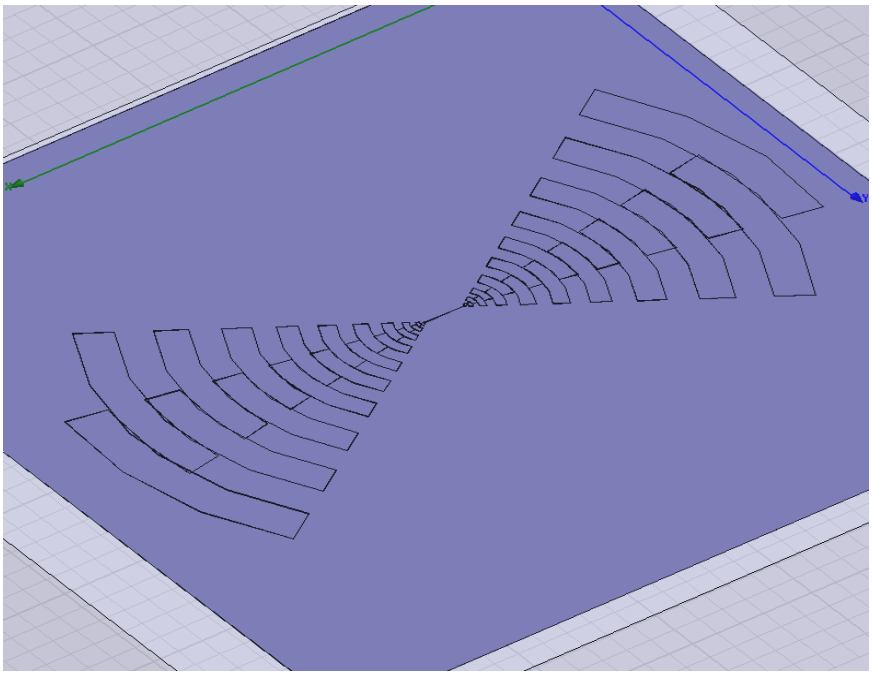

Figure 83. Log periodic antenna over PEC and PMC

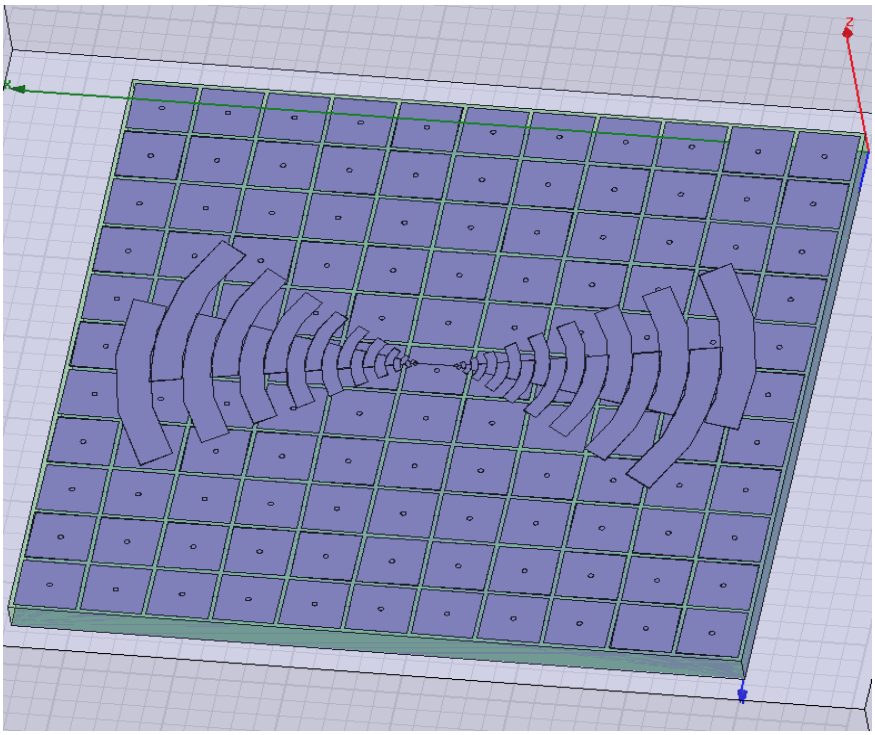

Figure 84. Log-periodic antenna over optimized square patch HIGP (w=5.5mm, g=0.4mm, h=3.175mm)

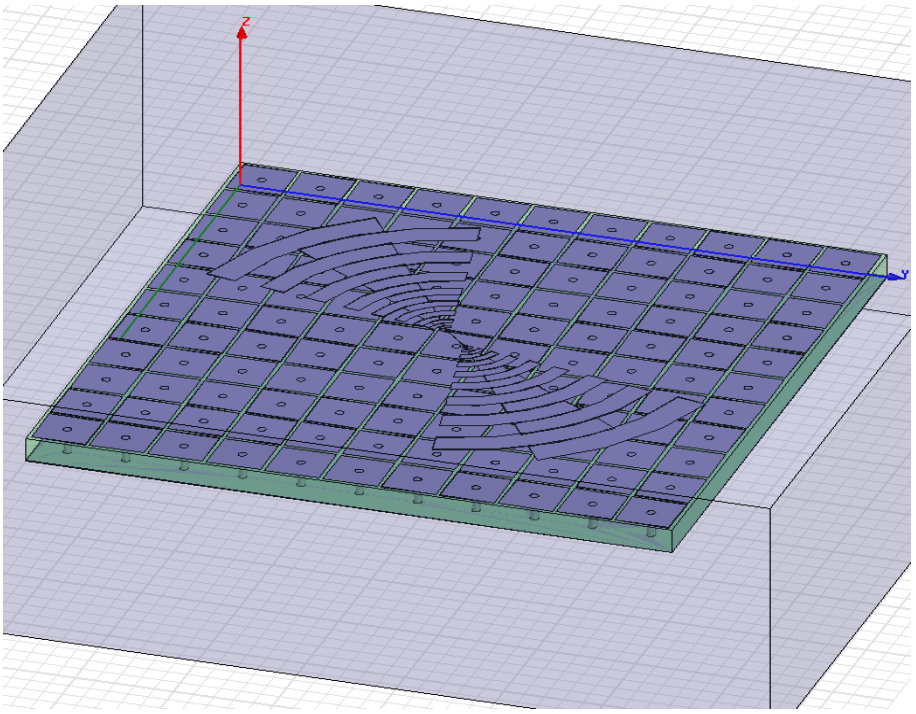

Figure 85. Log-periodic antenna over optimized square patch HIGP (diagonal)

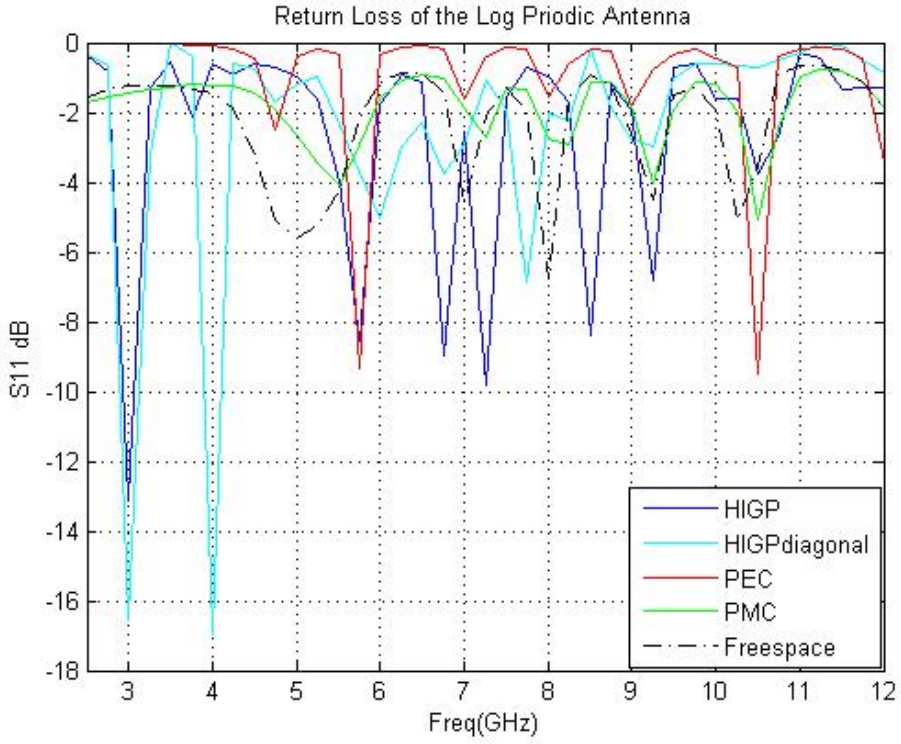

Figure 86. S_{11} of the log periodic antenna over HIGP, HIGPdiagonal, PEC, PMC and in free space

Many resonant frequencies occur because of the log periodic antenna arms. According to the results of Fig. 86, log-periodic antenna mounted over both parallel to HIGP and diagonal to HIGP provides less return loss in the frequency region of 5-10 GHz than PEC and PMC, because this frequency region is inside the frequency band gap of the optimized square patch HIGP.

Log-periodic Antenna Over Round Patch HIGP

The same type of log periodic antenna is mounted over round patch HIGP which was previously introduced in Fig. 76 (Fig 87). In this application 3 different patch widths are used: 5.5, 6.5, 7.5mm (Figs. 87 and 88).

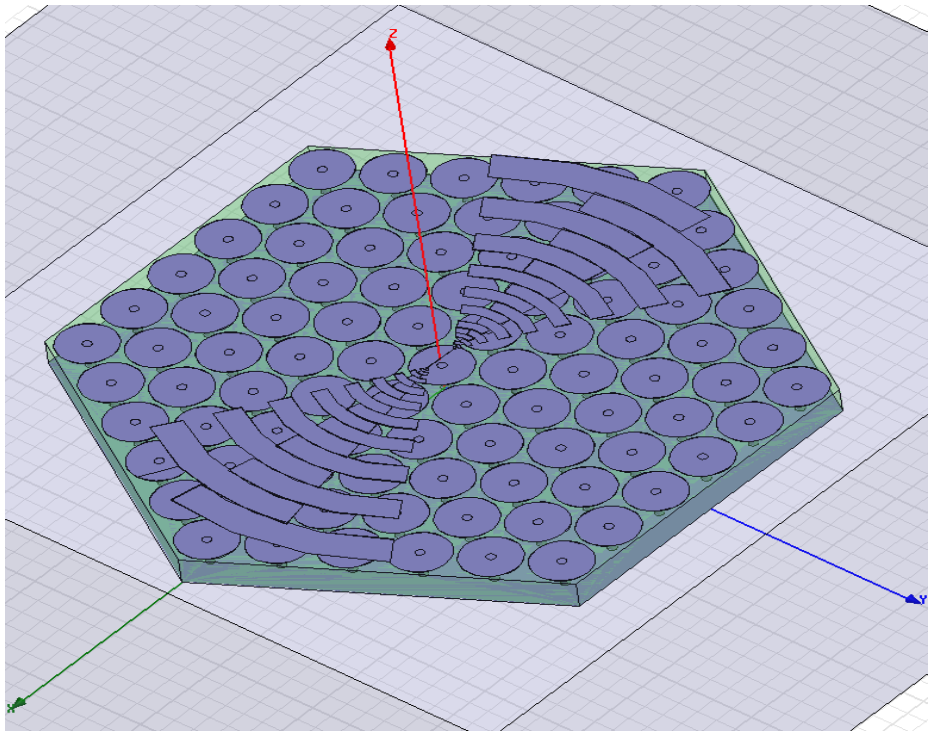

Figure 87. Log periodic antenna over round patch HIGP

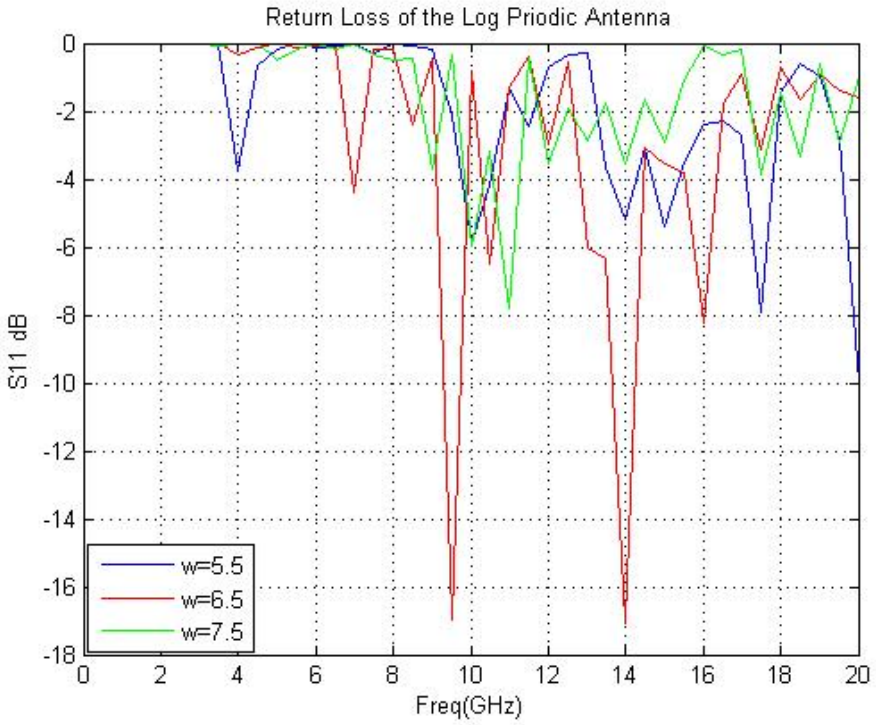

Figure 88. S_{11} of the log-periodic antenna over round patch HIGP (w=5.5mm, 6.5mm, 7.5mm)

Fig. 88 shows that 6.5mm and 5.5mm patch widths are more efficient than 7.5mm patch width, which is consistent with the optimized round patch HIGP result in Figs. 78, 79 and 80.

Hexagon Patch HIGP Optimization (patch width optimization)

In this optimization process, hexagon patches are used instead of round patches and optimum patch width is found by changing patch width value with 3.5mm, 4.5mm, 5.5mm, 6.5mm, 7.5mm and 8.5mm (Figs. 89, 90, 91, 92, 93, 94 and 95). In all of the examples RT/duroid 5880 is used as the substrate material, where 3.175mm is used as the substrate thickness (h) and 0.4mm is used as gap width (g).

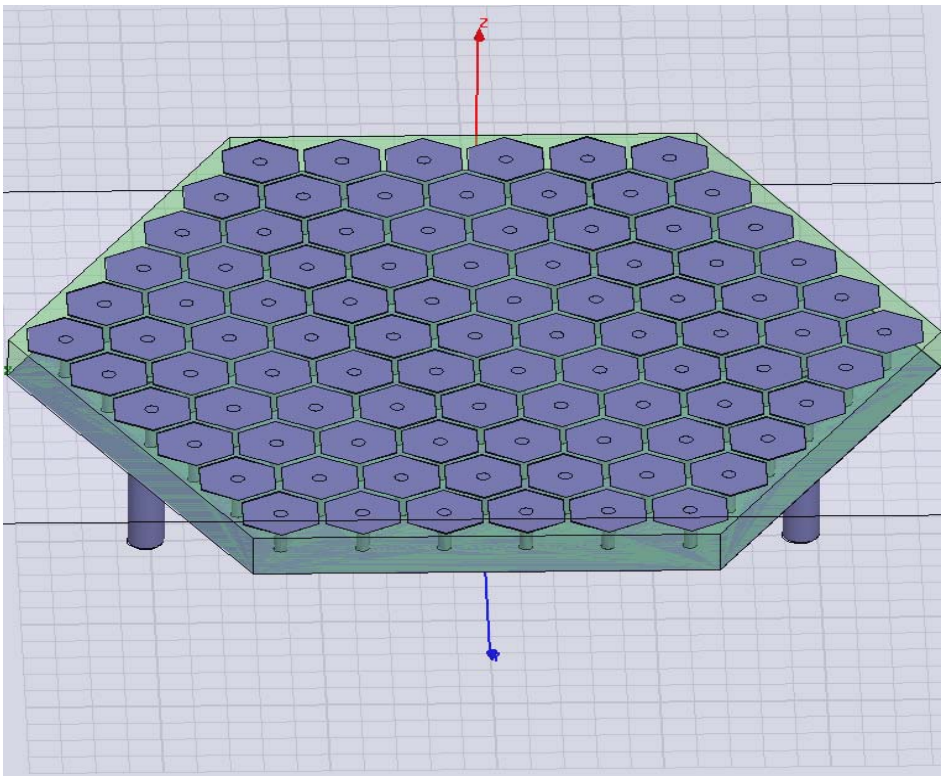

Figure 89. Hexagon patch HIGP design

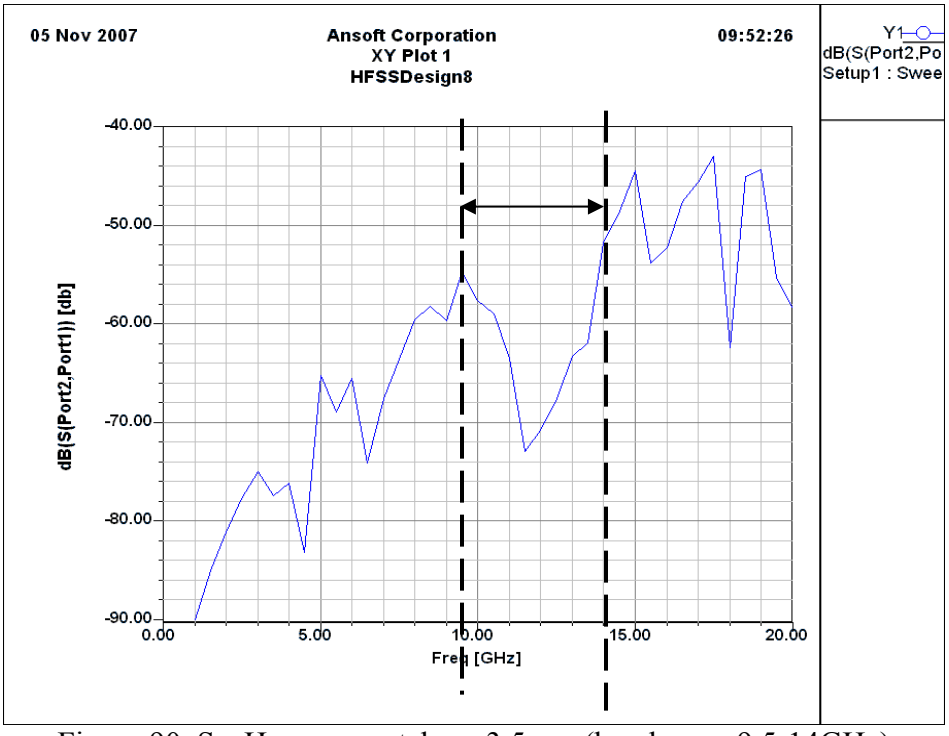

Figure 90. S_{21} Hexagon patch w=3.5mm (band gap= 9.5-14GHz)

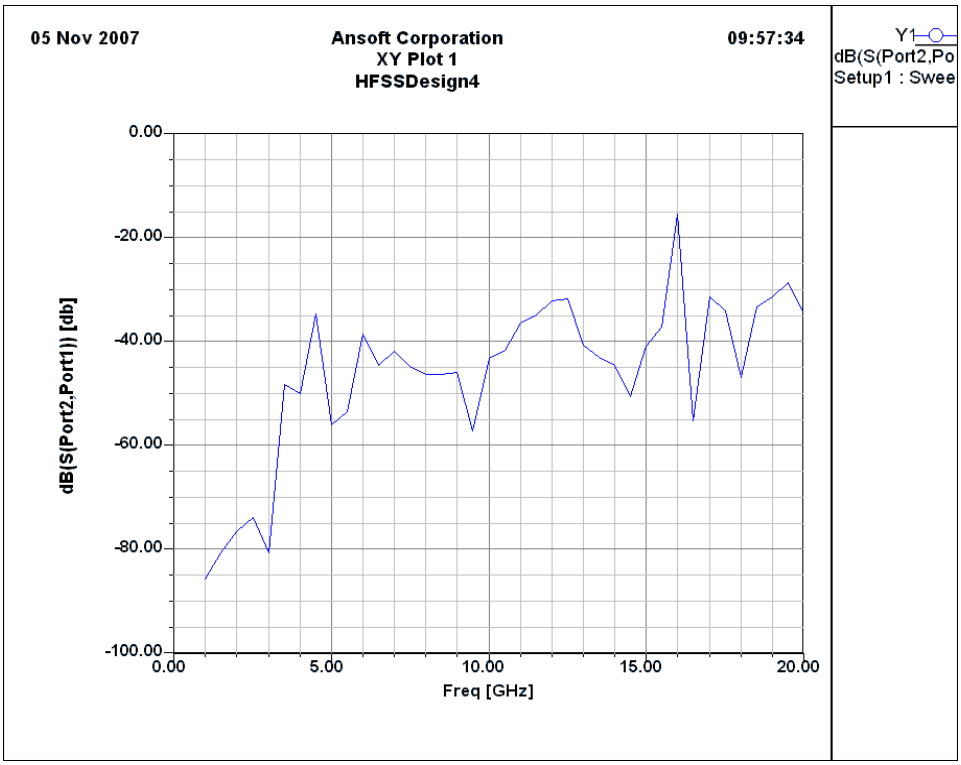

Figure 91. S_{21} Hexagon patch w=4.5mm (there is no clear band gap)

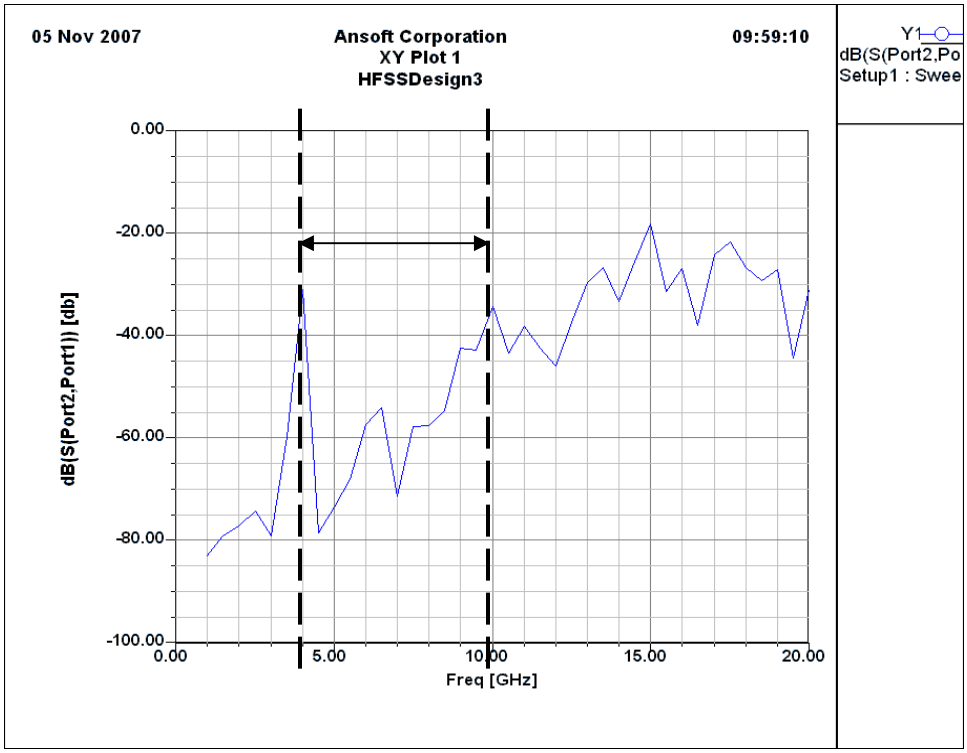

Figure 92. S_{21} Hexagon patch w=5.5mm (band gap= 4-10GHz)

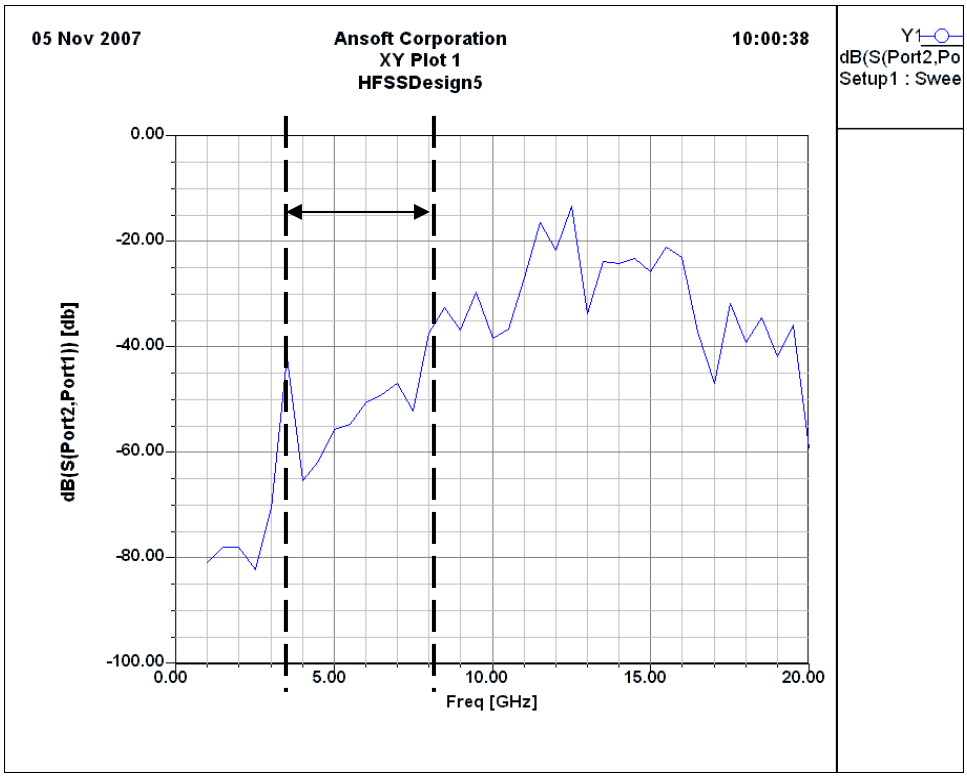

Figure 93. S_{21} Hexagon patch w=6.5mm (band gap= 3.5-8 GHz)

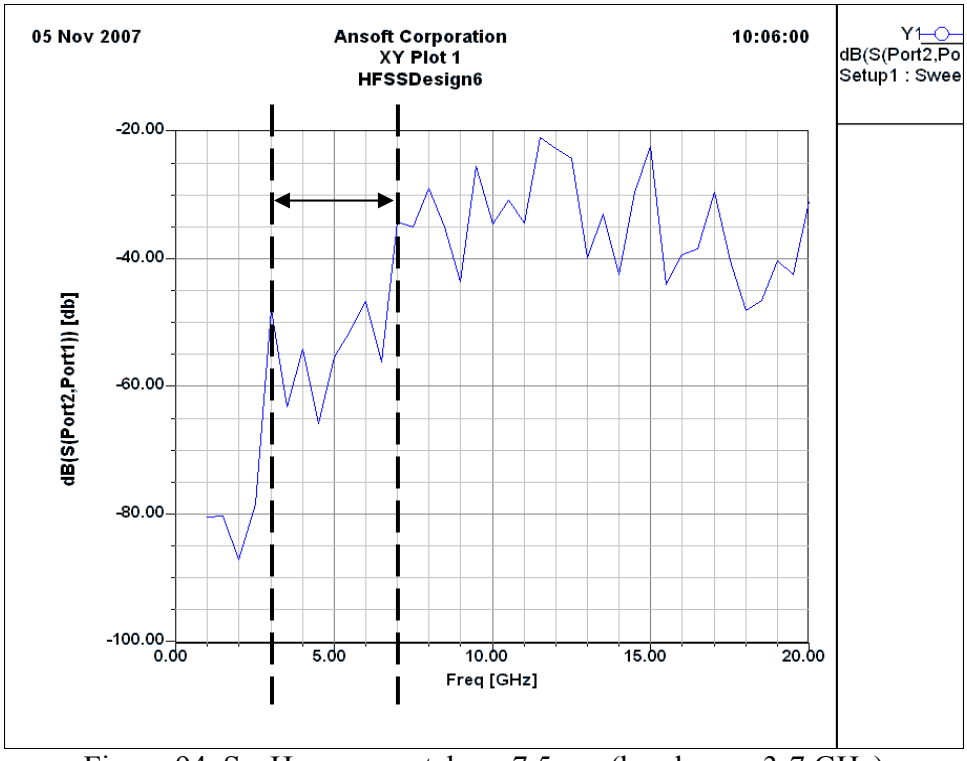

Figure 94. S_{21} Hexagon patch w=7.5mm (band gap= 3-7 GHz)

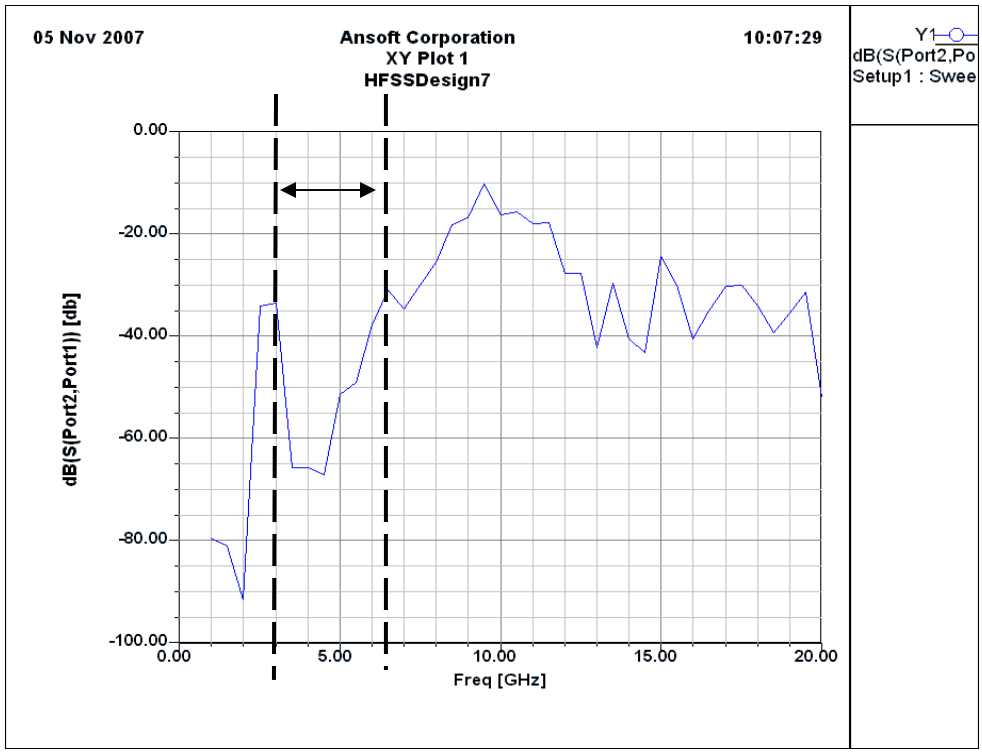

Figure 95. S_{21} Hexagon patch w=8.5mm (band gap= 3-6.5 GHz)

It's obviously seen from the results above that, using 5.5mm as the patch width for the hexagonal HIGP gives the widest suppression band gap (4-10 GHz). These results show that there is no significant band gap change between the hexagon patch and round patch HIGPs. Band gaps are very close to each other on the same patch widths.

Triangle Patch HIGP and Bow Tie Antenna Applications

In this part triangle shape is used as the patch shape both to see the difference with the previous designs and to combine these triangle patch HIGPs with the triangle shape bow tie antennas. Another important point of this part is to combine two different patch widths on the same HIGP-Bow Tie Antenna design to increase the total operating bandwidth.

Triangle Patch HIGPs

Triangle patch HIGPs are designed as 17x18 elements. Each equilateral triangle patch element is connected to the bottom metal ground plane by the way of conductor vias through the center of the triangles. The ground plane is fed by two coaxial cables from the middle elements of the third rows of the opposite edges (Fig. 96). RT/Duroid 5880 is used as the substrate material, 0.406mm is used as the radius of the vias, 0.4mm is used as gap width (g), 3.175mm is used as the thickness of the substrate (h). Four different patch widths (5.2mm, 7.6mm, 8mm, 16mm) are used to see the proper band gap (Figs. 97, 98, 99 and 100).

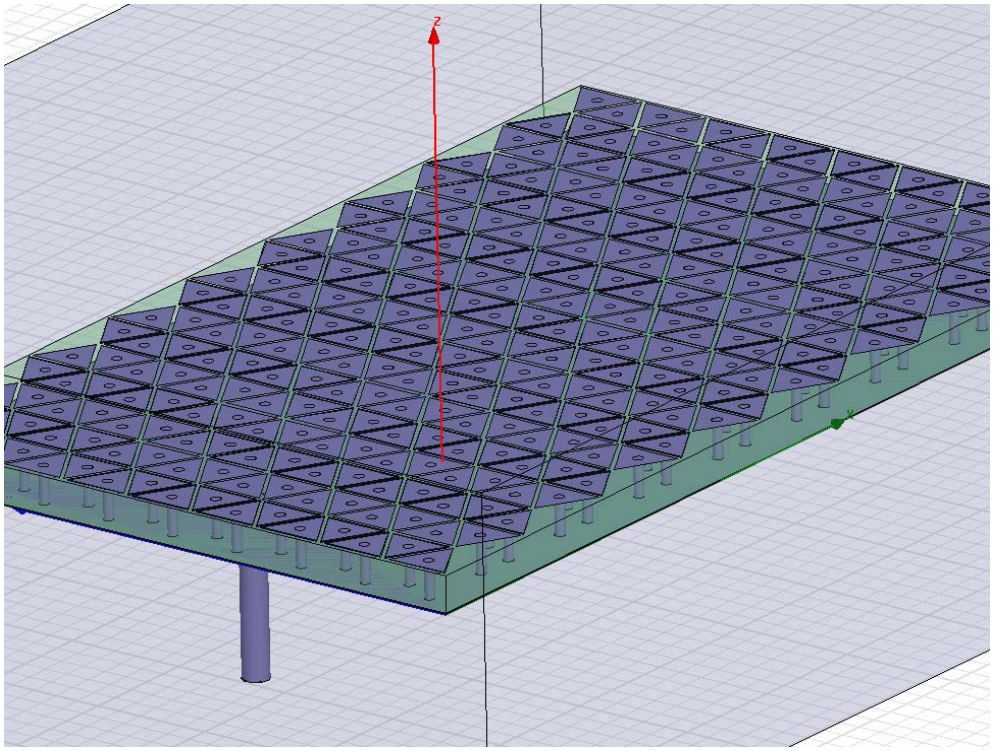

Figure 96. Triangle patch HIGP

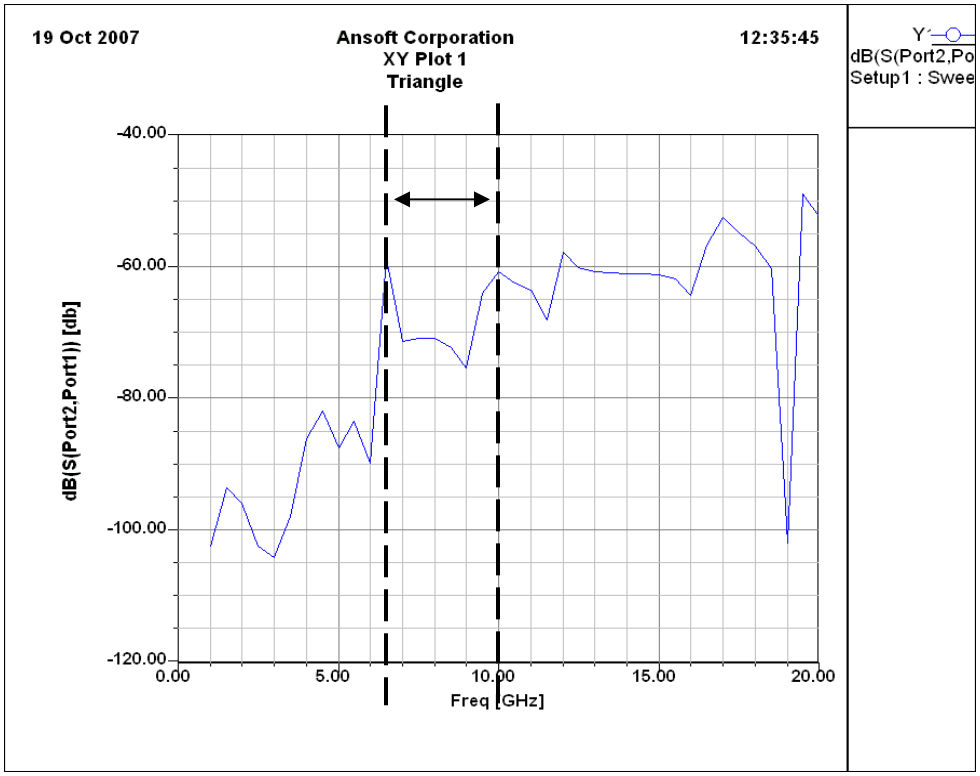

Figure 97. S_{21} triangle patch w=5.2mm (band gap=6.5-10 GHz)

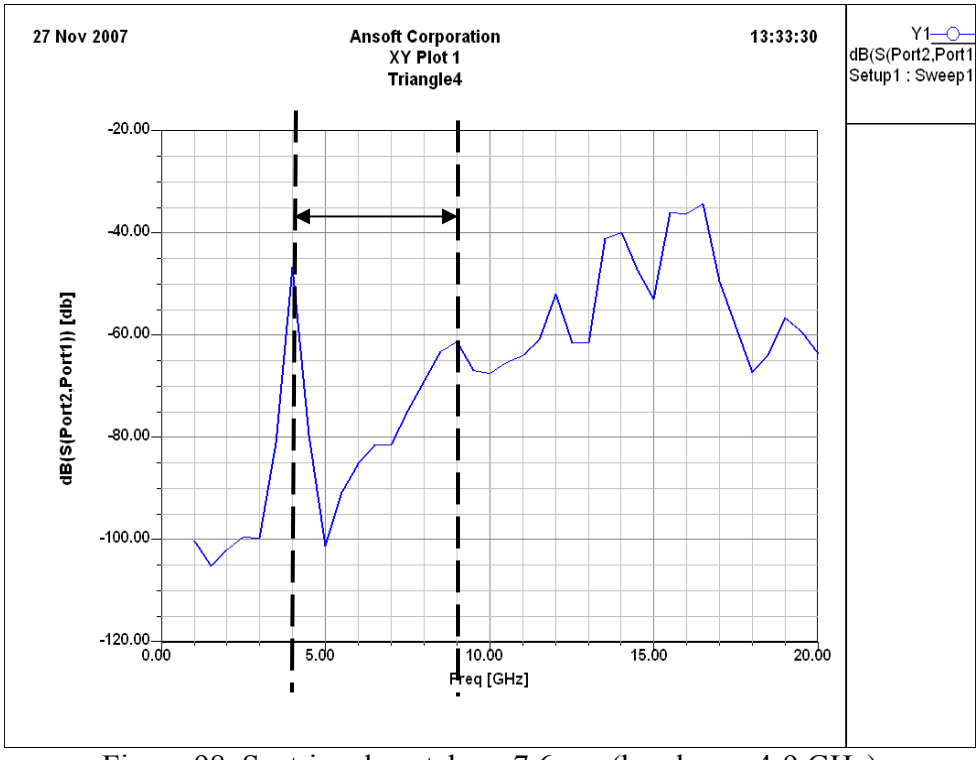

Figure 98. S_{21} triangle patch w=7.6mm (band gap=4-9 GHz)

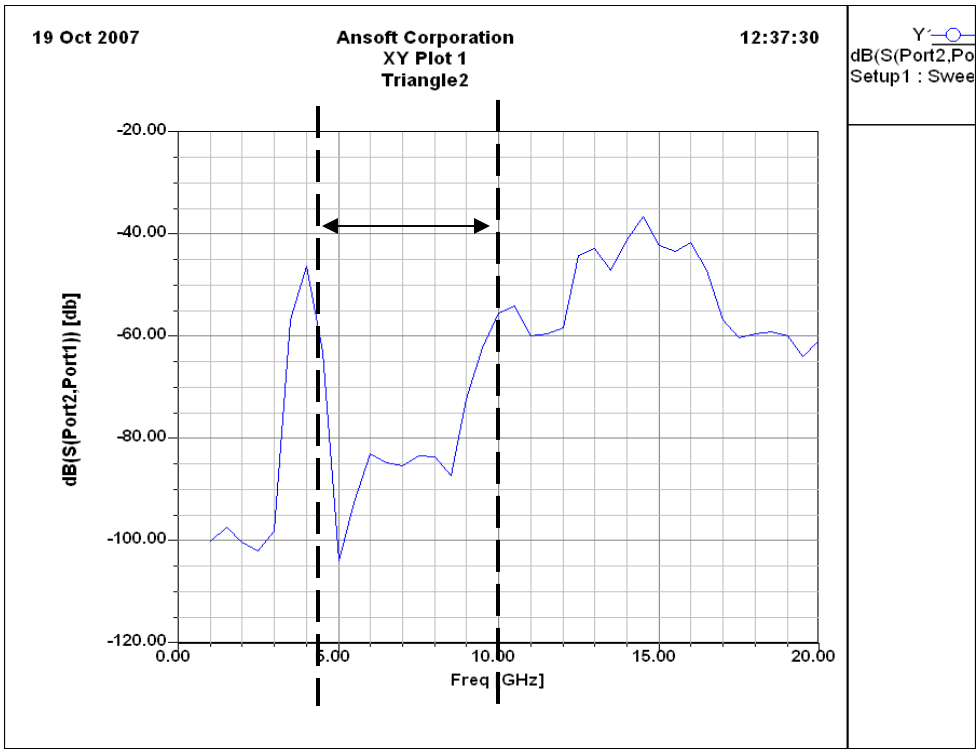

Figure 99. S_{21} triangle patch w=8mm (band gap= 4.5-10 GHz)

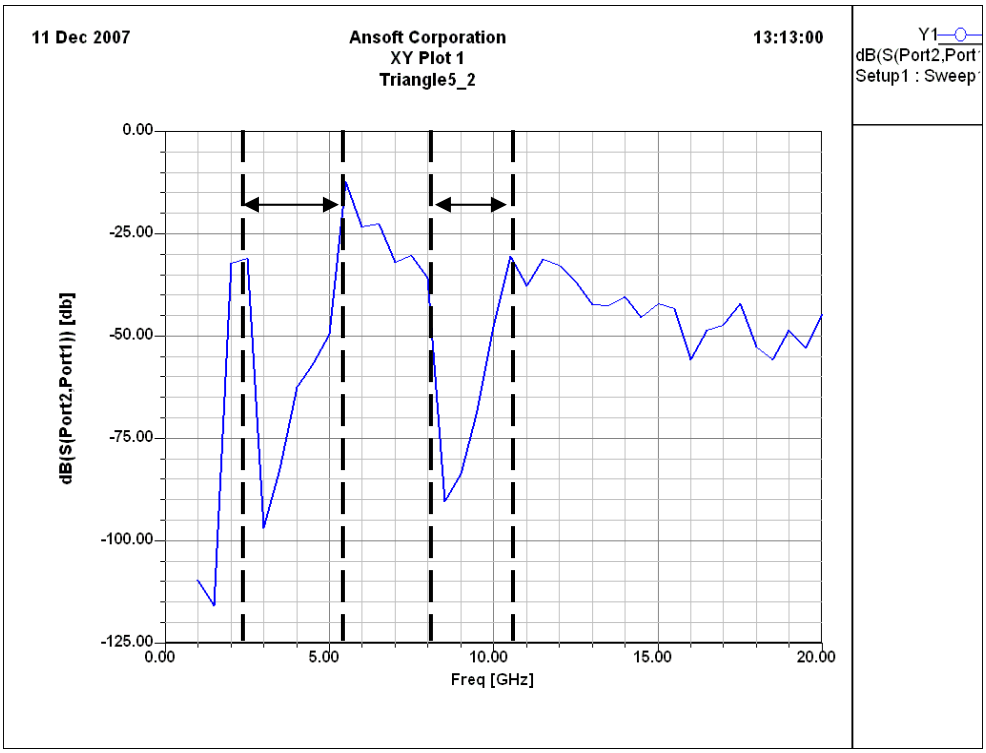

Figure 100. S_{21} triangle patch w=16mm (band gap= 2-5 GHz and 8-10.5 GHz)

8mm patch width design gives the widest frequency band gap (4.5-10 GHz). If lower frequency region is desired, 16mm patch width can be used to preserve bandwidth between 2-5 GHz as well.

HIGP-Bow Tie Antenna Applications

To provide a baseline for designing a broadband high impedance ground plane, a bow-tie antenna is first applied to a ground plane which the triangle patches surround the bow-tie antenna. The main difference of this HIGP-antenna structure is the placement of the antenna element. In the previous designs, antennas were mounted over the HIGP, but in this application, the bow–tie antenna is mounted inside the HIGP not only to reduce the overall thickness of the structure but also to preserve bandwidth.

In the first application, 7mm is used as both the triangle patch width and the length of the one edge of the two arm bow-tie antenna (Fig. 101). Other dimensions are left the same with the previous ones.

The same bow-tie antenna is mounted:

- over PEC (distance between the PEC and the antenna is the same substrate thickness but the material is vacuum),
- over close to PEC (distance between the PEC and the antenna is 1mm),
- over PMC (distance between the PMC and the antenna is the same substrate thickness but the material is vacuum),
- over close to PMC (distance between the PMC and the antenna is 1mm),
- and in free space.

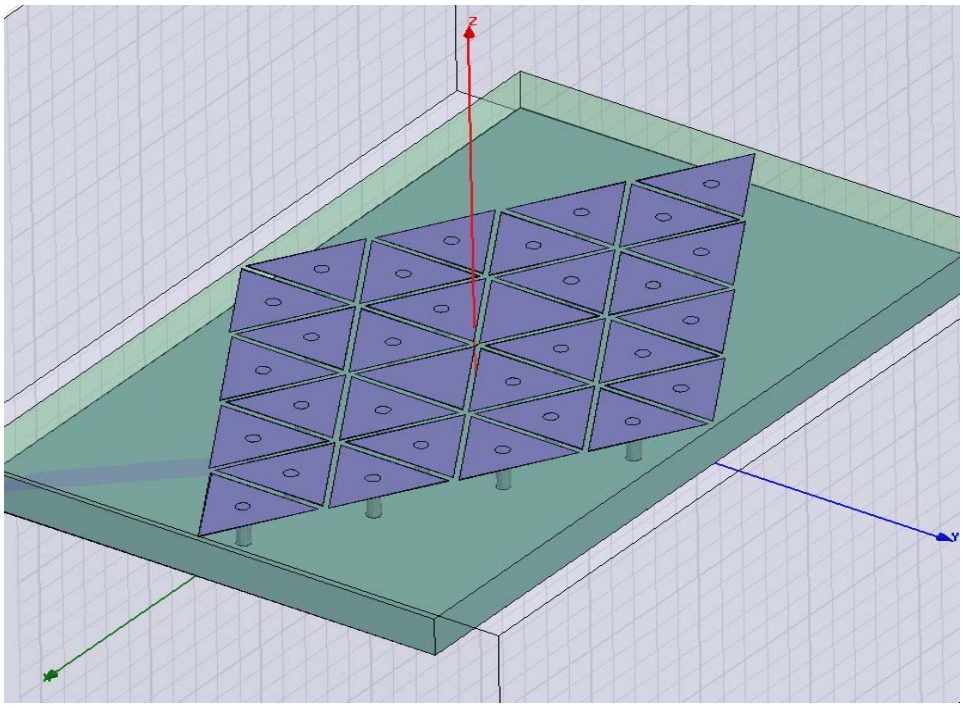

Figure 101. Bow Tie antenna inside HIGP (w=7mm)

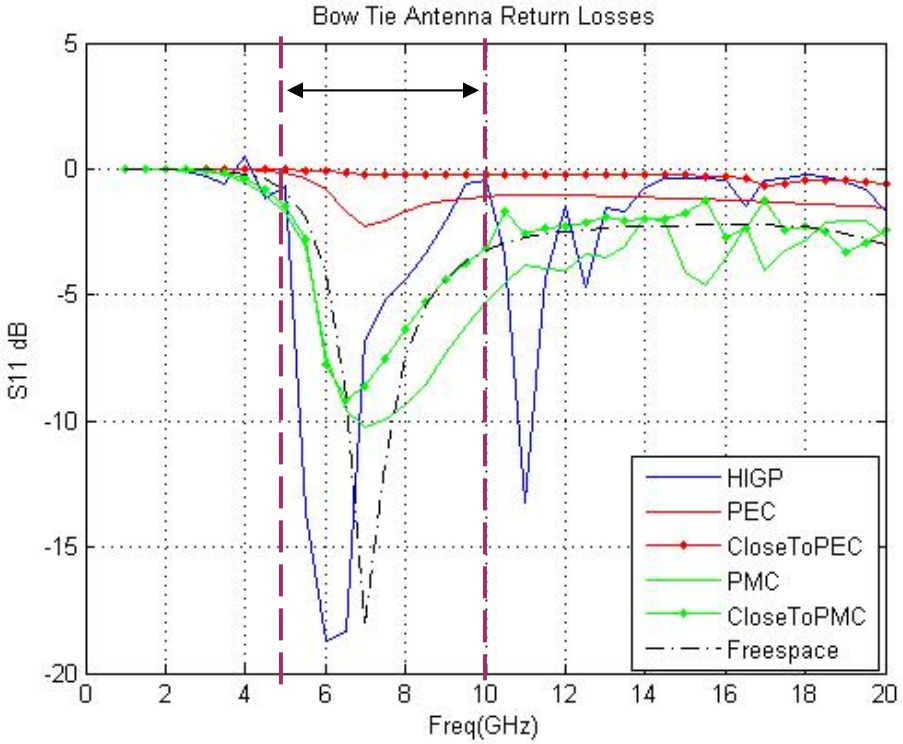

Figure 102. S_{11} results of Bow Tie antenna (w=7mm)

Overall S_{11} results are compared in Fig.102. According to these results, HIGP provides better S_{11} return loss than the other combinations between 5-7 GHz and provides better results between 7-10 GHz than PEC (behaves like almost PMC). Another resonant frequency occurs at 11 GHz when HIGP is used because of the coupling of the antenna and the HIGP.

The same application is repeated by increasing the patch width and the antenna triangle length to 16mm. Since the band gap for 16mm patch width is known as 2-5 GHz from Fig. 100 and free space resonant frequency of the 16mm bow tie antenna (3.5 GHz) is inside this frequency band gap, only 0-9 GHz frequency is observed (Fig. 103).

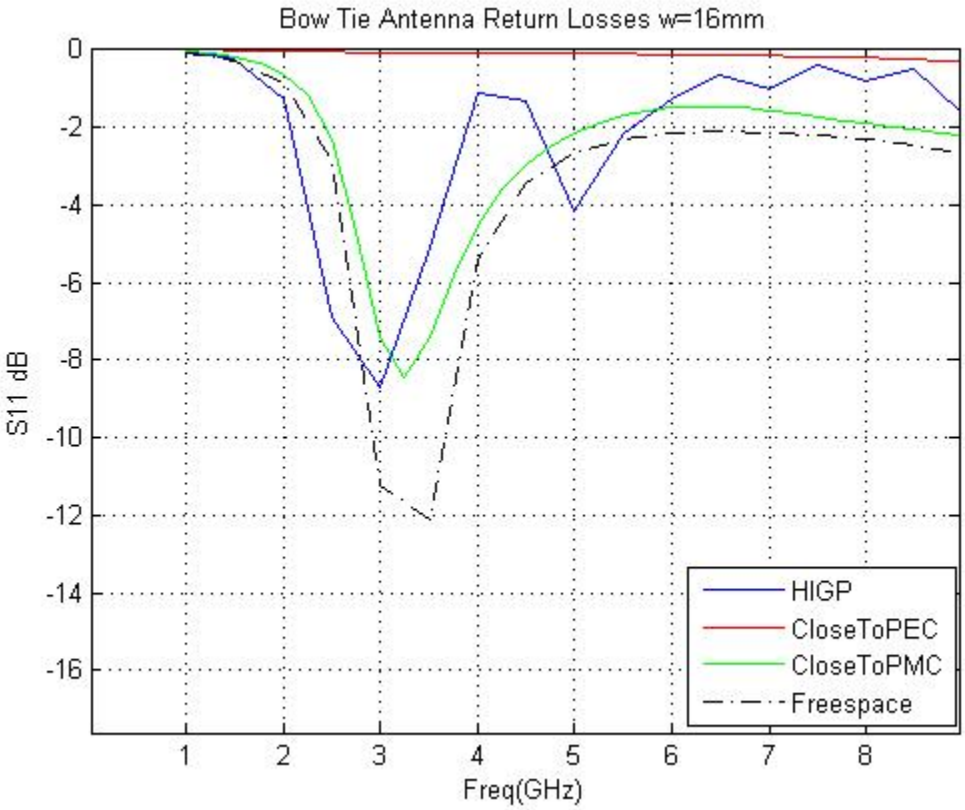

Figure 103. S_{11} results of Bow Tie antenna (w=16mm)

Fig. 103 shows that HIGP-Bow tie antenna structure operates well inside the band gap of the HIGP. Both Figs. 102 and 103 show that, if an Antenna-HIGP combination is desired to operate well, then the free space resonant frequency of the antenna should be inside the frequency band gap of the HIGP structure.

The following applications will discuss if it is possible to combine two different patch widths into one HIGP and if it might be possible to increase the bandwidth as the combination of the lower frequency bandwidth and higher frequency bandwidth of two different scale HIGPs.

In Fig. 104 both 7.6mm and 16mm patch widths are used to generate HIGP. The 16-mm scale is also used for the length of the edge of the bow-tie antenna. The inner part of the HIGP is made up of 7.6-mm patches, and the outer part is made up of 16-mm patches.

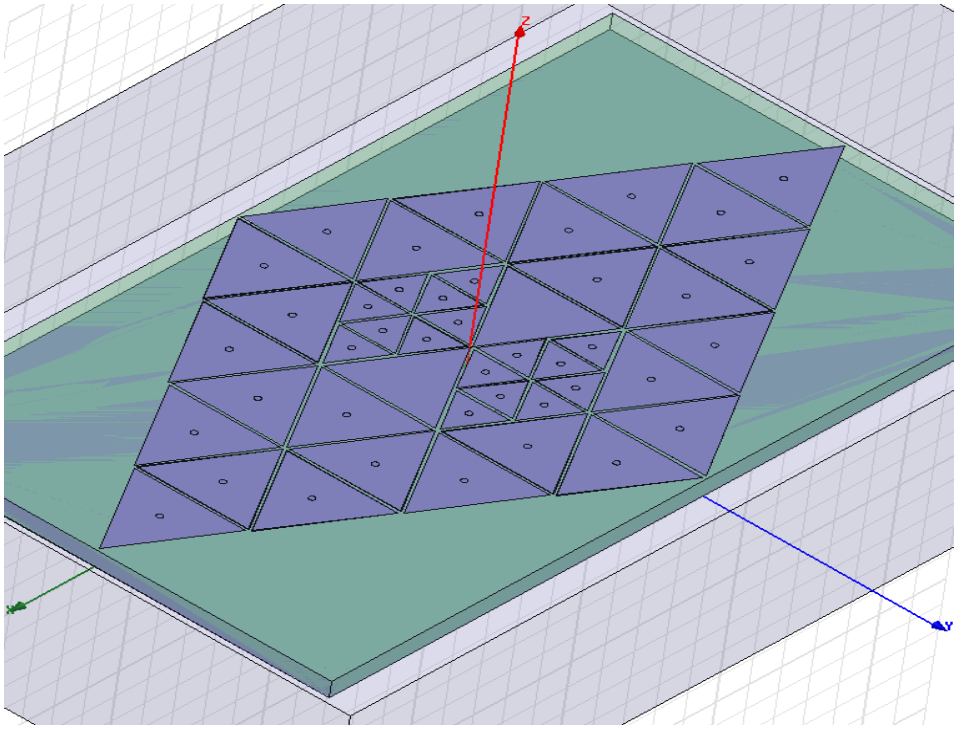

Figure 104. Combination of two different HIGP and 16mm bow-tie antenna

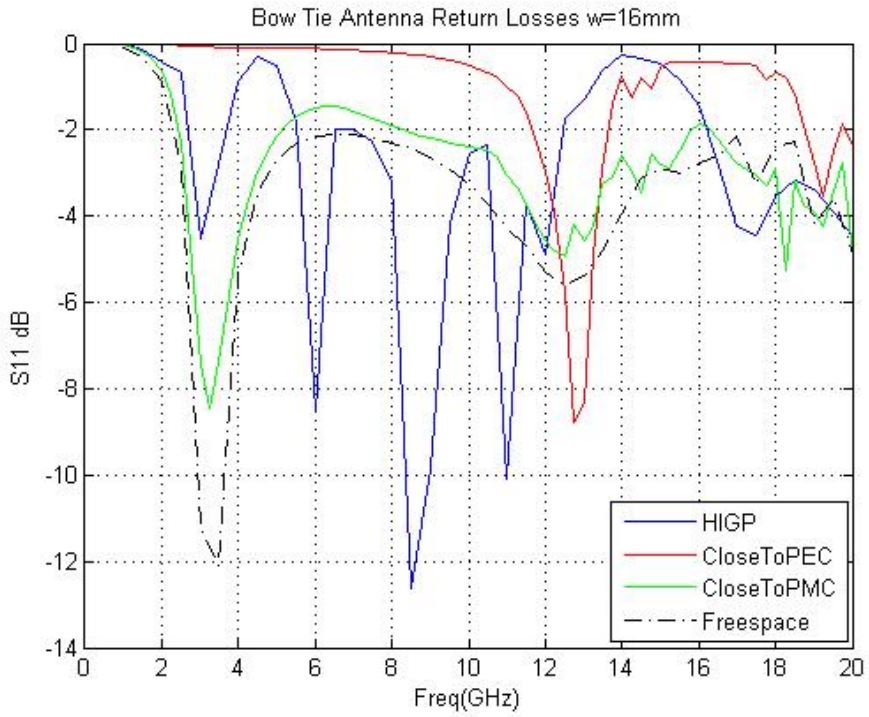

Figure 105. S_{11} of the 16mm bow-tie antenna and HIGP combination

Since the bow-tie antenna that is mounted inside the HIGP has a free space resonant frequency of 3.5 GHz and this frequency is inside the band gap of the larger scale (16mm) HIGP, it operates well between 2-5 GHz. Also, small scale (7.6mm) HIGP elements provide an operating bandwidth between 4-9 GHz. Large scale HIGP elements provide not only lower frequency bandwidth (2-5 GHz), but also higher frequency bandwidth (8-10.5 GHz) (Fig.100). So a total wide frequency bandwidth (2-10.5 GHz) is expected that includes both of the two HIGPs. Fig.105 shows that this combination confirms the expected results. HIGP-bow tie antenna combination operates between 2-12 GHz.

As a next step, two different 16-mm bow-tie antenna and 7.6-mm HIGP applications are made.

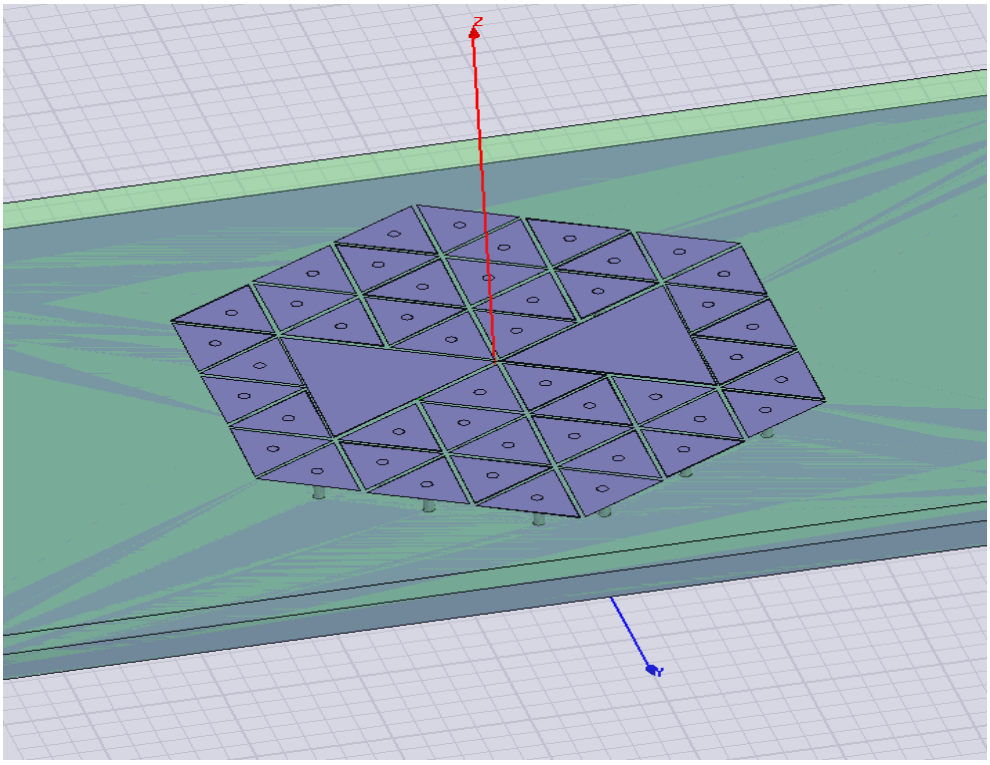

Figure 106. 7.6mm HIGP and 16mm bow-tie antenna (1)

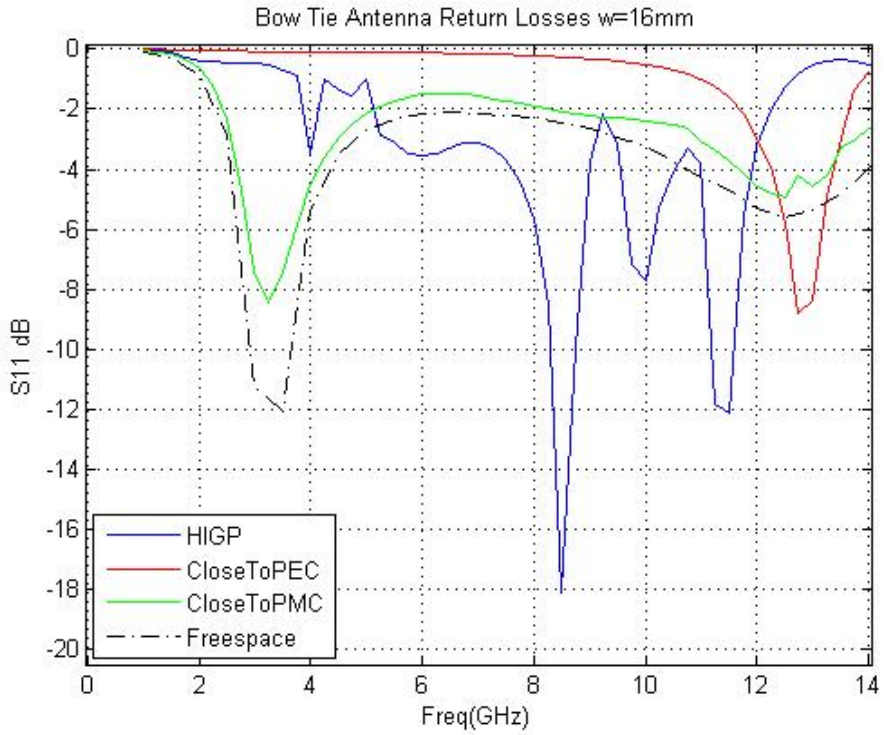

Figure 107. S_{11} of the 7.6mm HIGP and 16mm bow-tie antenna (1) (Fig. 106)

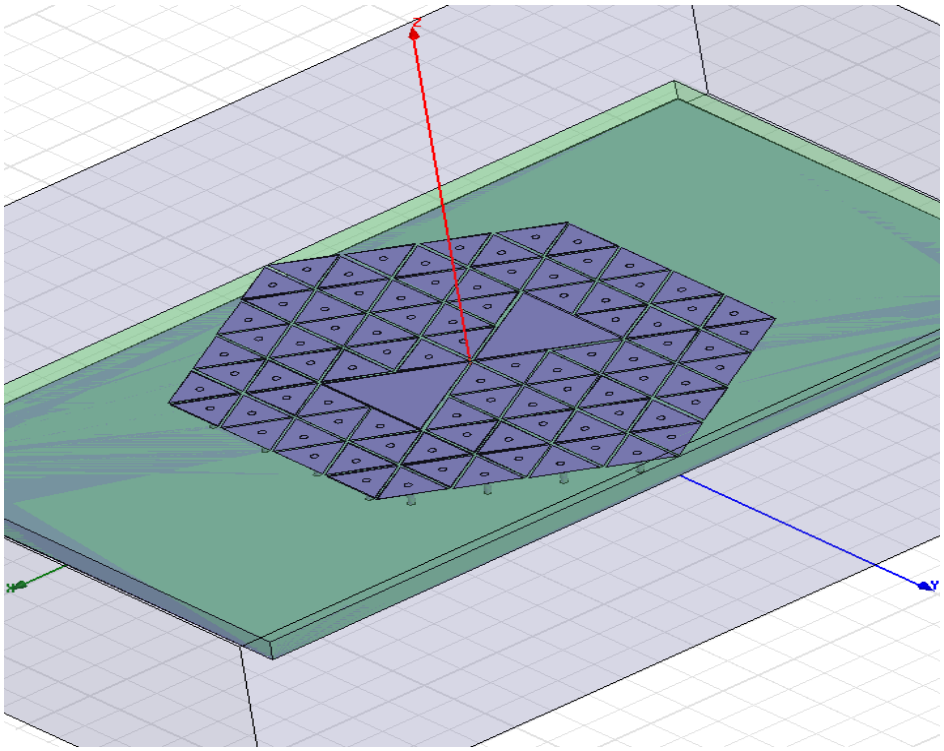

Figure 108. 7.6mm HIGP and 16mm bow-tie antenna (2) (one row added)

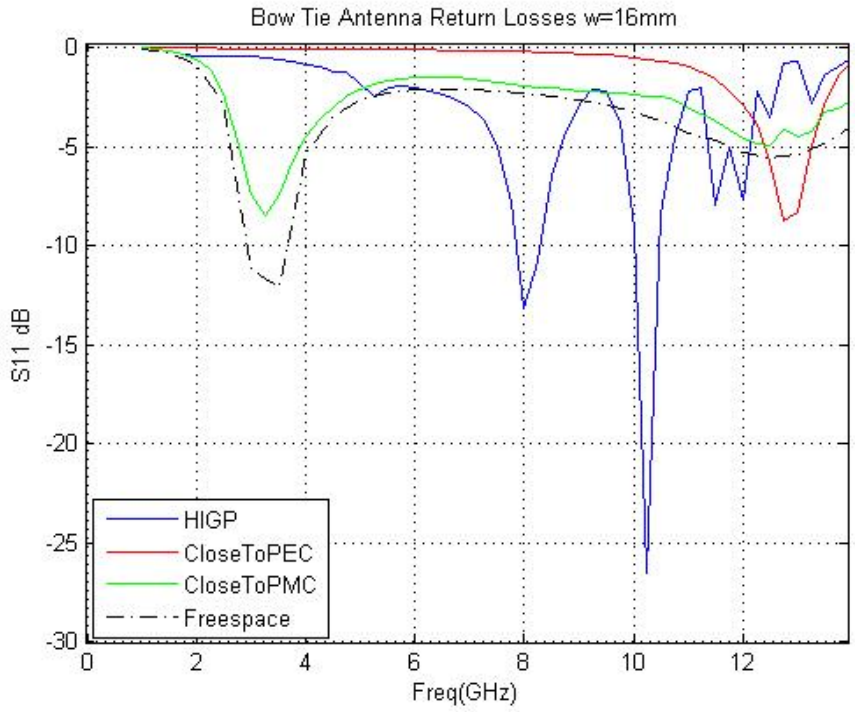

Figure 109. S_{11} of the 7.6mm HIGP and 16mm bow-tie antenna (2) (Fig. 108)

These two application results show that the16-mm bow-tie antenna does not work in the region of the free space resonant frequency, because 7.6-mm HIGP does not correspond in this region (Figs. 107 and 109). But it works between 5-12 GHz (inside the band gap of the 7.6-mm HIGP).

The following two designs discuss the combinations of HIGP, made up of two different scale (7.6-mm and 16-mm), and 7.6-mm bow-tie antenna (Figs. 110 and 112). At this time 7.6mm was used as the dimension of each edge of the bow-tie antenna for not only fitting the geometry of the HIGP and bow-tie antenna, but also having this 7.6mm bow-tie antenna a free space resonant frequency of 7 GHz which is inside the band gap of the 7.6mm HIGP. 16mm HIGP elements were also used to obtain wider frequency bandwidth

for the operation of the bow-tie antenna. Inner elements were designed as small elements (7.6mm) and outer HIGP elements were designed as large elements (16mm).

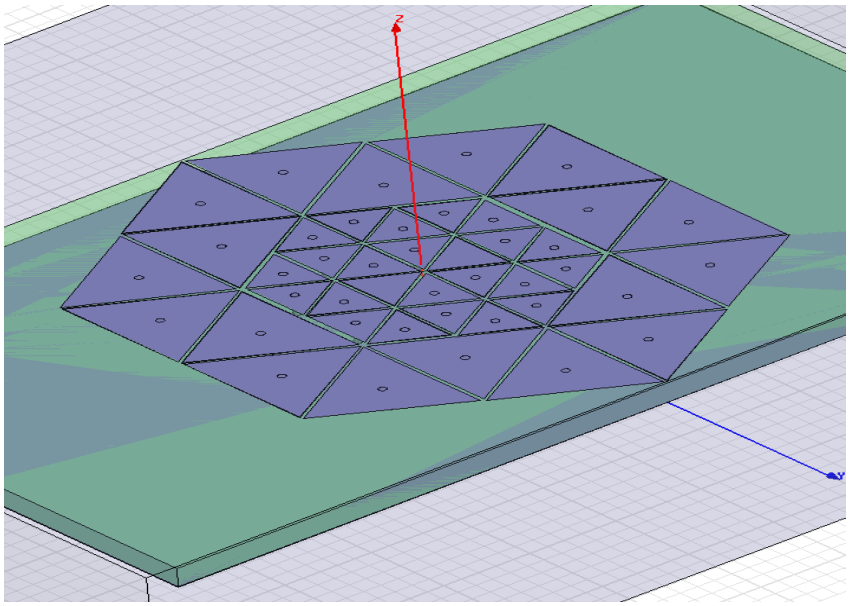

Figure 110. Combination of two different HIGP (7.6mm and 16mm) and 7.6mm bow-tie antenna (1)

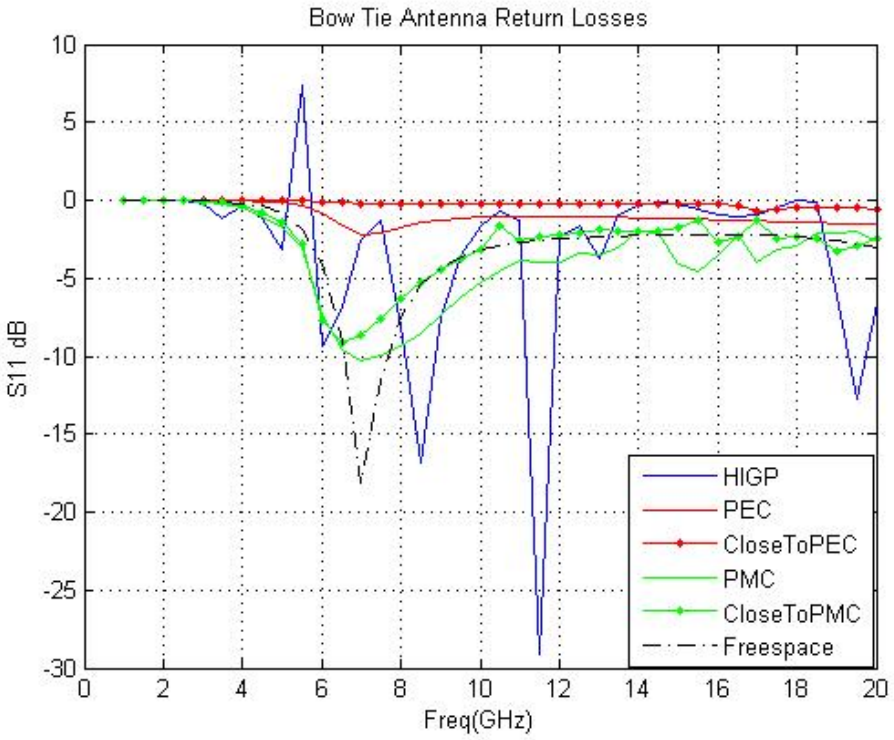

Figure 111. S_{11} of the 7.6mm bow-tie antenna and HIGP combination (1) (Fig. 110)

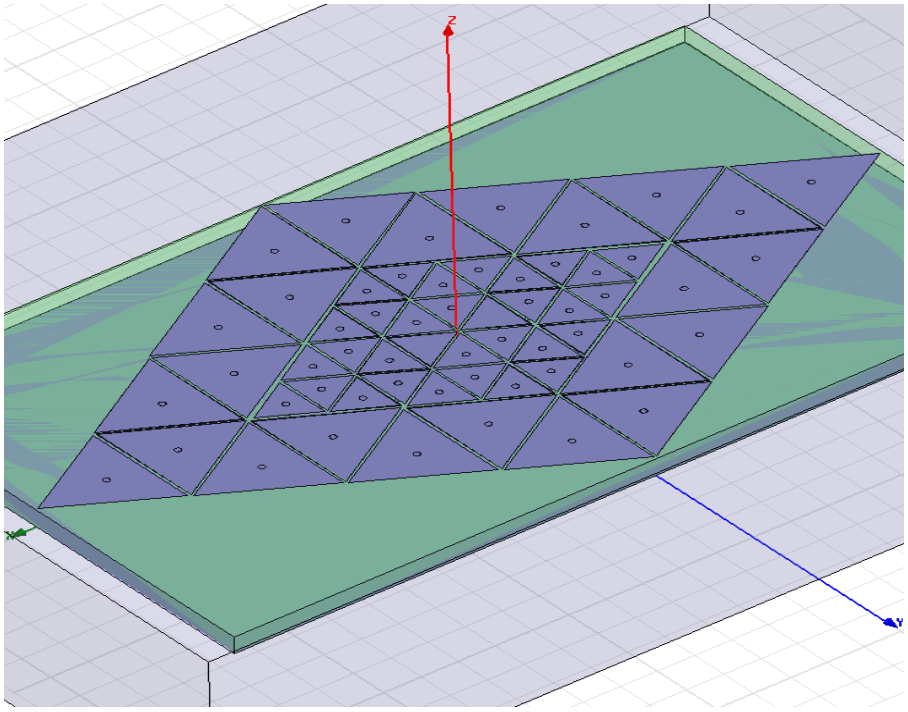

Figure 112. Combination of two different HIGP (7.6mm and 16mm) and 7.6mm bow-tie antenna (2)

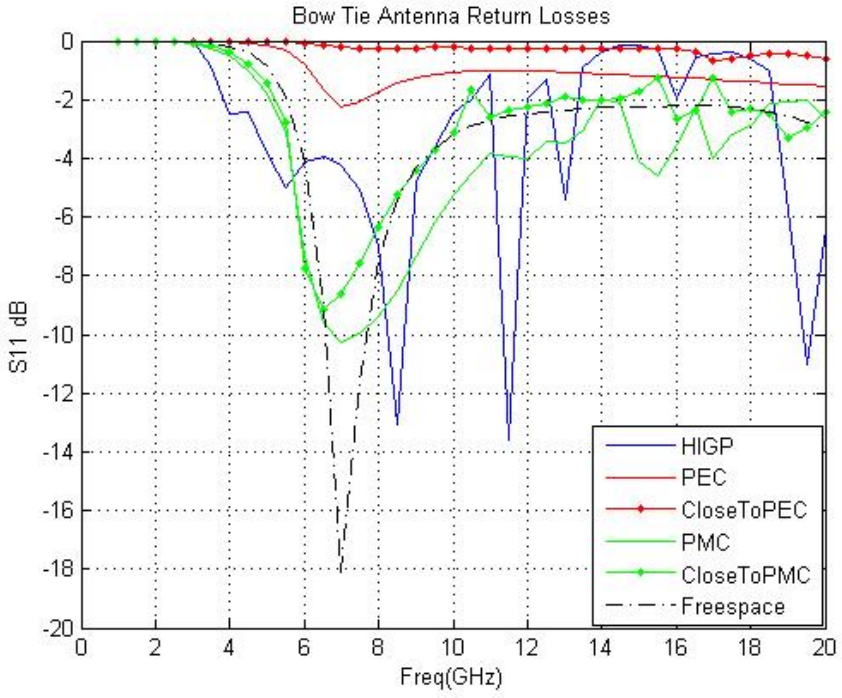

Figure 113. S_{11} of the 7.6mm bow-tie antenna and HIGP combination (2) (Fig. 112)

The design which is shown in Fig. 110 gives lower return loss than PEC. But it does not provide a wide operating bandwidth (Fig. 111).

The second 7.6-mm bow-tie antenna-HIGP design (Fig. 112) provides lower return loss than the antenna-PEC combinations in the frequency band of 3-13 GHz. These results are close to antenna-PMC results even though the PMC material does not exist in the nature itself. Also PEC results show that, when the antenna is brought close to a PEC surface, it shorts out and does not radiate (Fig. 113).

Both designs, which are introduced in Fig. 104 and Fig. 112 confirm the expected broadband return loss results. These two 7.6-mm and 16-mm bow-tie antenna-HIGP designs show that it is possible to take advantage of combining two different-scale HIGPs into one HIGP and provide a broadband operating range for an antenna that is designed to work in the frequency band gap of the HIGP structure.

Summary

In this chapter new HIGP designs and antenna-HIGP combinations were presented. The ways of obtaining the maximum surface wave suppression frequency band gap for HIGPs, and obtaining the minimum return loss in the suppression band gap of the HIGP for the Antenna-HIGP combinations were investigated.

Firstly, 7x7, 9x9 and 11x11 square patch HIGP designs were created and band gap characteristics of these designs were simulated and observed. These results were compared with the measurement results.

Secondly, optimization of 7x7 square patch design was created. Optimum patch width, gap width, substrate thickness and substrate material were determined within certain values and materials.

Afterwards, the performance of dipole antenna over square patch designs was simulated. Return loss of the antennas were compared in different combinations such as antenna-PEC and antenna-PMC and antenna-free space.

Next, log periodic antenna and antenna-HIGP designs were introduced and discussed. After trying different geometrical shapes for the HIGP designs, the triangle shape was used as the patch element for the HIGP. Bow-tie antenna and HIGP applications were simulated and discussed in the last part. Two different scale HIGPs were combined into one HIGP and broadband HIGP-antenna designs were introduced.

All the HIGP design parameters and surface wave suppression band gaps are shown on Table 2.

Table 2. HIGP Design Parameters and Band Gaps

	w(mm)	g(mm)	h(sub.thick.mm)	Permitivity	Band Gap
7x7 Square Patch	4.5	0.75	3.175	2.2	5-12 GHz
9x9 Square Patch	3.6	0.6	3.175	2.2	6-14 GHz
11x11 Square Patch	3	0.5	3.175	2.2	6-15 GHz
7x7 Patch Width Optimization	3.5	0.75	3.175	2.2	10-14 GHz
	4.5	0.75	3.175	2.2	5.5-14.5 GHz
	5.5	0.75	3.175	2.2	4-12.5 GHz
	6.5	0.75	3.175	2.2	4-8, 15-20 GHz
	7.5	0.75	3.175	2.2	3.5-7, 12-18 GHz
7x7 Gap Width Optimization	4.5	0.4	3.175	2.2	5-15 GHz
	4.5	0.6	3.175	2.2	5.5-13.5 GHz
	4.5	0.75	3.175	2.2	5.5-14 GHz
	4.5	1.2	3.175	2.2	5.5-12 GHz
	4.5	1.5	3.175	2.2	6-11.5 GHz
7x7 Substrate Thickness Optimization	4.5	0.4	3.175	2.2	5-15 GHz
	4.5	0.4	1.575	2.2	6.5-14 GHz
	4.5	0.4	0.787	2.2	9.5-14 GHz
	4.5	0.4	0.508	2.2	11.5-13 GHz
	4.5	0.4	0.381	2.2	-
7x7 Substrate Material Optimization	4.5	0.4	3.175	2.2	5-15 GHz
	4.5	0.4	3.175	2.33	4.5-14.5 GHz
	4.5	0.4	3.175	2.94	4.5-11.5 GHz
	4.5	0.4	3.175	10.2	-
Round Patch HIGP	4.5	0.4	3.175	2.2	-
	5.5	0.4	3.175	2.2	5-12 GHz
	6.5	0.4	3.175	2.2	4.5-9 GHz
	7.5	0.4	3.175	2.2	4-7.5 GHz
Hexagon Patch HIGP	3.5	0.4	3.175	2.2	9.5-14 GHz
	4.5	0.4	3.175	2.2	-
	5.5	0.4	3.175	2.2	4-10 GHz
	6.5	0.4	3.175	2.2	3.5-8 GHz
	7.5	0.4	3.175	2.2	3-7 GHz
	8.5	0.4	3.175	2.2	3-6.5 GHz
Triangle Patch HIGP	5.2	0.4	3.175	2.2	6.5-10 GHz
	7.6	0.4	3.175	2.2	4-9 GHz
	8	0.4	3.175	2.2	4.5-10 GHz
	16	0.4	3.175	2.2	2-5, 8-10.5 GHz

V. Conclusions and Recommendations

Chapter Overview

In this chapter, all of the research processes are broadly reviewed, conclusions of the thesis are made and recommendations are presented to the future researchers.

Conclusions of Research

This thesis is the design and optimization of broadband high-impedance ground planes for surface mount antennas which is complementary with a companion thesis involving construction and testing (Cakiroglu, 2008).

In this research, operating bandwidth of the different conformal antennas (dipole, log periodic and bow-tie antennas) were increased by changing the geometry and dimensions of the HIGPs and antennas. In order to achieve this goal, firstly HIGPs were designed by using different geometrical shapes (square, round, hexagon and triangle) as patches. And then, surface wave suppression band gaps of these designs were determined. Next, conformal antennas which operate in these band gaps were designed. Lastly, antennas and HIGPs were combined together and return loss results of these combinations were compared with antenna-PEC, antenna-PMC and antenna free space results. All the designs, simulations and optimizations were completed by using Ansoft HFSS v.10.

The 7x7, 9x9 and 11x11 square patch HIGP designs were created and band gap characteristics of these designs were simulated and observed. These results were

compared with the measurement results. Optimization of 7x7 square patch design was performed. Optimum patch width, gap width, substrate thickness and substrate material were determined within certain values and materials. Dipole antennas over square patch designs were simulated. Return loss of the antennas were compared in different combinations such as antenna-PEC and antenna-PMC and antenna-free space. Next, log periodic antenna and antenna-HIGP designs were introduced and discussed.

Lastly, triangle shape was used as the patch element for the HIGP. Bow-tie antenna and HIGP applications were simulated and discussed in the last part of the previous chapter. Two different scale HIGPs were combined into one HIGP and multi-scale broadband HIGP-antenna designs were introduced. It was shown that using multi-scale patches in a proper direction and order could preserve increased operation bandwidth of the antenna in comparison with the same antenna over PEC and PMC.

Significance of Research

The feasibility of designing multi-scale patch HIGPs were introduced in this research. It was demonstrated that it was possible to combine two different scale HIGPs into one, and increase the band gap. It is considered that the different scale patch usage gives more preserved operating bandwidth.

Other significance of this research is that the HIGP-antenna structures are very thin for mounting on metal surfaces such as aircraft, satellite or UAV. These kinds of thin low profile HIGP-antenna structures will not affect the aerodynamic properties of the surface

severely, in contrast to the protruding antennas, if they are mounted properly. And also it is going to be possible to combine all the antennas on a flying object, which operates in different frequencies into one broadband low profile antenna.

Recommendations for Future Research

Triangular multi-scale HIGP was introduced in this research, and some antenna applications were considered. Different multi-scale geometrical shapes such as squares, rounds and hexagons could be tried to improve the bandwidth. More than two different scales could be used to cover more bandwidth.

Log periodic antenna applications could be improved. A log periodic antenna which has a design of smooth and broadband radiation can be used together with a multi-scale HIGP.

Other research can be performed on the feasibility of mounting the HIGP-antennas over the surfaces of the aircraft, UAVs or satellites.

Combining all the antennas of the aircraft into one low profile broadband surface mount HIGP-antenna can be another research project for the future.

Ansoft HFSS v.10 software program was used in the designs and simulations of this research. This software will be quite adequate and accurate to solve the problems for the designs and simulations of the future research recommendations discussed above.

Bibliography

Balanis, Constantine A., *Antenna Theory (3rd Edition)*. New York: John Wiley & Sons Inc., 2005.

Broas, Romulo F. Jimenez, Daniel F. Sievenpiper and Eli Yablonovitch. "A High-Impedance Ground Plane Applied to a Cellphone Handset Geometry," *IEEE Trans. On Microwave Theory Tech.*, vol. 49, 7:1262-1265 (July 2001).

Broas, Romulo F. Jimenez, Daniel F. Sievenpiper and Eli Yablonovitch. "An Application of High-Impedance Ground Planes to Phased Array Antennas," *IEEE Trans. On Microwave Theory Tech.*, vol. 53, 4:1377-1381 (April 2005).

Cakiroglu, Bora, *Construction and Testing of Broadband High-Impedance Ground Plane for Surface Mount Antennas*, MS thesis, AFIT/GE/ENG/08M-02. School of Engineering, Air Force Institute of Technology, Wright-Patterson AFB OH, March 2008.

DuHamel, R. H. and D.E. Isbell, "Broadband Logarithmically Periodic Antenna Structures," *IRE National Convention Record*, 119-128, 1957.

DuHamel, R.H. and F.R. Ore, "Logarithmically Periodic Antenna Designs," *IRE National Convention Record*, 139-152, 1958.

Golla, Kevin J. *Broadband Application of High Impedance Ground Planes*. MS thesis, AFIT/GE/ENG/01M-11. Graduate School of Engineering and Management, Air Force Institute of Technology (AU), Wright Patterson AFB OH, March 2001.

Kshetrimayum, Rakhesh S. "A Brief Intro to Metamaterials," *IEEE Potentials,* vol. 23, 5:44-46 (December 2004).

Linton, David and William Scanlon. "Continuously Conformable Antenna Element for Advanced Wearable Communications Under Hostile Channel Conditions," First Report, USAF EOARD, Queen's University, Belfast, UK. March 2006.

Saville, Michael, *Investigation of conformal High-Impedance Ground Planes*, MS thesis, AFIT/GE/ENG/00M-17. School of Engineering, Air Force Institute of Technology, Wright-Patterson AFB OH, March 2000.

Sievenpiper, Dan, Lijun Zhang, Ramulo F. Jimenez Broas, Nicholas G. Alexopolous and Yablonovitch. "High-Impedance Electromagnetic Surfaces with a Forbidden Frequency Band," *IEEE Trans. On Microwave Theory Tech.*, vol. 47, 11:2059-2074 (November 1999).

Stutzman, Warren L. and Gary A.Thiele, Antenna Theory and Design. New York: John Wiley & Sons Inc., 1981.

Yablonovitch, Eli, "Inhibited Spontaneous Emission in Solid State Physics and Electronics," *Physical Review Letters*, vol. 58, 2059-2062 (May 1987).

Yang, Fan and Yahya Rahmat-Samii. "Reflection Phase Characterizations of the EBG Ground Plane for Low Profile Wire Antenna Applications," *IEEE Trans. On Antennas and Propagation,* vol. 51, 10:2691-2703 (October 2003).

Vita

Second Lieutenant Murat Dogrul was born in 1980 in Kocaeli, Turkiye. He attended Kocaeli Science High School. Upon graduation in 1998, he entered undergraduate studies at the Turkish Air Force Academy, Istanbul, where he graduated with a Bachelor of Science degree in Electrical Engineering in August 2002.

After that, he finished his basic pilot training at 2nd Main Jet Base in Izmir in 2004, F-5 fighter training at 3rd Main jet Base in Konya in 2004, F-16 fighter training at 4th Main Jet Base in Ankara in 2005. His first assignment was at 9th Main Jet Base 192nd Squadron in Balikesir in July 2005. In September 2006, he entered the Graduate School of Engineering and Management, Air Force Institute of Technology.

REPORT DOCUMENTATION PAGE

Form Approved
OMB No. 074-0188

1. REPORT DATE *(DD-MM-YYYY)*	2. REPORT TYPE	3. DATES COVERED *(From – To)*
27-03-2008	Master's Thesis	Sep 2006– Mar 2008

4. TITLE AND SUBTITLE

DESIGN AND OPTIMIZATION OF BROADBAND HIGH IMPEDANCE GROUND PLANES (HIGP) FOR SURFACE MOUNT ANTENNAS

5a. CONTRACT NUMBER

5b. GRANT NUMBER

5c. PROGRAM ELEMENT NUMBER

6. AUTHOR(S)

Dogrul, Murat, 1st Lt., TuAF

5d. PROJECT NUMBER

5e. TASK NUMBER

5f. WORK UNIT NUMBER

7. PERFORMING ORGANIZATION NAMES(S) AND ADDRESS(S)

Air Force Institute of Technology
Graduate School of Engineering and Management (AFIT/EN)
2950 Hobson Way, Building 640
WPAFB OH 45433-8865

8. PERFORMING ORGANIZATION REPORT NUMBER

AFIT/GE/ENG/08-08

9. SPONSORING/MONITORING AGENCY NAME(S) AND ADDRESS(ES)

George W. York, Deputy CC and RF Sensors
AFRL/AF Office of Scientific Research, European Office of Aerospace Research & Development,
email: george.york@london.af.mil phone #:+44 (0) 207 514-4354

10. SPONSOR/MONITOR'S ACRONYM(S)

11. SPONSOR/MONITOR'S REPORT NUMBER(S)

12. DISTRIBUTION/AVAILABILITY STATEMENT

APPROVED FOR PUBLIC RELEASE; DISTRIBUTION UNLIMITED.

13. SUPPLEMENTARY NOTES

14. ABSTRACT

Gain and bandwidth metrics of broad-band low-profile antennas severely deteriorate when they are placed conformally onto the conductive skins of air, sea, and ground platforms. This detrimental effect is primarily due to out-of-phase reflections from the conductive body interfering with the antenna's self radiation. Furthermore, lateral waves launched by the antenna couple into the thin substrate placed between the antenna and the platform, giving rise to surface waves resulting in significant diffraction from the edges of the substrate. To remedy these two major mechanisms degrading antenna performance, high impedance ground planes (HIGP) were designed. HIGPs made of a 2-dimentional periodic arrangement of a mushroom structure not only provide perfect-magnetic-conductor (PMC)-like reflection but also suppress the surface waves within the stop-band of the substrate modes. This study presents new geometrical shape HIGP-antenna designs and optimizations. Dipole antenna, log periodic antenna and finally bow-tie antennas are used in the study. Multi-scale HIGP and antenna designs are introduced in the final part of the thesis.

15. SUBJECT TERMS

High Impedance Ground Plane (HIGP), Electronic Band Gap (EBG), Photonic Band Gap (PBG), Dipole Antennas, Log Periodic Antennas, Bow-tie Antennas.

16. SECURITY CLASSIFICATION OF:			17. LIMITATION OF ABSTRACT	18. NUMBER OF PAGES	19a. NAME OF RESPONSIBLE PERSON
a. REPORT	b. ABSTRACT	c. THIS PAGE			Dr. Peter J. Collins
U	U	U	UU	135	19b. TELEPHONE NUMBER *(Include area code)* (937) 255-3636, ext 7256 (peter.collins@afit.edu)